Final Report

Project Title Improving efficacy of anticancer drugs in P-gp overexpressing cells by flavonoid incorporated into mPEG-b-OCL-Bz micelles

By Assist. Prof. Dr. Ruttiros Khonkarn

May/2020

Contract No. MRG6180038

Final Report

Project Title Improving efficacy of anticancer drugs in P-gp overexpressing cells by flavonoid incorporated into mPEG-b-OCL-Bz micelles

Researcher	Institute
Assist. Prof. Dr. Ruttiros Khonkarn	Faculty of Pharmacy Chiang Mai University

This project granted by the Thailand Research Fund

Abstract

Project Code : MRG6180038

Project Title : Improving efficacy of anticancer drugs in P-gp overexpressing cells by flavonoid incorporated into mPEG-b-OCL-Bz micelles

Investigator : Assist. Prof. Dr. Ruttiros Khonkarn

E-mail Address : ruttiros.khonkarn@cmu.ac.th; pharrutty@gmail.com

Project Period : 2 May 2018 – 1 May 2020

Abstract:

Over expression of cell-membrane transporters is one of the major mechanism of multidrug resistant (MDR) phenomenon which is associated with failure of cancer treatment. Therefore, inhibition of drug transporter function is challenge in cancer therapy. Two flavonoid glycosides; quercetrin (QRT) and rutin (RUT) as well as their aglycone, quercetin (QCT) are inhibitors of the P-glycoprotein (P-gp) which is overexpressed in cancer cells and is one of the mechanism for the resistance towards cytostatic drugs. However, their pharmaceutical application is limited according to their low aqueous solubility. In this study, the polymeric micelles of benzoylated methoxy-poly(ethylene glycol)-*b*-oligo(ε-caprolactone) or mPEG-*b*-OCL-Bz loading with the flavonoids were prepared to solve these problems. The flavonoid-loaded micelles showed average size of 13-20 nm and maximum loading capacity of 35% (w/w). The release of QCT (21%, 3 h) was lower than QTR (51%, 3 h) and RUT (58%, 3 h). QCT (free and micelle forms) exhibited significantly higher cytotoxicity against P-glycoprotein overexpressing leukemia (K562/ADR) cells than QTR and RUT ($p<0.05$). The results demonstrated that QCT-loaded micelles effectively reversed cytotoxicity of both doxorubicin (multidrug resistant reversing (δ) values up to 0.71) and daunorubicin (δ values up to 0.74) on K562/ADR cells. It was found that QCT-loaded micelles as well as empty polymeric micelles inhibited P-gp efflux of tetrahydropyranyl adriamycin. Besides, mitochondrial membrane potential was decreased by QCT (in its free form and micellar formation). Our results suggested that a combination effects of polymeric micelles (inhibiting P-gp efflux) and QCT (interfering mitochondrial membrane potential) might be critical factors contributing to the reversing multidrug resistant of K562/ADR cells by QCT-loaded micelles. We concluded that QCT-loaded mPEG-b-OCL-Bz micelles are the attractive systems for overcoming multidrug-resistant cancer cells.

Keywords : Flavonoid; Polymeric micelle; Resistance; Cancer; P-gp

บทคัดย่อ

กระบวนการขนส่งสารผ่านเยื่อหุ้มเซลล์ที่มีจำนวนมากในเซลล์มะเร็งที่ดื้อยาเป็นสาเหตุหลักของการดื้อยา ซึ่งส่งผลให้การรักษามะเร็งล้มเหลว ดังนั้นการยับยั้งกระบวนการขนส่งสารผ่านเยื่อหุ้มเซลล์จึงเป็นวิธีที่น่าสนใจในการนำมารักษามะเร็ง สารฟลาโวนอยด์ชนิดเควอซิทริน รูทิน และเควอซิทิน สามารถยับยั้งพี-ไกลโคโปรตีนที่ทำหน้าที่ขนส่งยาต้านมะเร็งออกจากเซลล์มะเร็งทำให้เซลล์มะเร็งดื้อยารักษามะเร็ง อย่างไรก็ตามการนำสารเหล่านี้มารักษามะเร็งยังมีข้อจำกัดเนื่องจากสารมีค่าการละลายน้ำที่ต่ำ ในการศึกษานี้จึงได้นำสารฟลาโวนอยด์มากักเก็บในพอลิเมอริกไมเซลล์ชนิดเบนโซอิล เมทอกซี โพลิ เอทิลีน ไกลคอล โอลิโกคาโพลแลคโทน เพื่อเพิ่มการละลาย ผลการศึกษาพบว่าสารฟลาโวนอยด์ที่กักเก็บในพอลิเมริกไมเซลล์มีขนาด 13-20 นาโนเมตร และมีประสิทธิภาพการกักเก็บสารสูงสุดที่ 35 เปอร์เซ็นต์ การศึกษาการปลดปล่อยสารพบว่าสารเควอซิทิน (21 เปอร์เซ็นต์, 3 ชั่วโมง) ปลดปล่อยจากพอลิเมอริกไมเซลล์ช้ากว่าสารเควอซิทริน (51 เปอร์เซ็นต์, 3 ชั่วโมง) และรูทิน (58 เปอร์เซ็นต์, 3 ชั่วโมง) สารเควอซิทินมีประสิทธิภาพฆ่าเซลล์มะเร็งเม็ดเลือดขาวที่ดื้อยาได้มากกว่าสารเควอซิทรินและรูทิน สารเควอซิทินที่กักเก็บในพอลิเมอริกไมเซลล์สามารถเพิ่มประสิทธิภาพต้านมะเร็งของยาดอกโซรูบิซิน (ค่าการย้อนกลับการดื้อยา สูงถึง 0.71) และยาดาวโนรูบิซิน (ค่าการย้อนกลับการดื้อยา สูงถึง 0.74) ในเซลล์มะเร็งเม็ดเลือดขาวที่ดื้อยา นอกจากนี้สารเควอซิทินที่กักเก็บในพอลิเมอริกไมเซลล์และพอลิเมอริกไมเซลล์เปล่าสามารถยับยั้งการขนส่งยาเตตราไฮโดรไพรานิล อะเดรียมัยซิน โดยยับยั้งการทำงานของพี-ไกลโคโปรตีน อีกทั้งสารเควอซิทินในรูปอิสระและที่กักเก็บในพอลิเมอริกไมเซลล์สามารถลดศักย์เยื่อเซลล์ของไมโทคอนเดรีย ผลการศึกษานี้แสดงให้เห็นว่าการที่สารเควอซิทินที่กักเก็บในพอลิเมอริกไมเซลล์สามารถเพิ่มประสิทธิภาพการต้านมะเร็งของยารักษามะเร็งเนื่องจากผลที่เกิดจากการรวมกันของพอลิเมอริกไมเซลล์ที่ไปยังยั้งการขนส่งยารักษามะเร็งโดยพี-ไกลโคโปรตีน และผลของเควอซิทินที่ไปลดศักย์เยื่อเซลล์ของไมโทคอนเดรีย การศึกษานี้จึงสรุปได้ว่าสารเควอซิทินที่กักเก็บในพอลิเมอริกไมเซลล์เป็นระบบนำส่งยาที่น่าสนใจในการรักษามะเร็งที่ดื้อยา

คำสำคัญ : ฟลาโวนอยด์; พอลิเมอริกไมเซลล์; ดื้อยา; มะเร็ง; พี-จีพี

TABLE OF CONTENTS

1. Executive Summary

Multidrug resistance (MDR), among others, caused by over expression of cell-membrane transporters, is a major factor for the clinical failure of chemotherapy for many types of cancer. Therefore, inhibition of these drug transporters is an attractive modality in cancer therapy to enhance the therapeutic potential of cytotoxic drugs. It has been reported that flavonoids which are quercetin (QCT) quercetrin (QTR) and rutin (RUT), inhibit MDR efflux proteins. However, the solubility of QCT and also its glycoside derivatives, QTR and RUT, is very low (0.1-500 μM) which limits their use in clinical oncology. Polymeric micelles consist of a hydrophobic core that can improve solubility of hydrophobic drugs. Additionally, a recent study reported that polymeric micelles can inhibit P-gp (cell-membrane transporters) function. In this study, we aimed to encapsulate QCT, QTR and RUT into mPEG750-b-OCL-Bz micelles to improve their solubility and evaluate the MDR-reversing effect.

The results show that flavonoid-loaded mPEG-b-OCL-Bz micelles were successfully prepared by film hydration method with the particle size around 13-20 nm and zeta potential of -1.99 to -8.86 mV. The flavonoid loaded polymeric micelles exhibited a regular spherical shape as determined by TEM. The highest entrapment efficiency was found from QTR (91.1±1.1%), followed by QCT (73.1±5.0%) and RUT (71.7±1.9%). Besides, QTR had the maximum loading capacity, followed by RUT and QCT with LC values of 36.4±0.4%, 11.5±0.3% and 7.3±0.5%, respectively. These results present that the efficiency of incorporation of flavonoids into polymeric micelles was influenced by the balance between the hydrophobicity and the hydrophilicity. Moreover, the studied flavonoid-incorporated polymeric micelles were stable for 14 days at 37°C in the absence of BSA. The *in vitro* release study exhibited that QCT was significantly slower than that of QTR and RUT at releasing time of 15 min to 6 h. The interaction between the drug and the micellar core effected the drug release. The π-π interaction between QCT (aglycone) and the micellar core of mPEG-b-OCL-Bz micelles was stronger than that of QCT glycosides.

The cytotoxicity results present that QCT in its free form or micellar formulation had higher cytotoxicity activity than QTR and RUT. The cytotoxicity results also reveal that free QCT and QCT-loaded micelles might not be substrates of P-gp. Interestingly, empty mPEG-b-OCL-Bz micelles had MDR-reversing effect. A stronger MDR-reversing effect to both doxorubicin (DOX) and daunorubicin (DAU) of K562/ADR cells was observed from QCT-loaded micelles (at QCT

concentration of 1-3 μM) with maximum MDR-reversing values around 70%. In order to study the mode of action by which QCT-loaded micelles increased the efficacy of DOX or DAU in P-gp overexpressing cells, the modulation of QCT-loaded micelles in the kinetics of P-gp-mediated pumping and mitochondrial membrane potential were investigated. For the assessment of kinetics of P-gp-mediated pumping, it was found that P-gp pump was inhibited by QCT-loaded micelles and empty mPEG750-b-OCL-Bz micelles with maximum P-gp inhibiting effect of 70% and 18%, respectively. The ratio of $C_{n(i)} / C_N$ of QCT-loaded micelles and empty polymeric micelle continuously increased in dose dependent manner. For the assessment of mitochondrial membrane potential, it found that QCT (in its free form and micellar formation) had an effect on mitochondrial membrane potential. The deceasing of JC-1 R/G ratio in resistant cells treated with free QCT and QCT loaded polymeric micelles for 15 min was 30% and 36% of cell control, respectively. This decreasing did not change in time dependent manner. Taken together, the potential mechanisms of reversing multidrug resistant of K562/ADR cells by QCT loaded polymeric micelles might be the combination effects of polymeric micelles and QCT, interfering with P-gp function and mitochondrial membrane potential, respectively.

2. Objectives

2.1. To improve the solubility of QCT glycosides by incorporation these compounds into mPEG750-b-OCL-Bz micelles

2.2. To evaluate the MDR-reversing effect of interesting flavonoid-loaded mPEG750-b-OCL-Bz micelles for anticancer drugs (doxorubicin (DOX) and daunorubicin (DAU))

2.3. To determine mechanism of cancer cell death of interesting flavonoid-loaded mPEG750-b-OCL-Bz micelles

2.4 To investigate mechanism of sensitization of MDR cancer cells by interesting flavonoid-loaded mPEG750-b-OCL-Bz micelles

3. Methodology

3.1 Preparation flavonoid-loaded mPEG750-b-OCL-Bz micelles

The film hydration method was used to prepare flavonoid-loaded amphiphilic block oligomers, mPEG750-*b*-OCL-Bz.

- Stock solution of flavonoids (quercetrin, rutin and quercetin) and oligomer was dissolved in ethanol and/or dichloromethane.
- Stock flavonoid solution and oligomer solution were mixed into round bottom flask to achieve flavonoid/oligomer ratios of 2.5%, 5%, 10%, 20%, and 40% (w/w).
- The solvent of this mixture was evaporated under N_2 stream for 1 h.
- Micellization was induced by hydration of the obtained film with DI water.
- The micellar suspension (size around 20 nm) was filtered through a 0.45 μm filter to eliminate non entrapped (precipitated) flavonoids.

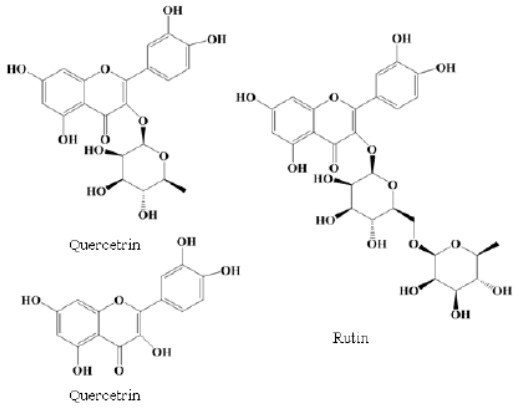

Fig. 1. The chemical structures of quercetin, quercetrin, rutin

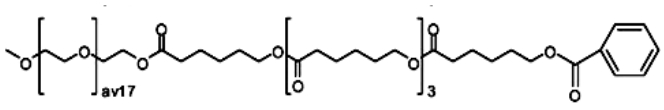

Fig. 2. The chemical structures of mPEG750-b-OCL-Bz

3.2 Loading efficiency

- The amount of flavonoid loaded micelles in the filtrate was determined by diluting the micelles with suitable solvent and measured the absorbance using UV-vis spectrophotometer.
- The entrapment efficiency (EE) and loading capacity (LC) were calculated by the following formula:

$$\% \text{ EE} = \frac{\text{Amount of measured flavonoid}}{\text{Amount of added flavonoid}} \times 100\%$$

$$\% \text{ LC} = \frac{\text{Amount of measured flavonoid}}{\text{Amount of added polymer}} \times 100\%$$

3.3 Dynamic light scattering

The particle size and zeta potential of loaded and unloaded polymeric micelles was measured by dynamic light scattering (DLS), using a Malvern system (Malvern Ltd., U.K.) which consisting of auto-titrate and a computer with DLS software. Scattering of the micellar solutions was measured at room temperature in an optical quality concentration thereby giving the average diameter of the micelles (Zave).

3.4 Transmission electron microscopy

Transmission electron microscopy (TEM, JEM 2010) was used to examine morphology and particle size of flavonoid loaded micelles. TEM samples were prepared by dropping the micelles onto copper grid, followed by air drying. TEM images of flavonoid load polymeric micelles were subsequently examined.

3.5 Release study

The *in vitro* release of flavonoid from flavonoid-loaded micelles was determined by dialysis method.

- Flavonoid-loaded micelles obtained from fresh preparation were added into pre-swollen dialysis bag with molecular weight cut-off at 3,500 daltons.

- The dialysis bag then was tightly closed and immersed into suitable receiving medium with gentle stirring.
- The received medium was sampling periodically and the fresh medium was replaced.
- The amount of flavonoid released was measured spectroscopy using UV-vis spectrophotometer.

3.6 Cell culture

Human erythromyelogenous leukemic (K562) cells and their corresponding DOX-resistant cells (K562/ADR; a cell line that overexpresses P-gp) were used in this study.

- The cells were cultured in RPMI 1640 supplemented with 10% FBS, 100 U/ml of penicillin, and 0.1 mg/ml of streptomycin, and grown in a humidified atmosphere at 37°C in 5% CO_2.
- The trypan-blue dye exclusion method was used to evaluate cell viability.
- The cells were seeded at a density of 5×10^5 cells/ml and allowed to grow for 24 h in order to let them get into the exponential growth phase before starting the experiments.

3.7 Cytotoxicity

- Cancer cells were seeded into 24-well plates for mono-treatment.
- The media contained doxorubicin, daunorubicin, free interesting flavonoid, empty mPEG750-*b*-OCL-Bz micelles and interesting flavonoid-loaded mPEG750-*b*-OCL-Bz micelles was added.
- The cells were consecutively incubated for 72 h.
- To evaluate the inhibition of cell growth, the number of cell was counted using a flow cytometer (Coulter® Epics® XL™).
- The cell growth inhibition was calculated.

$$\%\ \text{Cell growth inhibition} = \frac{C_{c\text{-}72\ h} - C_{s\text{-}72\ h}}{C_{c\text{-}72\ h} - C_{c\text{-}0\ h}} \times 100\%$$

where $C_{c\text{-}72\ h}$ and $C_{c\text{-}0\ h}$ represent the number of viable cells in the control cells at 72 h and 0 h, respectively, and $C_{s\text{-}72\ h}$ represents the number of viable cells in the samples

at 72 h. The drug concentration that inhibits 50% of the cell growth (IC_{50}) was obtained from the dose-response curves of the percentages of cell growth inhibition versus drug concentration.

3.8 Co-treatment assay

The potential MDR-reversing action of free interesting flavonoid or interesting flavonoid-loaded micelles was investigated by the co-treatment assays using conventional chemotherapeutic drugs (doxorubicin or daunorubicin) in combination with free flavonoid or flavonoid-loaded micelles as P-gp modulators.

- The cells were incubated with medium containing both interesting flavonoid (in its free form or micellar formulation) and doxorubicin or daunorubicin
- The inhibition of cell growth was investigated after 72 h of incubation at 37°C.
- The number of cell was counted using a flow cytometer (Coulter® Epics® XL™)
- The efficacy (δ) of interesting flavonoid in increasing the cytotoxicity effect of the used chemotherapeutic drugs on MDR cells was calculated.

$$\text{MDR reversing } (\delta) \text{ value} = \frac{IC_{50}(RD) - IC_{50}(RM)}{IC_{50}(RD) - IC_{50}(SD)}$$

where IC_{50}(RD) is the 50% inhibitory drug concentration of MDR cell (K562/ADR) growth, IC_{50}(RM) is the 50% inhibitory drug concentration of MDR cell growth in the presence of QCT (in its free form or as micellar formulation) and IC_{50}(SD) is the 50% inhibitory drug concentration of drug-sensitive cell (K562) growth. δ = 0 when IC_{50}(RD) = IC_{50} (RM). This means that there is no effect of QCT; in the other words, QCT does not act as inhibitor of Pgp. δ = 1 when IC_{50}(RM) = IC_{50} (SD). This means that QCT fully inhibits P-gp.

3.9 Determination of kinetics of P-gp-mediated efflux of tetrahydropyranyl adriamycin (THP) modulated by free flavonoids and flavonoid-loaded micelles

The kinetics of the active efflux of P-gp-mediated THP in cells were studied based on quenching of the fluorescence of THP after its intercalation in DNA.

- A 1 cm quartz cuvette was filled with 2 ml of HEPES-Na^+ buffer solutions pH 7.25 with vigorous stirring at 37°C.

- The cancer cells were incubated in the HEPES-Na^+ buffer in the presence of 10 mM NaN_3 for 30 min.
- Then, 20 µl THP was added to the cell suspension.
- The fluorescence intensity of THP was recorded as a function of time (using excitation and emission wavelengths of 480 nm and 590 mm, respectively). When THP is taken up by cells and subsequently intercalates in DNA, its fluorescence is quenched (Fig 1). The kinetics of the quenching of the THP fluorescence is a measure for the rate of cellular uptake of THP.
- Then, free interesting flavonoids and interesting flavonoid-loaded micelles were added.
- Glucose was added.
- The rate of THP efflux was calculated from the slope of the tangent to the curve.
- The cell membranes were permeabilized by the addition of 0.01% Triton X-100.

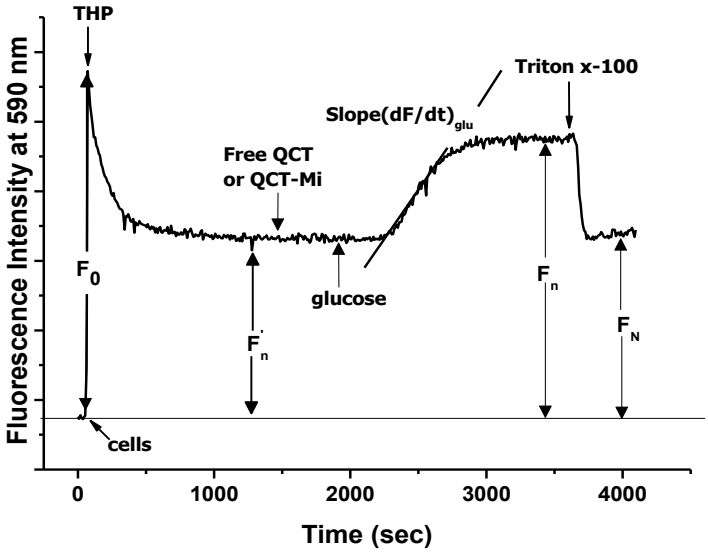

Fig. 3. Determination of the active kinetic efflux of THP mediated by P-gp in the presence of free interesting flavonoid, empty polymeric micelles or interesting flavonoid-loaded micelles.

3.10 Annexin V-FITC apoptosis assay

Annexin V-Fluorescein isothiocyanate (Annexin V-FITC) assay was performed for apoptosis detection.

- The cells were treated with QCT (in its free form or micellar formulation, at concentrations of 25 μM) and empty polymeric micelles.
- The cells were washed with PBS and subsequently fixed with 70% ethanol overnight.
- The cells were washed with PBS and subsequently added binding buffer.
- Then Annexin V-FITC and PI were added.
- The prepared cells were incubated at room temperature with light protection for 10 min.
- The fluorescence of the cells was determined immediately with a flow cytometer.
- The flow cytometer was set excitation at 488 nm and emission at 530 nm. PI and FITC fluorescence intensity were collected on FL2 and FL1, respectively.
- The apoptosis analyzed was done by Flowing Software.

3.11 ATP content assay

- K562/ADR cells were treated with with QCT (in its free form or micellar formulation, at concentrations of 25 μM) and empty polymeric micelles.
- The cells were washed twice with ice-cold PBS and solubilized into cell lysates
- The mixture was centrifuged (12000 × *g*) at 4 °C for 10 min.
- The supernatant was collected to quantify the ATP concentrations using a luciferin/luciferase assay kit. The ATP content was normalized to the protein content in each sample, as determined using a BCA kit.
- Blank medium was used as a control.

3.12 Assessment of mitochondrial membrane potential

Mitochondrial membrane potential ($\Delta\psi m$) was assessed by tetraethyl benzimidazolyl carbocyanine iodide (JC-1), according to the manufacturer's instructions.

- K562/ADR cells at a density of 1.5×10^4 cells/well were seeded into 96-well plates and incubated overnight.

- Next, the cells were washed once with buffer.
- These cells were then stained with 20 μM JC-1 for 10 min at 37°C in the dark and were washed twice with buffer.
- Subsequently, the cells were treated with QCT (in its free form or micellar formulation, at concentrations of 25 μM) and empty polymeric micelles for 15, 30 and 60 min.
- The treated cells were measured using a microplate reader at λ ex (475 nm)/λ em (590 nm) for red fluorescence or λ ex (475 nm)/λ em (530 nm) for green fluorescence.
- The obtained values were then expressed as JC-1 Red/Green fluorescent intensity (JC-1 R/G) ratio.

4. Results and Discussion

4.1 Formulations and characterizations

Table 1 reveals that the average particle size of flavonoid-loaded mPEG-b-OCL-Bz micelles was around 13-20 nm. There was no difference in the particle sizes between the different molecular structures of the loaded flavonoids. Besides, the zeta potential was range of -1.99 to -8.86 mV as shown in Table 2. The less negatively charge surfaces prevent clearance by mononuclear phagocytic cells [Levchenko et al., 2002]. Morphological investigation of flavonoid loaded polymeric micelles was observed by TEM. All flavonoid loaded polymeric micelles exhibited a regular spherical shape with the particle size around 14 nm (Fig. 4A-C). The particle size determined by TEM was similar to that determined by DLS and there was no significant difference in the particle size between the micelles loaded with the different flavonoids.

Table 1 Average particle sizes of quercetin (QCT), quercetrin (QTR) and rutin (RUT) incorporated mPEG-b-OCL-Bz micelles

Polymer: conpound ratio	QCT		QTR		RUT	
(w/w)	Z_{ave} (nm)	PDI	Z_{ave} (nm)	PDI	Z_{ave} (nm)	PDI
10:0	15.85±0.46	0.259±0.04	-	-	-	-
40:1	14.36±0.32	0.143±0.03	13.9±0.4	0.16±0.03	17.74±2.29	0.381±0.12
20:1	15.02±0.60	0.165±0.06	14.0±0.2	0.17±0.01	13.10±0.41	0.114±0.05
10:1	14.84±0.22	0.117±0.03	14.2±1.4	0.19±0.09	13.68±0.28	0.162±0.05
10:2	15.66±1.14	0.215±0.08	13.3±0.3	0.20±0.03	13.00±0.19	0.109±0.00
10:4	20.00±0.69	0.402±0.03	15.4±1.3	0.33±0.06	12.86±0.24	0.111±0.01

Table 2 Zeta potential of quercetin (QCT), quercetrin (QTR) and rutin (RUT) loaded mPEG-b-OCL-Bz micelles. The values are presented as mean±S.D. (n=3).

Flavonoid:Oligomer	Zeta (mV)		
(%)	QCT	QTR	RUT
0*	-1.99±2.17	-	-
2.5	-2.56±0.28	-3.89±0.48	-2.81±0.15
5	-2.26±0.12	-2.71±2.03	-2.31±0.62
10	-4.18±0.25	-4.51±1.15	-2.27±0.15
20	-6.28±0.40	-2.00±1.24	-6.05±0.98
40	-8.86±2.03	-2.25±0.14	-5.63±2.80

* = Empty micelles

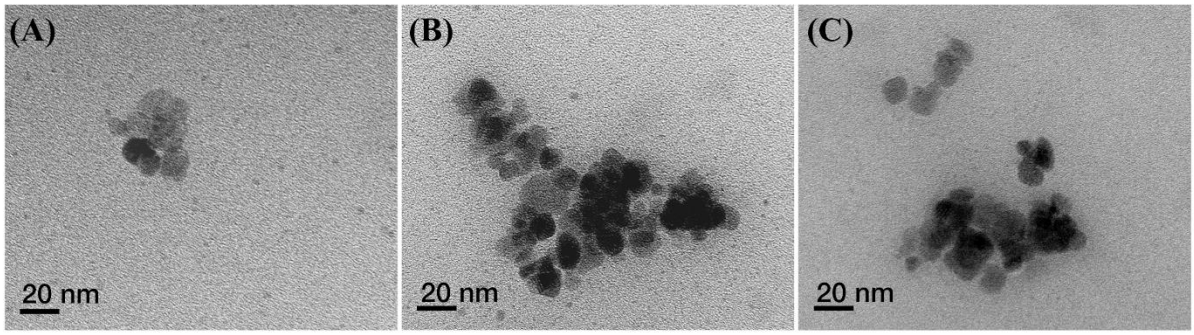

Fig. 4. TEM images of mPEG-b-OCL-Bz micelles loading with QCT (a), QTR (b), and RUT (c)

The loading efficiency values of the polymeric micelles loading quercetin with different sugar moieties are shown in Fig. 5 and Fig. 6. The y-axis shows the flavonoid entrapment efficiency (Fig. 5) and the loading capacity (Fig. 6), and the x-axis reveals the initial amounts of the flavonoid/polymer ratios used in the formulation. The loading efficiency of quercetin was about the same as that of the quercetin glycosides, at 10% of the flavonoid/polymer ratio. On a decrease in the flavonoid/polymer ratio, the entrapment efficiency of QCT was around the same as that of RUT but lower than that of QTR. On an increase in the flavonoid/polymer ratio, the incorporation efficiency of QCT was found to be higher than that of RUT but lower than that of QTR. Fig. 5 shows that the highest entrapment efficiency was found from QTR (91.1±1.1%), followed by QCT (73.1±5.0%) and RUT (71.7±1.9%). Fig. 6 presents, in line with the result illustrated in Fig. 5, that QTR had the maximum loading capacity, followed by RUT and QCT with LC values of 36.4±0.4%, 11.5±0.3% and 7.3±0.5%, respectively. Fig. 6 also demonstrates that the loading capacity of QTR increased when an increase in the QTR/polymer ratio was affected. However, a reduction in the loading capacity of QCT and RUT was observed at 40% of the flavonoid/polymer ratio. This characteristic is probably due to the limited capacity to incorporate flavonoids into the hydrophobic core of mPEG-b-OCL-Bz micelles. So, for that season, the optimal loading ratio of QCT and RUT was 30%, while QTR was 40%.

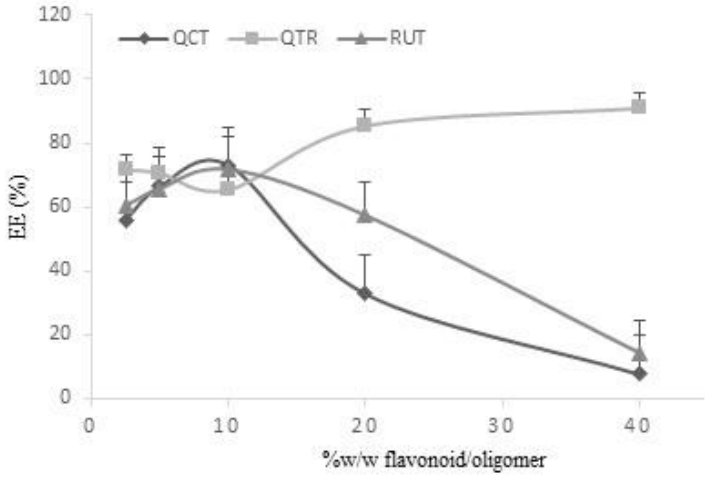

Fig. 5. The entrapment efficiency of quercetin (QCT), quercetrin (QTR) and rutin (RUT) incorporated mPEG-b-OCL-Bz micelles

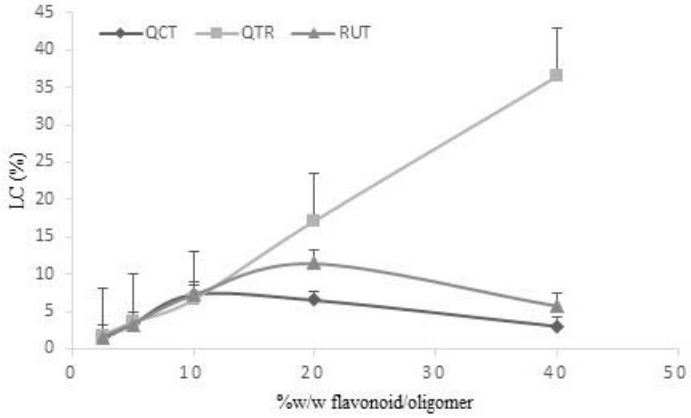

Fig. 6. The loading capacity of quercetin (QCT), quercetrin (QTR) and rutin (RUT) incorporated mPEG-b-OCL-Bz micelles

4.2. *In vitro* stability

Fig. 7 presents that all the studied flavonoid-incorporated polymeric micelles were stable for 14 days at 37°C in the absence of BSA. In contrast, the incorporation stability

was interestingly different between the loaded QCT and QCT glycosides in the presence of BSA. The contents of QTR and RUT remained constant during at least 4 days (Fig 8), which suggests that the QCT glycoside loaded mPEG-b-OCL-Bz micelles was stable and that the release of the QCT glycosides was not affected by the presence of BSA. On the other hand, QCT slowly leaked from the polymeric micelles. The QCT content was observed todecrease to 83% on the first day and to 76% on the fourth day of incubation.

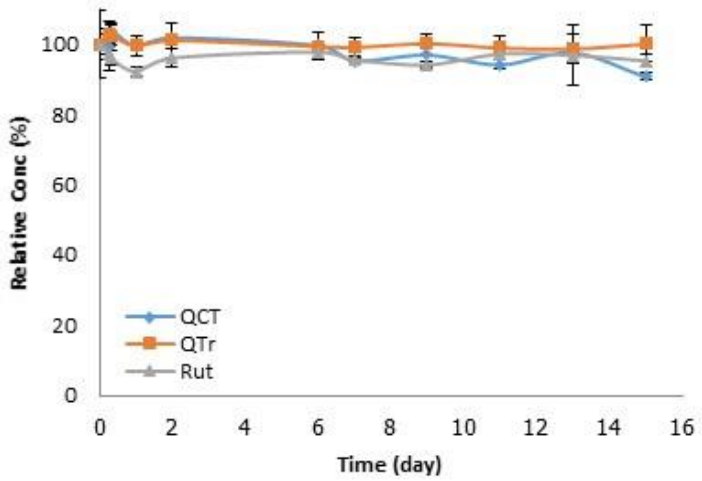

Fig. 7. The stability of quercetin (QCT), quercetrin (QTR) and rutin (RUT) incorporated mPEG-b-OCL-Bz micelles by incubation at 37°C in PBS in the absence of BSA

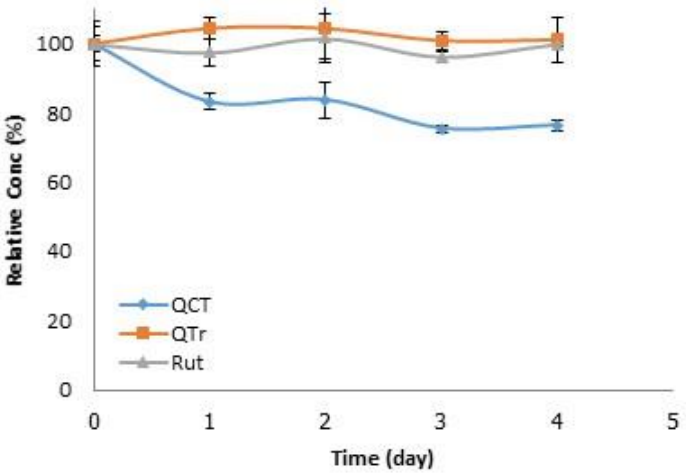

Fig. 8. The stability of quercetin (QCT), quercetrin (QTR) and rutin (RUT) incorporated mPEG-b-OCL-Bz micelles by incubation at 37°C in PBS in the presence of BSA

4.3 In vitro release

The *in vitro* release was analyzed to determine the release behavior of flavonoids (aglycone and glycoside of flavonoid) from polymeric micelles and to confirm the degree of the flavonoid-polymer interaction. In our previous studies, a method based on dialysis of a micellar dispersion against a Tween micellar was developed and this method was validated to maintain the sink condition. The destabilization of polymeric micelles like mPEG-b-p(HPMAm-Lac2) micelles, PEG-HPMA-Bz micelles and mPEG-b-OCL-Bz micelles is not affected by adding surfactants to the receiving medium, as determined by the DLS analysis [Khonkarn et al., 2011; Khonkarn et al., 2012]. Phosphate buffer (pH 7.4) with Tween 20 (0.2%) was then used in this study as the release medium of the aqueous insoluble compounds (QCT, QTR and RUT). It was found that approximately 30% of the loaded QTR and RUT was released within the first hour of the release study. This observed burst release was considered to be the relatively high water soluble of the glycosidic form of both QTR and RUT located in the region near the PEG outer shells. However, the burst release was not observed from QCT-loaded mPEG-b-OCL-Bz micelles. When the releasing time was 3 h, the amount of QCT, QTR and RUT released from mPEG-b-OCL-Bz micelles was approximately 21%, 51%, and 58%, respectively, and they were subsequently released to a maximum of approximately 80% in 24 h. In the releasing time between 15 min to 6 h, it was observed that the release rate of QCT was significantly slower than that of QTR and RUT approximately 21% and 26%, respectively ($p<0.05$). However, the amount of released QCT was not statistically significant difference from the amount of released QTR and RUT at releasing time of 8 h, 12 h and 24 h.

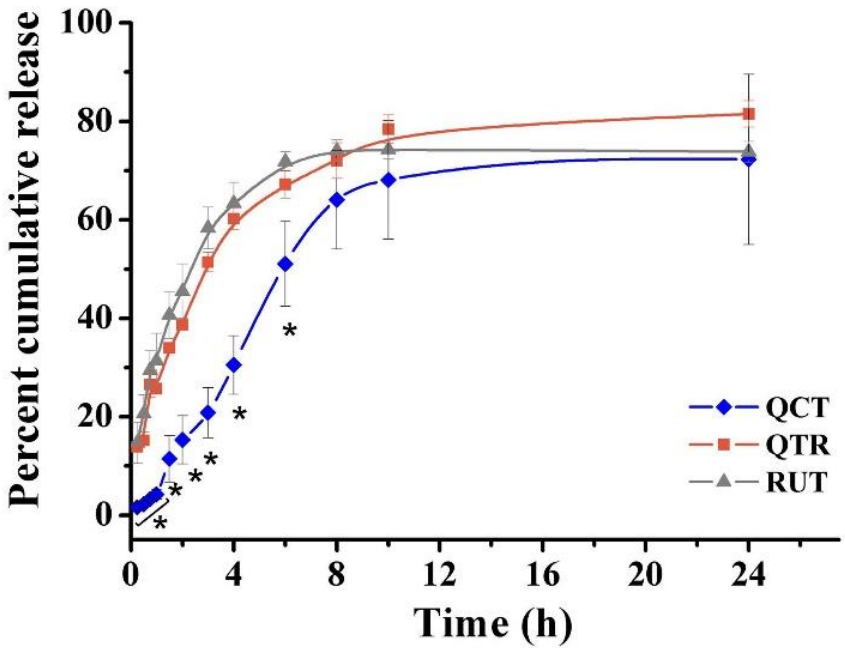

Fig. 9. The release study of of quercetin (QCT), quercetrin (QTR) and rutin (RUT) incorporated mPEG-b-OCL-Bz micelles

4.4. Cytotoxicity of anthracyclines, free QCT and QCT-loaded micelles

The cytotoxicity results of sensitive K562 and resistant K562/ADR cells treated with anthracycline anticancer drugs (DOX and DAU), free QCT, and QCT-loaded mPEG-b-OCL-Bz micelles are demonstrated by the concentrations of compound causing 50% of cell growth inhibition (IC_{50} values) and resistance factor (RF), as summarized in Table 3. DOX and DAU inhibited the growth of sensitive K562 cells, with IC_{50} values of 19.1±0.6 nM and 17.5±0.9 nM, respectively. In resistant K562/ADR cells, the IC_{50} values were higher than those for their sensitive cells, with the values of 678.4±137.2 nM for DOX and 387.5±75.2 nM for DAU. As expected, it was found that the cytotoxic effect of DOX and DAU in the resistant cells was less than their cytotoxic effect in the sensitive cells, with the resistant factor values of 35.5 and 22.1, respectively. These data demonstrate a decrease in the cytotoxic effect of the anthracyclines that were pumped out from the K562/ADR cells. This result, therefore, confirmed the P-gp phenotype of the K562/ADR cell line.

Even both QTR and RUT in its free form or micellar formulation had low cytotoxicity activity (IC_{50} values >100 μM). Free QCT and QCT-loaded micelles strongly exhibited anticancer properties against K562 and K562/ADR, with the IC_{50} values ranged from 6.95±2.58 μM to 14.98±4.00 μM. The RF values of free QCT (0.70± 0.23) and QCT-loaded micelles (0.78± 0.15) were a bit lower than 1, indicating similar cytotoxic efficacy in P-gp overexpressing cells and their corresponding sensitive cell lines. Similar to the finding of a previous study, quercetin was observed to exhibit cytotoxic effect on both human T lymphoblastoid leukemia MOLT-4/DNR and DNR-resistant cells [Ishii et al., 2010]. These results suggested that free QCT and QCT-loaded micelles might not be substrates of P-gp.

Table 3 IC_{50} values of various compounds against K562 and K562/ADR cells. The values are presented as mean±S.D. (n=3).

Compounds	**IC_{50} value (μM)**		**RF**
	K562	**K562/ADR**	
DOX	0.019±0.001	0.678±0.137	35.5
DAU	0.018±0.001	0.388±0.075	22.1
Free QCT	15.0±4.0	10.0±0.7	0.7
QCT-loaded mPEG-*b*-OCL-Bz micelles	8.7±1.6	7.0 ± 2.6	0.8
Empty mPEG-*b*-OCL-Bz micelles	ND	ND	-

Abbreviations: DOX, doxorubicin; DAU, daunorubicin; QCT, quercetin; mPEG-b-OCL-Bz, (poly[ethylene glycol]-b-oligo[e-caprolactone]) with benzoyl end groups; $IC_{50,}$ half maximal inhibitory concentration; RF, resistance factor; ND, Not detectable.

4.5 Co-treatment assay

The efficacy of free QCT or QCT-loaded micelles in reversing the MDR phenomenon and/or re-sensitizing the MDR cells to DOX or DAU was demonstrated in cell growth curves as indicated in Fig. 10 - Fig. 13 and the MDR-reversing values (δ) are

also summarized in Table 4. The cytotoxicity in K562/ADR of both DOX and DAU in combination with verapamil (2 μM), a well-known inhibitor of P-gp, was recovered by 93%. Free QCT (1-3 μM) had no effect in sensitizing K562/ADR cells to DOX (Fig. 10) or DAU (Fig. 11). Interestingly, QCT-loaded micelles clearly improved the cytotoxicity of both doxorubicin (Fig. 12) and daunorubicin (Fig. 13) when a similar series of experiments was carried out with drug-resistant K562/ADR cell lines in a dose-dependent manner. From this finding, it can be suggested that QCT-loaded micelles can efficiently increase the cytotoxicity of DOX (δ ranged from 0.39 ± 0.19 to 0.71 ± 0.15) and DAU (δ ranged from 0.29 ± 0.21 to 0.74 ± 0.20). This results show that P-gp pump was inhibited by QCT-loaded micelles around 30-40% at QCT concentration of 1 μM and around 70% at QCT concentration of 3 μM. Interestingly, empty mPEG750-b-OCL-Bz micelles (concentrations of 10-30 μg/mL) also exhibited MDR-reversing effect to DOX with δ values ranged from 0.11±0.04 to 0.18±0.05, resulting in maximum P-gp inhibiting effect of 18% at empty micelles concentration of 30 μg/mL.

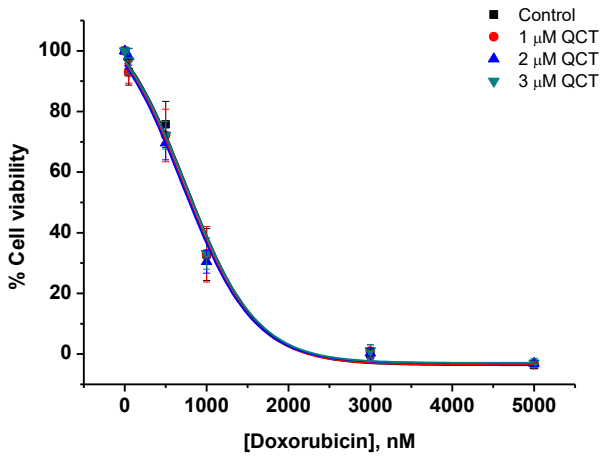

Fig. 10. The P-gp reversing effect of free QCT with various concentrations of DOX against K562/ADR. The cell viability assay was conducted by counting the cell numbers using a flow cytometer after 72 h of incubation.

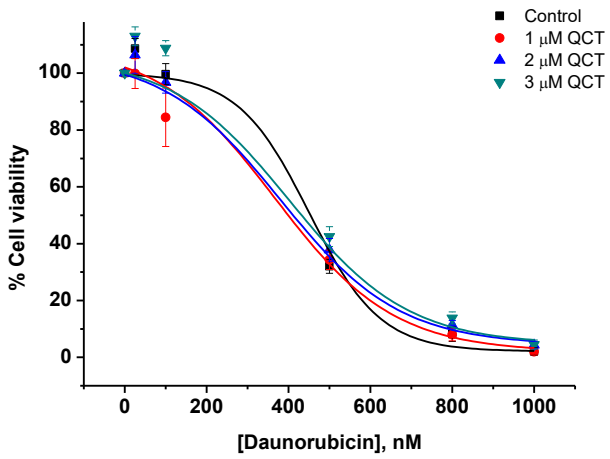

Fig. 11. The P-gp reversing effect of free QCT with various concentrations of DAU against K562/ADR. The cell viability assay was conducted by counting the cell numbers using a flow cytometer after 72 h of incubation.

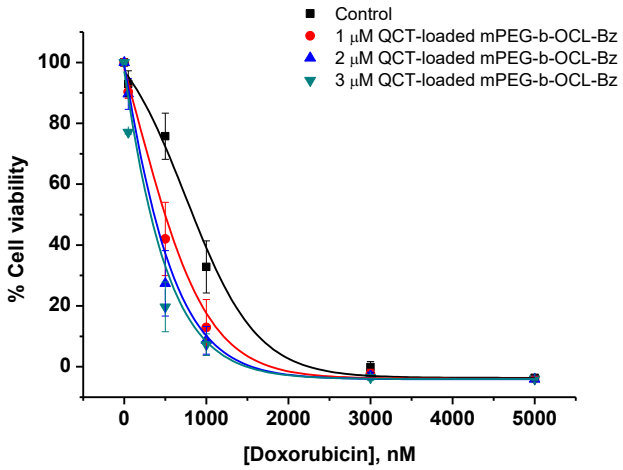

Fig. 12. The P-gp reversing effect of QCT-loaded mPEG-*b*-OCL-Bz micelles with various concentrations of DOX against K562/ADR. The cell viability assay was conducted by counting the cell numbers using a flow cytometer after 72 h of incubation.

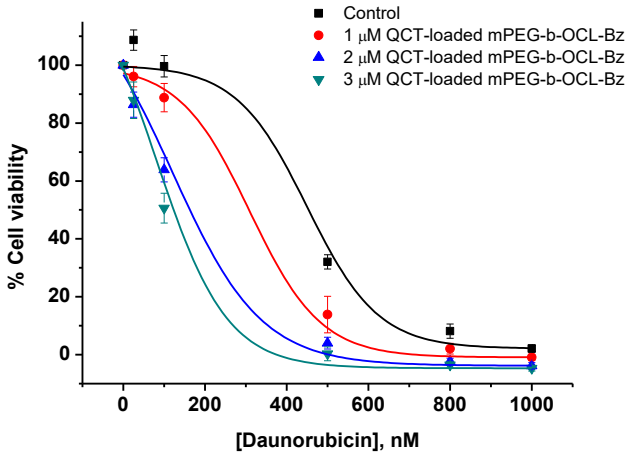

Fig. 13. The P-gp reversing effect of QCT-loaded mPEG-*b*-OCL-Bz micelles with various concentrations of DAU against K562/ADR. The cell viability assay was conducted by counting the cell numbers using a flow cytometer after 72 h of incubation.

Table 4 The MDR-reversing efficacy of QCT-loaded mPEG-*b*-OCL-Bz micelles in increasing cytotoxicity effect of DOX and DAU on P-gp expressing K562 (K562/ADR) cells. The values are presented as mean±S.D. (n=3).

Test Compound	MDR reversing efficacy (δ)	
	DOX	DAU
1 μM QCT loaded mPEG-*b*-OCL-Bz micelles	0.39±0.19	0.29±0.21
2 μM QCT loaded mPEG-*b*-OCL-Bz micelles	0.54±0.05	0.63±0.19
3 μM QCT loaded mPEG-*b*-OCL-Bz micelles	0.71±0.15	0.74±0.20
10 μg/mL mPEG-*b*-OCL-Bz micelles	0.11±0.04	ND
20 μg/mL mPEG-*b*-OCL-Bz micelles	0.13±0.06	ND
30 μg/mL mPEG-*b*-OCL-Bz micelles	0.18±0.05	ND
2 μM VER	0.93±0.03	0.93±0.07

* Not determine

4.6 Determination of kinetics of P-gp-mediated efflux of THP modulated by free QCT and QCT-loaded micelles

In order to understand the direct interaction of QCT-loaded micelle with P-gp, the spectrofluorometric method was used to study the P-gp -mediated efflux. THP is a good substrate of P-gp with fluorescence property. It is therefore suitable to use as a molecular probe to measure P-gp function [Laochariyakul et al., 2003]. The results are presented in Fig. 14-17. The typical kinetic uptake of THP in K562/ADR cell lines in the presence of VER, well known P-gp inhibitor, was shown in Fig. 14. The quenching of THP fluorescence intensity referred to the accumulation of THP within the cells. The THP accumulation was low because of the function of P-gp pump. The fluorescent intensity of THP was continued decreased when VER was added. This result presents the pattern of P-gp inhibition by P-gp inhibitor. The low THP quenching was observed after adding free quercetin (Fig. 15). Whereas, QCT loaded polymeric micelles revealed the high THP quenching (Fig. 16). This results indicated that QCT loaded polymeric micelles had much stronger P-gp inhibition than free QCT. Interestingly, empty polymeric micelles also had inhibition effect on P-gp function (Fig. 17).

The ability of P-gp inhibitor to inhibit the P-gp function was present in the ratio of $C_{n(i)}/C_N$ as shown in Fig. 18-19. The efficacy of VER to inhibit the P-gp function increased as a function of concentration (Fig. 18). Interestingly, the ratio of $C_{n(i)}/C_N$ of QCT-loaded micelles and empty polymeric micelle continuously increased in dose dependent manner (Fig. 19). However, it was found that the ratio of $C_{n(i)}/C_N$ of free QCT did not changed in dose dependent manner. Taken together, QCT loaded polymeric micelles had excellent ability to inhibit the function of P-gp.

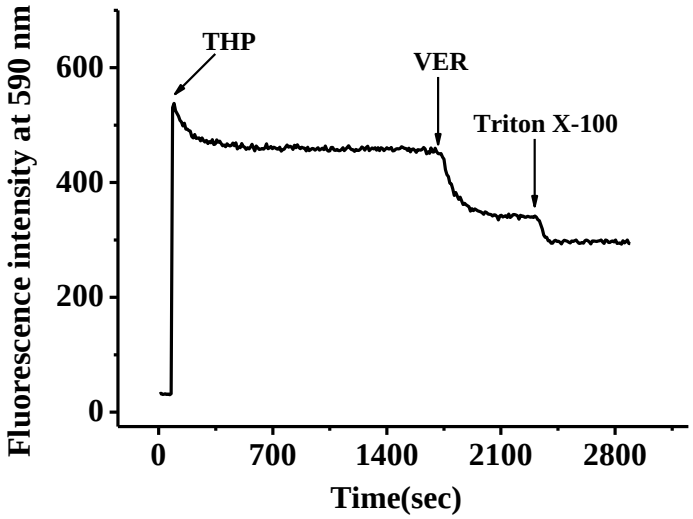

Fig. 14. Typical kinetic uptake of pirarubicin (THP) in K562/ADR in the presence of 2.5 μM verapamil (VER)

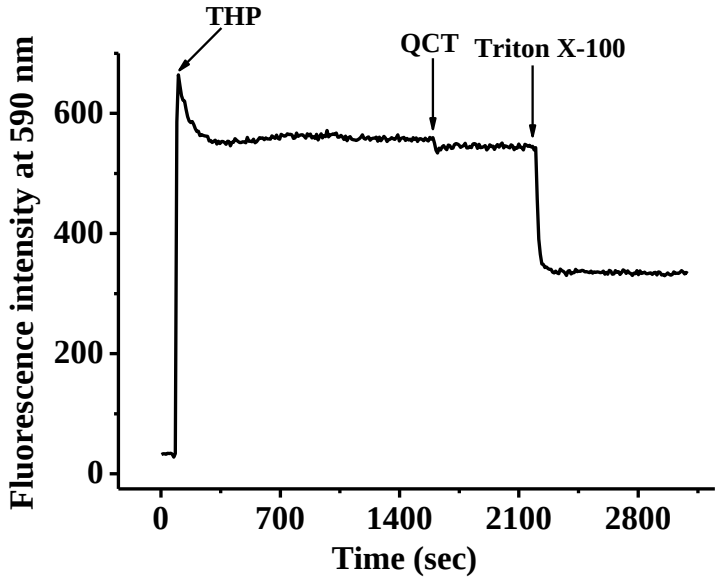

Fig. 15. Typical kinetic uptake of pirarubicin (THP) in K562/ADR in the presence of 2.5 μM free quercetin (QCT)

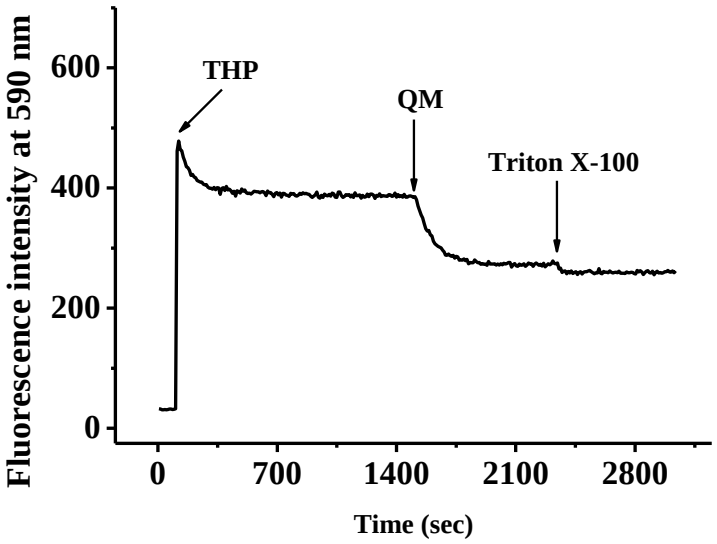

Fig. 16. Typical kinetic uptake of pirarubicin (THP) in K562/ADR in the presence of 2.5 μM quercetin-loaded micelles (QM)

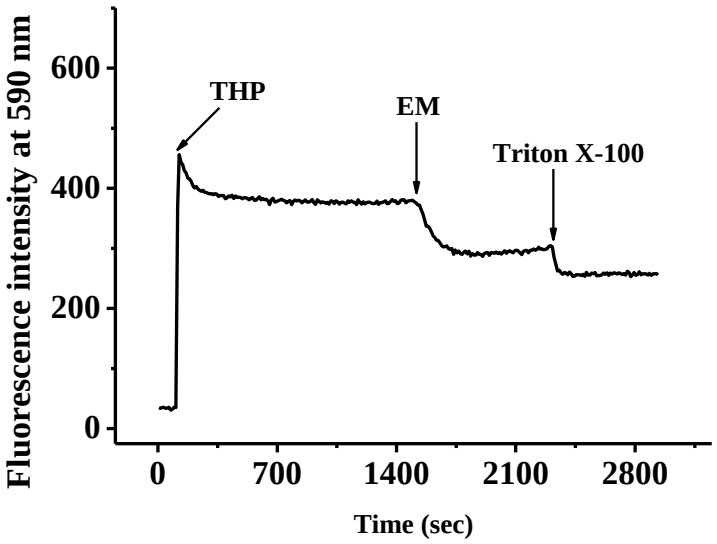

Fig. 17. Typical kinetic uptake of pirarubicin (THP) in K562/ADR in the presence of 2.5 μM micelles (EM)

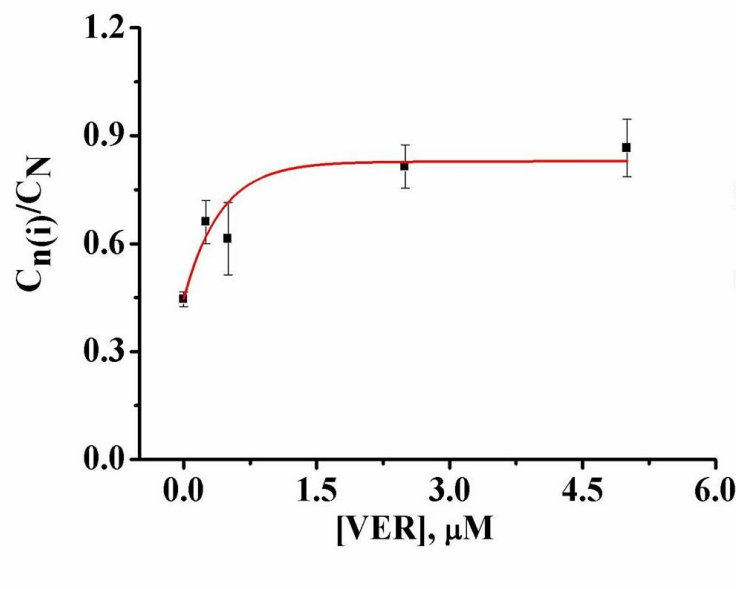

Fig. 18. The effect of verapamil on the drug accumulation in K562/ADR. The values of $Cn(i)/C_N$ are plotted as a function of the concentration of molecules. Each value represents mean±S.D.

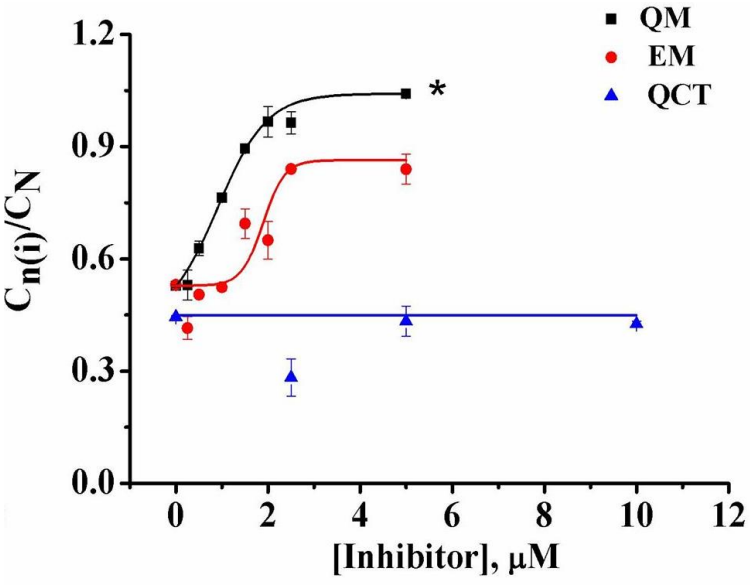

Fig. 19. The effect of free quercetin (free QCT), quercetin-loaded micelles (QM) and micelles (EM) on the drug accumulation in K562/ADR. The values of $Cn(i)/C_N$ are plotted as a function of the concentration of molecules. Each value represents mean±S.D.

4.7 Annexin V-FITC apoptosis assay

The apoptotic cell death induced by QCT (in its free form or micellar formulation) and empty polymeric micelles was not clearly found by Annexin V-FITC-PI assay

4.8 ATP content assay

The effect of QCT (in its free form or micellar formulation) and empty polymeric micelles on ATP content of K562/ADR cells was not clearly observed.

4.9 Assessment of mitochondrial membrane potential

JC-1 was used to evaluate mitochondrial membrane potential. JC-1 yields red fluorescence at high mitochondrial membrane potential while JC-1 yields green fluorescence at low mitochondrial membrane potential. A decrease in the JC-1 R/G ratio is indicative of mitochondrial depolarization (non-functional mitochondria). The JC-1 R/G ratio in K562/ADR cells treated with empty polymeric micelles was not significantly different from cell control (p<0.05). Whereas, The JC-1 R/G ratio in resistant cells treated with free QCT for 15 min, decreased to 36% of cell control. This decreasing did not change in time dependent manner as shown in Fig. 20. Moreover, the deceasing of JC-1 R/G ratio in resistant cells treated with QCT loaded polymeric micelles (decreased to 30% of the cell control) was not significantly different from free QCT, suggesting that QCT (in its free form and micellar formation) had an effect on mitochondrial membrane potential.

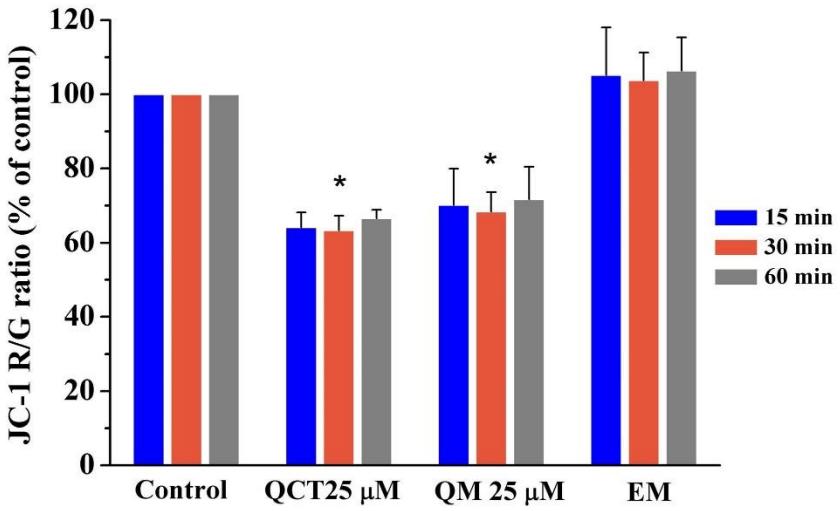

Fig. 20. The effect of quercetin (QCT), quercetin-loaded polymeric micelles (QM) and empty polymeric micelles (EM) on mitochondrial membrane potential of K562/ADR cells.

5. Discussion

Quercetin glycosides incorporated mPEG-b-OCL-Bz micelles were successfully prepared using film hydration method, with the particle size around 13-18 nm. The sugar moieties of quercetin did not show any effect on the particle size of flavonoid-loaded mPEG-b-OCL-Bz micelles, but a different in the loading efficiency was found. Many recently studies reported that compatibility optimization between the micellar hydrophobic segment and the incorporated drug improved the drug-loading efficiency and its retention, resulting in a long circulation time in the biological system [Liu et al., 2004; Yamamoto et al., 2007]. The hydrophobic interaction between the hydrophobic moieties of polymer and the entrapped hydrophobic drugs was successful in improving the efficiency of loading drug into polymeric micelles [Yokoyama et al., 2004]. However, the results from this study demonstrated that the loading content of QTR loaded into the mPEG-b-OCL-Bz micelles was significantly higher than that of both QCT and RUT. This may be due to the optimum affinity between the aglycone (non-polar) and the glycone (polar) groups of QTR and the amphiphilic molecules of the mPEG-b-OCL-Bz oligomers. QTR is a molecules that is more hydrophilic than QCT but more hydrophobic than RUT. These results

present that the efficiency of incorporation of flavonoids into polymeric micelles was influenced by the balance between the hydrophobicity and the hydrophilicity.

Long circulation of the incorporated drugs in the bloodstream is a necessary condition for the passive targeting property of polymeric micelles based on the EPR effect. To provide a long circulation time, protection of the loaded component from the interaction with the serum protein by a potential hydrophilic shield is also a prerequisite so that the clearance at the reticulo-endothelial system can be avoided. Moreover, the drug release from the polymeric micelles may be accelerated by the blood components [Opanasopit et al., 2005]. In this study, the stability as regards flavonoid incorporation was therefore observed by the incubation of flavonoid-loaded polymeric micelles with or without BSA at 37°C. It was discovered that both the QCT glycosides-loaded polymeric micelles were stable under condition of 37°C in PBS with or without BSA. It has been reported that there was neither BSA adsorption nor destabilization of mPEG-b-OCL-Bz micelles and that paclitaxel (at 5% w/w loading) was not extracted from this micellar core by BSA [16]. Even quercetin-incorporated micelles were stable at 37°C in the absence of BSA, but there was some leaking quercetin (less than 25%) at 37°C in the presence of BSA. This result demonstrates that the presented serum protein extracted QCT from the micelle core which was probably due to the higher protein affinity of QCT.

On the other hand, the release study by a dialysis bag using 0.2% Tween in PBS as the received medium revealed that QCT had a better interaction in the mPEG-b-OCL-Bz micelles. The difference in the release rate between aglycone and the glycosides of the flavonoids contributed to the degree of interaction between the flavonoids and the mPEG-b-OCL-Bz polymer. The interaction between the drug and the micellar core effected the drug release. The π-π interaction between QCT (aglycone) and the micellar core of mPEG-b-OCL-Bz micelles was stronger than that of QCT glycosides. The less π-π interaction, which was found from the QCT glycosides, was probably due to steric factor of the sugar moieties of the QCT glycosides. Besides, the released quercetin glycosides were easier driven to the receiving medium than its aglycone by Tween as the assistance in solubilization, based on the amphiphilic characteristic of the QCT glycosides and considering the “like dissolves like” theory, thus leding to the higher release rate. In contrast with the release result, the QCT glycosides-loaded polymeric micelles

presented higher loading content and stability as regards incorporation in the presence of the protein serum than in the presence of quercetin. The QCT glucosides had better compatibility with the mPEG-b-OCL-Bz micelles. It is not only the π-π interaction of the micellar core that affects the loading efficiency, the incorporation stability and the drug release rate. Other factors such as the hydrophobicity-hydrophobicity balance, the hydrogen bonding, and the steric factor of the polymeric micelles can contribute to these micellar characteristics.

Chemotherapy is the most frequently used approach in the treatment of cancer. Unfortunately, multidrug resistance (MDR) leads to the limitation in the success of cancer chemotherapy. The most common established mechanism of MDR is overexpression of ATP Binding-Cassette ((ABC) membrane. These membrane transporters pump anticancer drugs out of the cells by ATP consumption; therefore, only a small proportion of the administered drug reaches its intended target sites, leading to therapeutic failure. One of the main investigated efflux pump is P-gp, a 170 k-Da transport protein, which is known to limit the distribution of a broad spectrum of drugs. Strategies to overcome the P-gp protein have been extensively studied, including silencing MDR-related miRNAs, combinative drug strategy, applying monoclonal antibodies against P-gp and designing novel agents that are not recognized as P-gp substrate. Among these strategies, reversing drug resistance by inhibition of the drug efflux of P-gp, including the use of MDR chemosensitizers, is a major challenge to overcome MDR in cancer treatment. Moreover, nano drug delivery system is one of the novel strategies in the approach to fight MDR.

Natural substances could be potent anticancer agent or MDR transporter inhibitors with less cytotoxicity (Kuete et al., 2014; Michalak & Wesolowska, 2012.). The cytotoxicity results of this study present that free QCT and QCT-loaded micelles had stronger anticancer activity toward both sensitive and resistant leukemia cells than QTR and RUT (in its free form and micellar formations). Furthermore, similar efficacies in drug-resistant phenotypes and their corresponding sensitive cells (the low degree of the resistant factor) of both free QCT and QCT-loaded micelles, was observed. This result suggests that free QCT and QCT-loaded micelles were not transported by P-gp. Moreover, the result also showed that free QCT (at concentration of 1-3 μM) had no MDR-reversing effect to DOX or DAU. This result is in agreement with Choiprasert et al. [2010] who reported that MDR-reversing effect of QCT and QCT glycosides

to DAU of K562/ADR and GLC4/ADR cells, was not observed. Interestingly, empty mPEG-b-OCL-Bz micelles had MDR-reversing effect. A stronger MDR-reversing effect to both DOX and DAU of K562/ADR cells was observed from QCT-loaded micelles (at QCT concentration of 1-3 μM) with maximum MDR-reversing values around 70%.

In order to study the mode of action by which QCT-loaded micelles increased the efficacy of DOX or DAU in P-gp overexpressing cells, the modulation of QCT-loaded micelles in the kinetics of P-gp-mediated pumping and mitochondrial membrane potential were investigated. For the assessment of kinetics of P-gp-mediated pumping, the THP was studied as a model anticancer drug because its pKa is relatively low and it can move into the cells very rapidly [Mankhetkorn et al., 1996; Reungpatthanaphong & Mankhetkorn, 2002] In the present study, the efflux of THP by P-gp was slightly inhibited by free QCT. Moreover, QCT loaded micelles increased the inhibition of P-gp efflux of THP in dose-dependent manner. Interestingly, empty polymeric micelles also had ability to inhibit P-gp function. This finding reveals that empty mPEG750-b-OCL-Bz micelles could enhance the MDR reversal effects of the QCT loaded mPEG750-b-OCL-Bz micelles by inhibition of P-gp efflux. Polymeric micelles are amphiphilic molecules which may lead to membrane fluidization and enhance permeability of cell membrane, resulting in P-gp interfering [Agarwal et al., 2009]. It has been reported that drug resistance was altered by poly(ethylene oxide)–poly- (propylene oxide) copolymers (pluronic®) or poly(ethylene glycol)-poly(lactic acid) copolymers using several mechanisms such as affecting the membrane microviscosity, decreasing the P-gp ATPase activity, loss of the mitochondrial membrane potential, and a subsequent decrease in the ATP levels [Batrakova et al., 2000; Batrakova et al., 2001]. Moreover, cellular drug accumulation was enhanced using nanocrystals and nanotubes through bypassing P-gp via endocytosis [Li et al., 2010; Liu et al., 2010].

QCT has been recently recognized for use as an anticancer agent alone or in combination therapy with conventional chemotherapeutic drugs. QCT was found to cause DNA fragmentation, cell cycle arrest and apoptosis through the mitochondrial partway [Chou et al., 2010; Granado-Serrano et al., 2006]. It has been reported that QCT was an effective inhibitor towards P-gp by directly interaction with transporter protein [Limtrakul et al., 2005]. Whereas, the less efficient inhibitor of P-gp by QCT glycosides was observed which might result from the steric effect of their sugar moieties [Kitagawa et al., 2005]. In this study, the mitochondrial

membrane potential was altered by both QCT and QCT loaded micelles. The main mechanism of MDR proteins pumping the chemical agents uses the energy of ATP. Mitochondria play key roles in the energy production. Mitochondrial dysfunction has been shown to participate in the induction of apoptosis. Opening of the mitochondrial permeability transition pore induces depolarization of mitochondrial membrane potential, inhibition of ATP synthesis, release of apoptogenic factors and subsequent cell death [Vayssi`ere et al., 1994; Bernardi, 1996]. The mitochondria targeting of MDR cancer cells and trigger cell apoptosis is one of the mechanisms to overcome MDR. Taken together, the potential mechanisms of reversing multidrug resistant of K562/ADR cells by QCT loaded polymeric micelles might be the combination effects of polymeric micelles and QCT, interfering with P-gp function and mitochondrial membrane potential, respectively.

6. Conclusion

The results in this study exhibit that the potential anticancer flavonoids, QCT, QTR, and RUT, were successfully incorporated into mPEG-b-OCL-Bz micelles. The particle size of the flavonoid loaded mPEG-b-OCL-Bz micelles was not affected by the chemical structure of flavonoids. However, the chemical structure of flavonoids plays important roles on incorporation efficiency, and release behavior of the micelles. The study demonstrates that free QCT and QCT-loaded micelles are not the substrates of P-gp. Moreover, the QCT-loaded micelles possess potential MDR reversing action to the conventional chemotherapeutic drugs (DOX or DAU). It was found that empty polymeric micelles had ability to inhibit P-gp function. A higher inhibition of P-gp efflux of THP was found from QCT loaded micelles. On the other hand, the mitochondrial membrane potential was altered by both QCT and QCT loaded micelles. The combination effects of polymeric micelles, by interfering P-gp function, and QCT, by altering mitochondrial membrane potential, might be the potential mechanisms of reversing multidrug resistant of K562/ADR cells by QCT loaded polymeric micelles. Finally, it can be concluded that mPEG750-b-OCL-Bz micelles are a promising carrier system of flavonoids for enhancing MDR reversal effects.

7. References

Abdallah HM, Al-Abd AM, El-Dine RS, El-Halawany AM. 2015. P-glycoprotein inhibitors of natural origin as potential tumor chemo-sensitizers: A review. l Adv Res, 6, 45-62.

Agarwal A, Lariya N, Saraogi G, Dubey N, Agrawal H, Agrawal GP. 2009. Nanoparticles as novel carrier for brain delivery: a review. Current Pharmaceutical Design. 15(8), 917–25.

Ahmad I, Krishnamurthi K, Arif JM, Ashquin M, Mahmood N, Athar M, Rahman Q. 1995. Augmentation of chrysotile-induced oxidative stress by BHA in mice lungs. Food and Chemical Toxicology, 33 (3), 209-215.

Batrakova EV, Li S, Alakhov VY, Kabanov AV. 2000. Selective energy depletion and sensitization of multiple drug resistant cancer cells by Pluronic block copolymers. Polym Prepr. 41, 1639–40.

Batrakova EV, Li S, Vinogradov SV, Alakhov VY, Miller DW, Kabanov AV. 2001. Mechanism of pluronic effect on P-glycoprotein efflux system in blood-brain barrier: contributions of energy depletion and membrane fluidization. J Pharmacol Exp Ther, 299 (2), 483-493.

Bernardi P. The permeability transition pore. 1996. Control points of a cyclosporin A-sensitive mitochondrial channel involved in cell death. Biochim Biophys Acta. 1275, 5-9.

Biswas S, Kumari P, Lakhani PM, Ghosh B. 2016. Recent advances in polymeric micelles for anti-cancer drug delivery. Eur. J. Pharm. Sci., 83, 184-202.

Broxterman HJ, Gotink KJ, Verheul HMW. 2009. Understanding the causes of multidrug resistance in cancer: a comparison of doxorubicin and sunitinib. Drug Resist Update, 12, 114-126.

Cabral H, Matsumoto Y, Mizuno K, Chen Q, Murakami M, Kimura M, Terada Y, Kano M, Miyazono K, Uesaka M. 2011. Accumulation of sub-100 nm polymeric micelles in poorly permeable tumours depends on size. Nature Nanotechnology, 6, 815-823.

Cabral H, Kataoka K. 2014. Progress of drug-loaded polymeric micelles into clinical studies. Journal of Controlled Release, 190, 465-476.

Carstens MG, Bevernage JJL, Nostrum CF, Steenbergen MJ, Flesch FM, Verrijk R, Leede LGJ, Crommelin DJA, Hennink WE. 2007a. Small oligomeric micelles based on end group

modified mPEG- oligocaprolactone with monodisperse hydrophobic blocks. Macromolecules, 40, 116–122.

Carstens MG, Nostrum CF, Verrijk R, Leede LGJ, Crommelin DJA, Hennink WE. 2007b. A mechanistic study on the chemical and enzymatic degradation of PEG- oligo(e-caprolactone) micelles. J Pharm Sci, 97, 506–518.

Carstens MG, Jong PHJLF, Nostrum CF, Kemmink J, Verrijk R, Leede LGJ, Crommelin DJA, Hennink WE. 2008. The effect of core composition in biodegradable oligomeric micelles as taxane formulations. Eur J Pharm Biopharm, 68, 596–606.

Chen W, Zhong P, Meng F, Cheng R, Deng C, Feijen J, Zhong Z. 2013. Redox and pH-responsive degradable micelles for dually activated intracellular anticancer drug release. Journal of Controlled Release, 169, 171-179.

Choiprasert W, Dechsupa N, Kothan S, Garrigos M, Mankhetkorn S. 2010. Quercetin, Quercetrin Except Rutin Potentially Increased Pirarubicin Cytotoxicity by Non Competitively Inhibiting the P-Glycoprotein-and MRP1 Function in Living K562/ adr and GLC4/ adr Cells. American Journal of Pharmacology and Toxicology, 5 (1), 24-33.

Chou CC, Yang JS, Lu HF, Ip SW, Lo C, Wu CC, Lin JP, Tang NY, Chung JG, Chou MJ, Teng YH, Chen DR. 2010. Quercetin-mediated cell cycle arrest and apoptosis involving activation of a caspase cascade through the mitochondrial pathway in human breast cancer MCF-7 cells. Arch Pharm Res. 33, 1181-91.

Clerkin JS, Naughton R, Quiney C, Cotter TG. 2008. Mechanisms of ROS modulated cell survival during carcinogenesis. Cancer Lett, 266, 30-36.

Cuong NV, Li YL, Hsieh MF. 2012. Targeted delivery of doxorubicin to human breast cancers by folate-decorated star-shaped PEG–PCL micelle. J Mater Chem, 22, 1006–1020.

Deng C, Jiang Y, Cheng R, Meng F, Zhong Z. 2012. Biodegradable polymeric micelles for targeted and controlled anticancer drug delivery: promises, progress and prospects. Nano Today, 7, 467-480.

Du G, Li M, Ma F, Liang D. 2009. Antioxidant capacity and the relationship with polyphenol and vitamin C in Actinidia fruits. Food Chem, 113, 557-562.

Feng SL, Yuan ZW, Yao XJ, Ma WZ, Liu L, Liu ZQ, Xie Y. 2016. Tangeretin, a citrus pentamethoxyflavone, antagonizes ABCB1- mediated multidrug resistance by inhibiting its transport function. Pharmacol Res, 110,193-204.

Geney R, Ungureanu IM, Li D, Ojima I. 2002. Overcoming multidrug resistance intaxane chemotherapy, Clin Chem Lab Med, 40 (9), 918–925.

Gianni L. 1997. Anthracycline resistance: the problem and its current definition. Semin Oncol, 24 (4 Su), S10-11-S10-17.

Granado-Serrano AB, Martin MA, Bravo L, Goya L, Ramos S. 2006. Quercetin induces apoptosis via caspase activation, regulation of Bcl-2, and inhibition of PI-3-kinase/Akt and ERK pathways in a human hepatoma cell line (HepG2). J Nutr. 136(11), 2715–21.

Hejazi R, Amiji M. 2003. Chitosan-based gastrointestinal delivery systems. J Control Rel, 89 (2), 151-165.

Huang K, Ma H, Liu J, Huo S, Kumar A, Wei T, Zhang X, Jin S, Gan Y, Wang PC. 2012. Size-dependent localization and penetration of ultrasmall gold nanoparticles in cancer cells, multicellular spheroids, and tumors in vivo. ACS Nano, 6, 4483-4493.

Ishii K., Tanaka S., Kagami K., Henmi K., Toyoda H., Kaise T., Hirano T. 2010. Effects of naturally occurring polymethyoxyflavonoids on cell growth, p-glycoprotein function, cell cycle, and apoptosis of daunorubicin-resistant T lymphoblas-toid leukemia cells, Cancer Invest 28, 220–229.

Jacob JK, Hakimuddin F, Paliyath G, Fisher H. 2008. Antioxidant and antiproliferative activity of polyphenols in novel high-polyphenol grape lines. Food Research International, 41 (4), 419-428.

Jin X, Zhou B, Xue L, San W. 2015. Soluplus® micelles as a potential drug delivery system for reversal of resistant tumor. Biomed Pharmacother, 69, 388–395.

Kabanov AV, Batrakova EV, Alakhov VY. 2002. Pluronic block copolymers for over-coming drug resistance in cancer. Adv Drug Deliv Rev, 54, 759-779.

Kaplan O, Navon G, Lyon RC, Faustino PJ, Straka EJ, Cohen JS. 1990. Effects of 2-deoxyglycose on drug-sensitive and drug-resistant human breast cancer cells: Toxicity and magnetic resonance spectroscopy studies of metabolism. Cancer Res, 50, 544–551.

Kathawala RJ, Gupta P, Ashby CR, Chen ZS. 2015. The modulation of ABC transporter-mediated multidrug resistance in cancer: a review of the past decade. Drug Resist Updat, 18, 1-17.

Khonkarn K, Mankhetkorn S, Hennink WE, Okonogi S. 2011. PEG-OCL micelles for quercetin solubilization and inhibition of cancer cell growth. Eur J Pharm Biopharm, 79, 268-75.

Khonkarn R, Samlee M, Talelli M, Hennink W E, Okonogi S. 2012. Cytostatic effect ofxanthone-loaded mPEG-b-p(HPMAm-Lac_2) micelles towards doxoruribin sensitive and resistant cancer cells. Colloids and Surfaces B: Biointerfaces. 94, 266-273.

Kitagawa S, Nabekura T, Takahashi T, Nakamura Y, Sakamoto H, Tano H, Hirai M, Tsukahara G. 2005. Structure–activity relationships of the inhibitory effects of flavonoids on P-glycoprotein mediated transport in KB-C2 cells. Biol Pharm Bull. 28, 2274-8.

Kuete V, Nkuete AH, Mbaveng AT, Wiench B, Wabo HK, Tane P, Efferth T. 2014. Cytotoxicity and modes of action of 4□-hydroxy-2□, 6□-dimethoxychalcone and other flavonoids toward drug-sensitive and multidrug-resistant cancer cell lines. Phytomedicine, 21, 1651-1657.

Lambert G, Fattal E, Couvreur P. 2001. Nanoparticulate systems for the delivery of antisense oligonucleotides. Adv Drug Deliver Rev, 47(1), 99-112.

Laochariyakul P, Ponglikitmongkol M, Mankhetkorn S. 2003. Functional study of intracellular P-gp- and MRP1-mediated pumping of free cytosolic pirarubicin into acidic organelles in intrinsic resistant SiHa cells. Can J Physiol Pharmacol. 81, 790-9.

Levchenko TS, Rammohan R, Lukyanov AN, Whiteman KR, Torchilin VP. 2002. Liposome clearance in mice: the effect of a separate and combined presence of surface charge and polymer coating. Int J Pharm. 240, 95-102.

Li W, Zhang H, Assaraf YG, Zhao K, Xu X, Xie J, Yang D-H, Chen Z-S. 2016. Overcoming ABC transporter-mediated multidrug resistance: Molecular mechanisms and novel therapeutic drug strategies. Drug Resist Updates, 27, 14–29.

Li R, Zou H, Xiao H, Wu R. 2010. Carbon nanotubes as intracellular carriers for multidrug resistant cells studied by capillary electrophoresis- laser- induced fluorescence. Methods Mol Biol, 625, 153-168.

Liang Y, Deng X, LZhang L, Peng X, Gao W, Cao J, Gu Z, He B. 2015. Terminal modification of polymeric micelles with p- conjugated moieties for efficient anticancer drug delivery. Biomaterials, 71, 1-10.

Liu Y, Huang L, Liu F. 2010. Paclitaxel nanocrystals for overcoming multidrug resistance in cancer. Mol Pharm, 7, 863-869.

Liu J, Xiao Y, Allen C. 2004. Polymer-drug compatibility: a guide to the development of delivery systems for the anticancer agent, ellipticine. J Pharm Sci. 93, 132-43.

Limtrakul P, Khantamat O, Pintha K. 2005. Inhibition of P-glycoprotein function and expression by kaempferol and quercetin. J Chemother. 17(1), 86-95

Maeda H, Wu J, Sawa T, Matsumura Y, Hori K. 2000. Tumor vascular permeability and the EPR effect in macromolecular therapeutics: a review. J Control Release, 65 (1), 271–284.

Maeda H. 2010. Nitroglycerin enhances vascular blood flow and drug delivery in hypoxic tumor tissues: analogy between angina pectoris and solid tumors and enhancement of the EPR effect. J Control Release, 142, 296–298.

Merz L, Höbel S, Kallendrusch S, Ewe A, Bechmann I, Franke H, Merz F, Aigner A. 2017. Tumor tissue slice cultures as a platform for analyzing tissue- penetration and biological activities of nanoparticles. European Journal of Pharmaceutics and Biopharmaceutics, 112, 45-50.

Mai Y, Eisenberg A. 2012. Self-assembly of block copolymers. Chem Soc Rev, 41, 5969-5985.

Mankhetkorn S, Teodori E, Scapecchi S, Garnier-Suillerot A. 1996. Study of P-glycoprotein functionality in living resistant K562 cells after photolabeling with a verapamil analogue. Biochem Pharmacol. 52, 213-7.

Michalak K, Wesolowska O. 2012. Polyphenols counteract tumor cell chemoresis-tance conferred by multidrug resistance proteins. Anticancer Agents Med Chem, 12, 880–890.

Moongkarndi P, Kosem N, Kaslungka S, Luanratana O, Pongpan N, Neungton N. 2004. Antiproliferation, antioxidation and induction of apoptosis by *Garcinia mangostana* (mangosteen) on SKBR3 human breast cancer cell line. Journal of Ethnopharmacology, 90 (1), 161-166.

Ofer M, Wolffram S, Koggel A, Spahn- Langguth H, Langguth P. 2005. Modulation of drug transport by selected flavonoids: Involvement of P- gp and OCT?. European Journal of Pharmaceutical Sciences, 25, 263-271.

Opanasopit P., Yokoyama M., Watanabe M., Kawano K., Maitani Y., Okano T. 2005. Influence of serum and albumins from different species on stability of camptothecin-loaded micelles, J. Control. Release 104, 313–321.

Pan L, Hu H, Wang X, Yu L, Jiang H, Chen J, Lou Y, Zeng S. 2015. Inhibitory effects of neochamaejasmin B on P- glycoprotein in MDCK- hMDR1 cells and molecular docking of NCB binding in P-glycoprotein. Molecules, 20, 2931–2948.

Peng CL, Shieh MJ, Tsai MH, Chang CC, Lai PS. 2008. Self-assembled starshaped chlorin-core poly(ε- caprolactone) – poly(ethylene glycol) diblock copolymer micelles for dual chemo-photodynamic therapies. Biomaterials, 29, 3599–3608.

Ravishankar D, Rajora AK, Greco F, Osborn HM. 2013. Flavonoids as prospective compounds for anti-cancer therapy. Int J Biochem Cell Biol, 45, 2821-2831.

Reungpatthanaphong P, Mankhetkorn S. 2002. Modulation of multidrug resistance by artemisinin, artesunate and dihydroartemisinin in K562/adr and GLC4/adr resistant cell lines. Biol Pharm Bull. 25, 1555-61.

Russo A, Cardile V, Lombardo L, Vanella L, Vanella A, Garbarino JA. 2005. Antioxidant activity and antiproliferative action of methanolic extract of Geum quellyon Sweet roots in human tumor cell lines. Journal of Ethnopharmacology, 100 (3), 323-332.

Ryu CS, Kwak HC, Lee KS, Kang KW, Oh SJ, Lee KH, Kim HM, Ma JY, Kim SK. 2011. Sulfur amino acid metabolism in doxorubicin- resistant breast cancer cells. Toxicol Appl Pharm, 255 (1), 94-102.

Thomas H, Coley HM. 2003. Overcoming multidrug resistance in cancer: an update on the clinical strategy of inhibiting p-glycoprotein. Cancer Control, 10 (2), 159–165.

Torchilin V. 2011. Tumor delivery of macromolecular drugs based on the EPR effect. Advanced drug delivery reviews, 63, 131-135.

Tsao AS, Kim ES, Hong WK. 2004. Chemoprevention of cancer. CA Cancer J Clin, 54, 150-180.

Vayssi`ere J-L, Petit PX, RislerY, Mignotte B. 1994. Commitment to apoptosis is associated with changes in mitochondrial biogenesis and activity in cell lines conditionally immortalized with simian virus 40. Proc Natl Acad Sci U S A. 91, 11752–6.

Whysner J, Williams GM. 1996. Butylated hydroxyanisole mechanistic data and risk assessment: Conditional species-specific cytotoxicity, enhanced cell proliferation, and tumor promotion. Pharmacology & Therapeutics, 71 (1-2), 137-151.

Xiao L, Xiong X, Sun X, Zhu Y, Yang H, Chen H, Gan L, Xu H, Yang X. 2011. Role of cellular uptake in the reversal of multidrug resistance by PEG- b- PLA polymeric micelles. Biomaterials, 32 (22), 5148-5157.

Xu P, Kirk EA, Li S, Murdoch WJ, Ren J, Hussain MD, Radosz M, Shen Y. 2006. Highly stable core- surface- crosslinked nanoparticles as cisplatin carriers for cancer chemotherapy. Colloids Surf. B Biointerfaces, 48, 50–57.

Yamamoto T, Yokoyama M, Opanasopit P, Hayama A, Kawano K, Maitani Y. 2007. What are determining factors for stable drug incorporation into polymeric micelle carriers? Consideration on physical and chemical characters of the micelle inner core. J Control Release. 123, 11-8.

Yokoyama M, Opanasopit P, Okano T, Kawano K, Maitani Y. 2004. Polymer design and incorporation methods for polymeric micelle carrier system containing water-insoluble anti-cancer agent camptothecin. J Drug Target. 12, 373-84.

Zhang S, Yang X, Morris ME. 2004. Flavonoids are inhibitors of breast cancer resistance protein (ABCG2)-mediated transport. Mol Pharmacol, 65, 1208-1216.

8. Output

- To get alternative treatment to overcome multidrug resistant problem of cancer therapy
- To publish this study on good international journal
    - **Khonkarn R**, Daowtak K, Okonogi S. Chemotherapeutic Efficacy Enhancement in P-gp-Overexpressing Cancer Cells by Flavonoid-Loaded Polymeric Micelles. *AAPS PharmSciTech* 2020;21**:**121.
    - Srisa-nga K, Mankhetkorn S, Okonogi S, **Khonkarn R**. Delivery of Superparamagnetic Polymeric Micelles Loaded with Quercetin to Hepatocellular Carcinoma Cells. *Journal of pharmaceutical sciences*. 2019;108(2):996-1006.

Appendix

AAPS PharmSciTech (2020) 21:121
DOI: 10.1208/s12249-020-01657-5

Check for updates

Research Article

Chemotherapeutic Efficacy Enhancement in P-gp-Overexpressing Cancer Cells by Flavonoid-Loaded Polymeric Micelles

Ruttiros Khonkarn,[1,2] Krai Daowtak,[3] and Siriporn Okonogi[1,2,4]

Received 14 October 2019; accepted 10 March 2020

Abstract. Multidrug resistance is the major problem in cancer treatment nowadays. Compounds from plants are the new targets to solve this problem. Quercetin (QCT), quercetrin (QTR), and rutin (RUT) are potential anticancer flavonoids but their poor water solubility leads to less efficacy. In this study, the polymeric micelles of benzoylated methoxy-poly (ethylene glycol)-*b*-oligo(ε-caprolactone) or mPEG-*b*-OCL-Bz loading with the flavonoids were prepared to solve these problems. The flavonoid-loaded micelles showed an average size of 13–20 nm and maximum loading capacity of 35% (w/w). The release of QCT (21%, 3 h) was lower than that of QTR (51%, 3 h) and RUT (58%, 3 h). QCT (free and micelle forms) exhibited significantly higher cytotoxicity against P-glycoprotein-overexpressing leukemia (K562/ADR) cells than QTR and RUT ($p < 0.05$). The results demonstrated that QCT-loaded micelles effectively reversed cytotoxicity of both doxorubicin (multidrug resistant reversing (δ) values up to 0.71) and daunorubicin (δ values up to 0.74) on K562/ADR cells. It was found that QCT-loaded micelles as well as empty polymeric micelles inhibited P-gp efflux of tetrahydropyranyl Adriamycin. Besides, mitochondrial membrane potential was decreased by QCT (in its free form and micellar formation). Our results suggested that the combination effects of polymeric micelles (inhibiting P-gp efflux) and QCT (interfering mitochondrial membrane potential) might be critical factors contributing to the reversing multidrug resistance of K562/ADR cells by QCT-loaded micelles. We concluded that QCT-loaded mPEG-*b*-OCL-Bz micelles are the attractive systems for overcoming multidrug-resistant cancer cells.

KEY WORDS: flavonoid; polymeric micelle; resistance; cancer; P-gp.

INTRODUCTION

Multidrug resistance (MDR), among others, caused by overexpression of cell membrane transporters, is a major factor for the clinical failure of chemotherapy for many types of cancer (1). ATP-dependent drug transporters such as the P-glycoprotein (P-gp), the multidrug resistance protein (MRP1), and the breast cancer resistance protein (BCRP) can pump structurally unrelated chemotherapeutic drugs from cancer cells, resulting in therapeutic ineffective intracellular concentrations of cytostatic drugs. Therefore, inhibition of these drug transporters is an attractive modality in cancer therapy to enhance the therapeutic potential of cytotoxic drugs (2,3).

It has been shown that flavonoids play important roles in the alterations of ROS signaling, cell cycle arrest, and apoptosis of several cancer cells (4). Moreover, it has been reported that flavonoids inhibit the growth of multidrug-resistant cancer cells (in the absence of anticancer drug) and MDR efflux proteins (in the presence of anticancer drug) (5,6). In previous study, structure-activity relationships of flavonoids to inhibit drug transporters in the MDR cells were investigated and it was found that quercetin (QCT) and QCT conjugated at the C^3position of ring C by rhamnoside (quercetrin; QTR) and rutinoside (rutin; RUT) as structures shown in Fig. 1 reverse the MDR cells to tetrahydropyranyl adriamycin (THP, anticancer drug) (7). For that reason, these flavonoids are of interest in cancer therapy as MDR inhibitors. However, the solubility of QCT and also its glycoside derivatives, QTR and RUT, is very low (0.1–500 μM, (8)) which limits their use in clinical oncology.

Polymeric micelles are under investigation as a drug delivery system (9,10). They consist of a hydrophobic core that can accommodate hydrophobic drugs and a hydrophilic shell that can give them stealth-like properties resulting in disposition in tissue of increased vascular permeability (*e.g.*, tumors) after intravenous

[1] Department of Pharmaceutical Sciences, Faculty of Pharmacy, Chiang Mai University, Chiang Mai, 50200, Thailand.
[2] Research Center of Pharmaceutical Nanotechnology, Chiang Mai University, Chiang Mai, 50200, Thailand.
[3] Department of Medical Technology, Faculty of Allied Health Sciences, Naresuan University, Phitsanulok, 65000, Thailand.
[4] To whom correspondence should be addressed. (e–mail: siriporn.okonogi@cmu.ac.th)

aaps
Published online: 26 April 2020

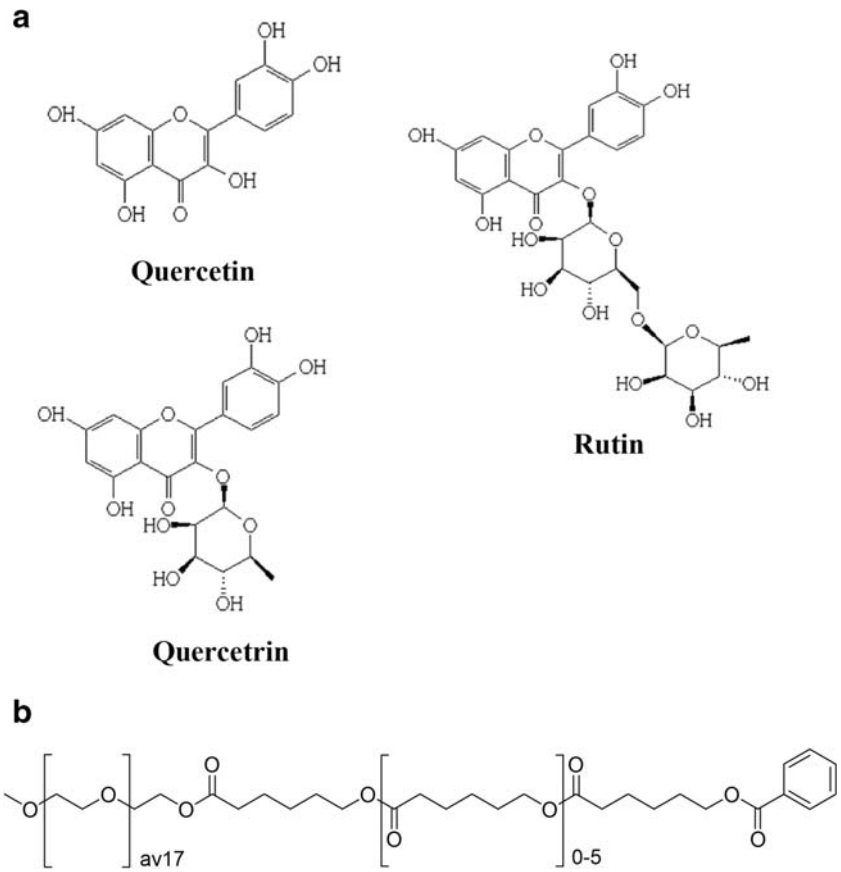

Fig. 1. The chemical structures of QCT, QTR, RUT (**a**), and mPEG750-*b*-OCL-Bz (**b**)

administration due to the so-called EPR effect (11). It has been also shown that cytostatic drugs delivered to cancer cells by polymeric micelles might overcome their MDR (12,13).

Because of its biodegradability and ease of synthesis, PEGylated poly (caprolactone) (PEG-PCL) recently gained attention as a micellar formulation for several chemotherapeutic agents including paclitaxel, doxorubicin, cisplatin, ellipticin, and rapamycin (14–16). It has been reported that π-π stacking interactions can be exploited to improve the drug loading and retention of hydrophobic drug in PEG-PCL-based micelles. That was accomplished by coupling aromatic functionalities (such as chrysin, cinnamic acid, 7-carboxymethoxy coumarin, benzyl, and napthyl) to the PCL OH end group of PEG-PCL block copolymers (17,18). Benzoylated methoxy-poly (ethylene glycol)-b-oligo(ε-caprolactone) (mPEG750-b-OCL-Bz) micelles are an interesting drug carrier because of their small (sub-20 nm) (19,20). It has been reported in a number of recent papers that these nanoparticles with a size smaller than 30 nm have substantially better tumor penetration properties than larger ones (21,22). In our previous publication, we demonstrated that the water solubility of QCT was successfully improved by loading QCT into mPEG750-*b*-OCL-Bz micelles. Furthermore, QCT-loaded mPEG750-*b*-OCL-Bz micelles had effective cytotoxicity on both sensitive and resistant cancer cells *via* a cell cycle arrest mechanism of the G2/M phase (20). However, mPEG750-*b*-OCL-Bz micelles with QCT glycosides encapsulation have not been investigated thus far.

In this study, the encapsulation of QCT glycosides into mPEG750-*b*-OCL-Bz micelles has been prepared by a film hydration method. Cytotoxicity of the obtained micelles toward human erythromyelogenous leukemic (K562) and their corresponding P-gp-overexpressing (K562/ADR) cells was investigated. The influence of the selected flavonoid-loaded micelles on the P-gp reversing effect of K562/ADR cells to certain important anticancer drugs such as doxorubicin (DOX) and daunorubicin (DAU) was presented. Finally, the effects of these micelles on P-gp function and mitochondrial membrane potential assay were also demonstrated.

MATERIALS AND METHODS

Materials

QCT, QTR, RUT, DOX, DAU, THP, and verapamil hydrochloride (VER) were purchased from Sigma-Aldrich (Saint Quentin Fallavier, France). RPMI 1640, trypsin–EDTA, and penicillin–streptomycin were obtained from GIBCO™ Invitrogen (Grand Island, NY, USA). Fetal bovine serum (FBS) was purchased from Biochrom AG (Berlin, Germany). Dichloromethane, ethanol, dimethylformamide, and Tween 80 were obtained from Merck (Darmstadt, Germany). All other chemicals were of the highest grade available. mPEG-*b*-OCL-Bz was synthesized and characterized as described previously (18,19). Average degrees of polymerization of mPEG and OCL were 17 and 4, respectively. Critical micellar concentration (CMC) of the mPEG-*b*-OCL-Bz polymer obtained with pyrene was 0.003–5 mg/mL (19).

Preparation of Flavonoid-Loaded Micelles

The polymeric micelles of mPEG750-*b*-OCL-Bz loading with the flavonoids were prepared by a film hydration method previously described by Carstens *et al.* (19). In brief, the flavonoids (QCT, QTR, and RUT at 5 mg/mL) and the oligomer (10 mg/mL) were dissolved in ethanol and dichloromethane, respectively. A stock flavonoid solution (0.1–1.6 mL) and oligomer solution (2 mL) were mixed in a round-bottomed flask to achieve flavonoid/oligomer ratios of 2.5, 5, 10, 20, and 40% (w/w). Next, the solvents were evaporated under an N_2 stream for 1 h. Micellization was induced by hydration of the obtained film with 2 mL of DI water under sonication. Finally, the dispersions were filtered through a 200-nm filter to remove non-entrapped (precipitated) flavonoids. The size and polydispersity and zeta potential of the micelles were analyzed by dynamic light scattering (Malvern Instruments, Ltd., Malvern, UK.) comprising computerized auto-titrate and DLS software. The measurement was made at a fixed angle of 173°. Transmission electron microscopy (TEM, JEM 2010) was used to examine the morphology and particle size of flavonoid-loaded micelles. TEM samples were prepared by dropping the micelles onto a copper grid, followed by air-drying. TEM images of flavonoid-loaded polymeric micelles were subsequently examined. The loading flavonoid content of the micelles was determined by UV–Vis spectroscopy at 372, 355, and 362 nm for QCT, QTR, and RUT, respectively. This measurement was employed by the addition of dimethylformamide (2 mL) to the micellar dispersions (20 μL) to dissociate the micelles and solubilize the flavonoids. The coefficients of linearity (r^2) for QCT, QTR, and RUT dissolved in dimethylformamide with a concentration range of 1–50 μg/mL was > 0.99. The loading capacity (LC) and entrapment efficiency (EE) were calculated as the following equations.

$$\%\mathrm{LC} = (\text{weight of loaded flavonoids} / \text{total weight of copolymer used for loading}) \times 100\%$$

$$\%\mathrm{EE} = (\text{weight of loaded flavonoids} / \text{total weight of flavonoids used for loading}) \times 100\%$$

For stability study, flavonoid-loaded micelles were stored at room temperature for 2 weeks. The physical appearance and flavonoid content were used to check the stability of the flavonoid-loaded micelles.

In Vitro Release

The release of QCT, QTR, and RUT from the micelles was studied by a dialysis method previously described by Khonkarn *et al.* (20). Briefly, 1 mL of micellar dispersion was transferred into a pre-swollen dialysis bag (Cellu Sep® Nominal T1, molecular weight cutoff 3500 Da, Membrane Filtration Products, Inc.) and transferred into a glass container containing 100 mL of 0.2% Tween 80 in PBS. Tween was added to solubilize the released flavonoids and to ensure sink conditions. The glass container was gently stirred at 37°C, and at different time points, 10-mL samples of the receiving medium containing the released flavonoid were taken and replaced by the same volume of fresh buffer. The concentration of the released flavonoids in the different samples was determined by means of UV–Vis spectroscopy as described in the Preparation of Flavonoid-Loaded Micelles section.

Cell Culture

Human erythromyelogenous leukemic (K562) cells and their corresponding DOX-resistant cells (K562/ADR; the cell lines that overexpresses P-gp) were used in this study. The cells were cultured in RPMI 1640 supplemented with 10% FBS, 100 U/mL of penicillin, and 0.1 mg/mL of streptomycin, and grown in a humidified atmosphere at 37°C in 5% CO_2. The trypan-blue dye exclusion method as described by Tennant (23) was used to evaluate cell viability. The cells were seeded at a density of 5×10^5 cells/mL and allowed to grow for 24 h in order to let them get into the exponential growth phase before starting the experiments.

Cytotoxicity Activity

To evaluate the inhibition of cell growth, the number of cells was counted using a flow cytometer (Coulter® Epics® XL™). For mono-treatment, cancer cells at a density of 5×10^4 cells/well were seeded into 24-well plates. The media contained DOX and DAU (concentration range of 25–1000 nM), and the flavonoids in its free form as well as micellar formulation (concentration of flavonoids (free/micelle forms) ranged from 2.5–200 μM) were added and incubated for 72 h. The cancer cell growth upon incubation with empty polymeric micelles (5–200 μg/mL) was also determined as the vehicle control. The cell growth inhibition was calculated as the following equation:

$$\%\text{Cell growth inhibition} = \frac{C_{c-72\ \mathrm{h}} - C_{s-72\ \mathrm{h}}}{C_{c-72\ \mathrm{h}} - C_{c-0\ \mathrm{h}}} \times 100\%$$

where $C_{c\text{-}72\ \mathrm{h}}$ and $C_{c\text{-}0\ \mathrm{h}}$ represent the number of viable cells in the control cells at 72 h and 0 h, respectively, and $C_{s\text{-}72\ \mathrm{h}}$ represents the number of viable cells in the samples at 72 h. The drug concentration that inhibits 50% of the cell growth (IC_{50}) was obtained from the dose-response curves of the percentages of cell growth inhibition *versus* drug concentration.

P-gp Reversing Effect

This assay was carried out to investigate chemosensitivity of resistant cancer cells with P-gp overexpression to conventional chemotherapeutic drugs (substrates of P-gp) by free QCT or QCT-loaded micelles (P-gp modulators). Therefore, the influence of free QCT or QCT-loaded micelles on the cytotoxicity of chemotherapeutic drugs (DOX or DAU) in K562/ADR cells was evaluated. Briefly, the cells were

incubated with medium containing both QCT (in its free form or micellar formulation, at concentrations of 1, 2, or 3 μM) and DOX or DAU (concentration range of 25–5000 nM and 25–1000 nM for DOX and DAU, respectively). The inhibition of cell growth was investigated after 72 h of incubation at 37°C by counting the cell number using a flow cytometer. The P-gp reversing effect of empty polymeric micelles (10–30 μg/mL) was also evaluated. The efficacy of QCT, QCT-loaded micelles, or empty polymeric micelles in increasing the cytotoxicity effect of the used chemotherapeutic drugs on MDR cells was calculated using the following equation:

$$\text{MDR reversing } (\delta) \text{ value} = \frac{IC_{50}(RD) - IC_{50}(RM)}{IC_{50}(RD) - IC_{50}(SD)}$$

where IC_{50}(RD) is the 50% inhibitory drug concentration of MDR cell (K562/ADR) growth, IC_{50}(RM) is the 50% inhibitory drug concentration of MDR cell growth in the presence of QCT (in its free form or as micellar formulation), and IC_{50}(SD) is the 50% inhibitory drug concentration of drug-sensitive cell (K562) growth. $\delta = 0$ when IC_{50} (RD) = IC_{50} (RM). This means that there is no effect of QCT; in other words, QCT does not act as an inhibitor of Pgp. $\delta = 1$ when IC_{50} (RM) = IC_{50} (SD). This means that QCT fully inhibits P-gp.

Effect on P-gp Function

The kinetics of the active efflux of P-gp-mediated THP (fluorescent P-gp substrate) in cells were studied using an assay previously described (24–26), based on the quenching of the fluorescence of THP after its intercalation in DNA. Briefly, a 1-cm quartz cuvette was filled with 2 mL of HEPES-Na^+ buffer solutions pH 7.25 containing 20-mM HEPES, 132-mM NaCl, 3.5-mM KCl, 1-mM $CaCl_2$, and 0.5-mM $MgCl_2$ with vigorous stirring at 37°C. Next, an exact amount of 2 mL of cell suspension (2×10^6 cells/mL) was added and incubated in the HEPES-Na^+ buffer in the presence of 10-mM glucose. Subsequently, 20 μL of a 100-μM THP was added to the cell suspension. As seen in Fig. 2, at starting state ($t = 0$), the fluorescence intensity of free THP in the extracellular medium (C_T) was equal to 1-μM THP. The fluorescence intensity was (using excitation and emission wavelengths of 480 nm and 590 mm, respectively) F_0. When THP is taken up by cells and subsequently intercalates in DNA, its fluorescence is quenched. The decrease fluorescence intensity of THP was then recorded as a function of time. At the 1st steady state (around 1000 s), the concentration of free THP in the extracellular medium is the same as in the cytosol and fluorescence intensity was equal to F_n. The concentration of THP intercalated in the base pairs of DNA in the nucleus was $C_n = C_T(F_0/F_n)/F_0$. At 1700 s, various concentrations of inhibitor, *i.e.*, free QCT (2–10 μM), QCT-loaded micelles (0.25–5 μM), or verapamil (a well-known Pgp inhibitor, 0.25–5 μM), were added, leading to a new steady. At the 2nd steady state (around 2000 s), the fluorescence intensity was equal to $F_{n(i)}$ and the concentration of THP intercalated between the base pairs of DNA in the nucleus was $C_{n(i)} = C_T(F_0/F_{n(i)})/F_0$. Next, the cell membranes were permeabilized by the addition of 0.01% Triton X-100 to yield the equilibrium state which resulted in the fluorescence intensity of F_N. The overall concentration of THP intercalated in DNA was $C_N = C_T(F_0/F_N)/F_0$. P-gp function was evaluated by the ratio value of $C_{n(i)}/C_N$ (27). In case of completed inhibition of the P-gp function, the ratio of $C_{n(i)}/C_N$ is equal to 1.

Assessment of Mitochondrial Membrane Potential

Mitochondrial membrane potential ($\Delta\psi m$) was assessed by tetraethyl benzimidazolyl carbocyanine iodide (JC-1), according to the manufacturer's instructions. Briefly, K562/ADR cells at a density of 1.5×10^4 cells/well were seeded into 96-well plates and incubated overnight. Next, the cells were washed once with buffer. These cells were then stained with 20-μM JC-1 for 10 min at 37°C in the dark and were washed twice with buffer. Subsequently, the cells were treated with QCT (in its free form or micellar formulation, at concentrations of 25 μM) and empty polymeric micelles for 15, 30, and 60 min. The treated cells were measured using a microplate reader at λ ex (475 nm)/λ em (590 nm) for red fluorescence or λ ex (475 nm)/λ em (530 nm) for green fluorescence. The obtained values were then expressed as JC-1 Red/Green fluorescent intensity (JC-1 R/G) ratio.

Statistic Analysis

The data are presented as mean ± standard deviation (SD) from three independent experiments. The statistical significance was assessed by a one-way ANOVA followed by Tukey's post-hoc test. Values of $p < 0.05$ were considered as statistically significant.

RESULTS

Formulations and Characterizations

After hydration of mPEG750-*b*-OCL-Bz films followed by sonication and filtration, different flavonoid-loaded mPEG-*b*-OCL-Bz micelles were obtained. The zeta potential and average size of obtained micelles determined by DLS were shown in Table I. The zeta potential ranged from −1.99 to −8.86 mV. The less negatively charge surfaces prevent

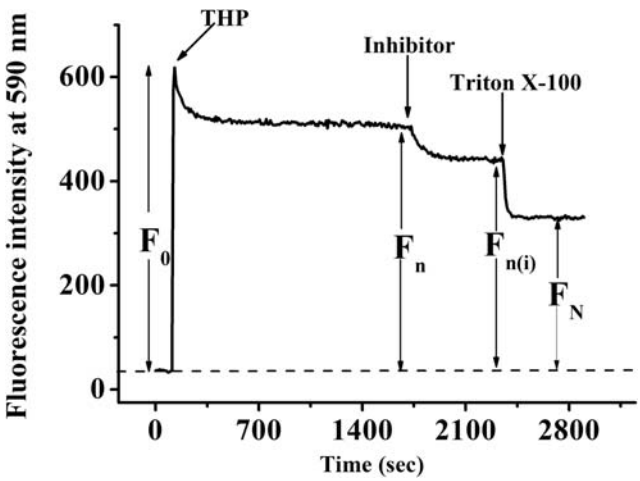

Fig. 2. Uptake of pirarubicin by K562/ADR, P-gp overexpression model, fluorescence intensity at 590 nm (λex = 480 nm) was recorded as a function of time until the steady state

Table I. Average Particle Size and Zeta Potential of Quercetin (QCT)–, Quercetrin (QTR)–, and Rutin (RUT)–loaded mPEG-b-OCL-Bz Micelles. The Values Are Presented as Mean ± S.D. ($n = 3$)

Flavonoid: oligomer	QCT			QTR			RUT		
(%)	Z_{ave} (nm)	PDI	Zeta (mV)	Z_{ave} (nm)	PDI	Zeta (mV)	Z_{ave} (nm)	PDI	Zeta (mV)
0*	15.9 ± 0.5	0.26 ± 0.04	− 1.99 ± 2.17	–	–	–	–	–	–
2.5	14.4 ± 0.3	0.14 ± 0.03	− 2.56 ± 0.28	13.9 ± 0.4	0.16 ± 0.03	− 3.89 ± 0.48	17.7 ± 2.3	0.38 ± 0.12	− 2.81 ± 0.15
5	15.0 ± 0.6	0.17 ± 0.06	− 2.26 ± 0.12	14.0 ± 0.2	0.17 ± 0.01	− 2.71 ± 2.03	13.1 ± 0.41	0.11 ± 0.05	− 2.31 ± 0.62
10	14.8 ± 0.2	0.12 ± 0.03	− 4.18 ± 0.25	14.2 ± 1.4	0.19 ± 0.09	− 4.51 ± 1.15	13.7 ± 0.28	0.16 ± 0.05	− 2.27 ± 0.15
20	15.7 ± 1.1	0.22 ± 0.08	− 6.28 ± 0.40	13.3 ± 0.3	0.20 ± 0.03	− 2.00 ± 1.24	13.0 ± 0.2	0.11 ± 0.00	− 6.05 ± 0.98
40	20.0 ± 0.7	0.40 ± 0.03	− 8.86 ± 2.03	15.4 ± 1.3	0.33 ± 0.06	− 2.25 ± 0.14	12.9 ± 0.2	0.11 ± 0.01	− 5.63 ± 2.80

*Empty micelles

clearance by mononuclear phagocytic cells (28), whereas the size was in the range of 13–20 nm which are in agreement with previously published data on the same micelles loaded with docetaxel and paclitaxel (18). Morphological investigation of flavonoid-loaded polymeric micelles was observed by TEM. All flavonoid-loaded polymeric micelles exhibited a regular spherical shape with the particle size around 14 nm (Fig. 3a–c). The particle size determined by TEM was similar to that determined by DLS, and there was no significant difference in the particle size between the micelles loaded with the different flavonoids. The loading efficiency and capacity of the polymeric micelles for the different flavonoids are quite different as shown in Fig. 3d, e. The loading efficiency for the different flavonoids was around 60–80% at a feed of 2.5–10%. At the feed of 20% and 40%, the entrapment efficiency of RUT was found to be significantly higher than that of QCT but lower than that of QTR (Fig. 3d). The micelles of QTR showed the highest entrapment efficiency (88.0 ± 6.8%), followed by that of RUT (72.4 ± 6.9%) and QCT (69.9 ± 6.4%). Figure 3 e presents, in line with the results illustrated in Fig. 3d, that the micelles of QTR had the maximum loading capacity (35.2 ± 2.7%), followed by that of RUT (10.7 ± 1.7%) and QCT (6.9 ± 0.6%). Figure 3 e also demonstrates that a reduction in the loading capacity of QCT and RUT was observed at 40% of the flavonoid feeding. This characteristic is probably due to a lack of polymer molecules available to encapsulate the flavonoids or the limited capacity to incorporate flavonoids into the hydrophobic core of mPEG-*b*-OCL-Bz micelles. For this reason, the optimal loading ratio of QCT and RUT was considered to be 30%, while QTR was 40%. For stability study, it was found that the physical appearance of flavonoid-loaded micelles was unchanged and precipitated flavonoids could not be observed after keeping flavonoid-loaded micelles at room temperature for 2 weeks. Moreover, the flavonoid content of the flavonoid-loaded micelles was not different (as shown in Fig. 4b).

In Vitro Release

The *in vitro* release of flavonoids (aglycone and glycoside of flavonoid) from the polymeric micelles was analyzed to investigate the release behavior and to confirm the degree of flavonoid–polymer interaction. In our previous studies, a method based on dialysis of micellar dispersion against the Tween micelles was developed and this method was validated to maintain the sink condition (20,29). From these reports, it was shown that the destabilization of polymeric micelles like mPEG-*b*-p (HPMAm-Lac2) micelles and mPEG-*b*-OCL-Bz micelles is not affected by adding surfactants to the receiving medium, as determined by the DLS analysis. Phosphate buffer (pH 7.4) with Tween 20 (0.2%) was then used in this study as the release medium of QCT, QTR, and RUT, which are water practically insoluble compounds. Figure 4 a exhibits the release profile of QCT, QTR, and RUT from the mPEG-*b*-OCL-Bz micelles. It was found that approximately 30% of the loaded QTR and RUT was released within the first hour of the release study. This observed burst release was considered to be the relatively high water solubility of the glycosidic form of both QTR and RUT located in the region near the PEG outer shells. However, the burst release was not observed from QCT-loaded mPEG-*b*-OCL-Bz micelles. When the releasing time was 3 h, the amount of QCT, QTR, and RUT released from mPEG-*b*-OCL-Bz micelles was approximately 21%, 51%, and 58%, respectively, and they were subsequently released to a maximum of approximately 80% in 24 h. In the releasing time between 15 min to 6 h, it was observed that the release rate of QCT was significantly slower than that of QTR and RUT at approximately 21% and 26%, respectively ($p < 0.05$). However, the amount of released QCT was not statistically significantly different from the amount of released QTR and RUT at releasing time of 8 h, 12 h, and 24 h.

Cytotoxicity Activity

The cytotoxicity results of sensitive K562 and resistant K562/ADR cells treated with anthracycline anticancer drugs (DOX and DAU), free flavonoids (QCT, QTR, and RUT), flavonoid-loaded mPEG-*b*-OCL-Bz micelles, and the empty mPEG-*b*-OCL-Bz micelles are demonstrated by the concentrations of compound causing 50% of cell growth inhibition (IC_{50}) and resistance factor (RF), as summarized in Table II. DOX and DAU inhibited the growth of sensitive K562 cells, with IC_{50} values of 19.1 ± 0.6 nM and 17.5 ± 0.9 nM, respectively. In resistant K562/ADR cells, the IC_{50} values were significantly higher than those for their sensitive cells, with the values of 678.4 ± 137.2 nM for DOX and 387.5 ± 75.2 nM for DAU ($p < 0.05$). As expected, it was found that the cytotoxic effect of DOX and DAU in the resistant cells was

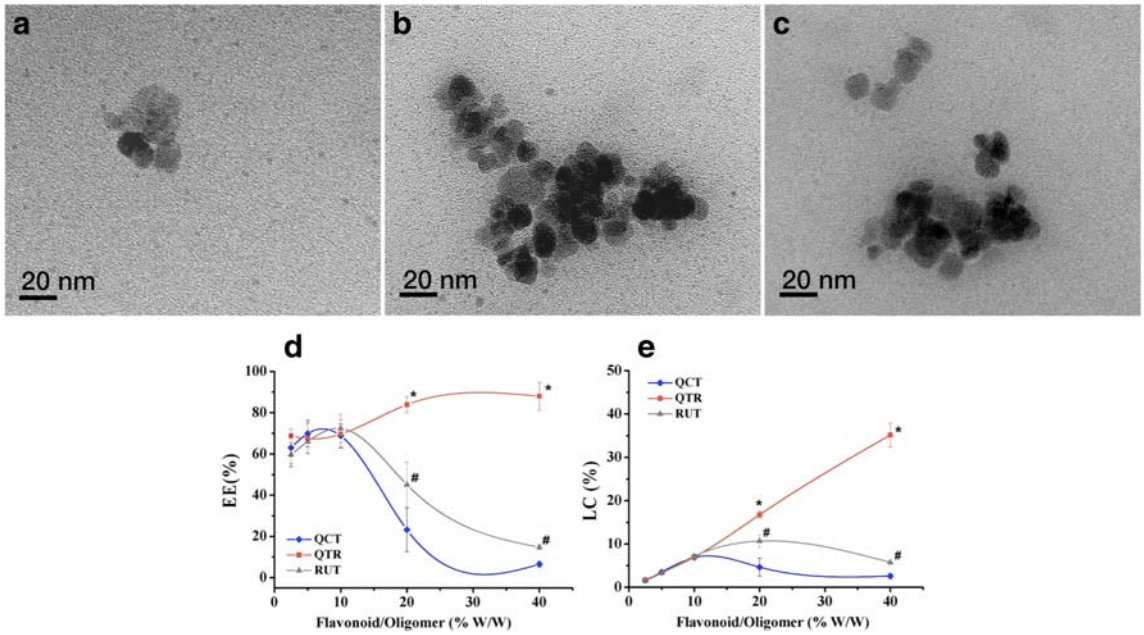

Fig. 3. TEM images of mPEG-*b*-OCL-Bz micelles loading with QCT (**a**), QTR (**b**), and RUT (**c**) and their entrapment efficiency (**d**) as well as loading capacity (**e**)

less than that in their sensitive cells, with the resistant factor values of 35.5 and 22.1, respectively. These data demonstrate a decrease in the cytotoxic effect of the anthracyclines that they were pumped out from the K562/ADR cells. This result therefore confirmed the P-gp phenotype of the K562/ADR cell line.

Even both QTR and RUT in its free form or micellar formulation had low cytotoxicity activity (IC_{50} values > 100 μM). QCT and QCT-loaded micelles exhibited potent anticancer properties against K562 and K562/ADR, with the IC_{50} values ranging from 7.0 ± 2.6 μM to 15.0 ± 4.0 μM. The RF values of free QCT (0.7) and QCT-loaded micelles (0.8) were a bit lower than 1, indicating the similar cytotoxic efficacy in P-gp-overexpressing cells and their corresponding sensitive cells. Similar to the finding of a previous study, QCT was observed to exhibit cytotoxic effect on both human T lymphoblastoid leukemia MOLT-4/DNR and DNR-resistant cells (30). These results suggested that free QCT and QCT-loaded micelles might not be substrates of P-gp. Besides, empty mPEG750-*b*-OCL-Bz micelles (up to 200 μg/mL) showed good cytocompatibility on both K562 and K562/ADR cells. Taken together, QCT-loaded micelles were therefore selected for further studies on P-gp reversing effect to anthracycline drugs of K562/ADR cells.

P-gp Reversing Effect

P-gp reversing effect of MDR cells to DOX or DAU by free QCT, empty polymeric micelles, or QCT-loaded micelles was demonstrated in cell growth curves as shown in Fig. 5. The MDR-reversing (δ) values were also summarized in Table III. The cytotoxicity in K562/ADR of both DOX and DAU in combination with VER (2 μM), a well-known inhibitor of P-gp, was reversed with a δ value of 0.93. Free QCT at concentrations of 1–3 μM, had no effect in reversing K562/ADR cells to DOX (Fig. 5a) or DAU (Fig. 5c). Interestingly, QCT-loaded micelles (at QCT concentrations of 1–3 μM) clearly increase chemosensitivity to DOX (Fig. 5b) and DAU (Fig. 5d) on multidrug resistance of K562/ADR cells in a dose-dependent manner. The δ values of QCT-loaded micelles in increasing P-gp reversing effect to DOX ranged from 0.39 ± 0.19 to 0.71 ± 0.15 and to DAU from 0.29 ± 0.21 to 0.74 ± 0.20. These results show that P-gp pump was inhibited by QCT-loaded micelles around 30–40% at QCT concentration of 1 μM and around 70% at QCT concentration of 3 μM. Interestingly, empty mPEG750-*b*-OCL-Bz micelles (concentrations of 10–30 μg/mL) also exhibited MDR-reversing effect to DOX with δ values ranging from 0.11 ± 0.04 to 0.18 ± 0.05, resulting in maximum P-gp inhibiting effect of 18% at empty micelles concentration of 30 μg/mL.

Effect on P-gp Function

In order to understand the direct interaction of QCT-loaded micelle with P-gp, the spectrofluorometric method was used to study the P-gp-mediated efflux. THP is a good substrate of P-gp with fluorescence property. It is therefore suitable to use as a molecular probe to measure P-gp function (31). The results are presented in Fig. 6. The typical kinetic uptake of THP in K562/ADR cell lines in the presence of VER, a well-known P-gp inhibitor, was shown in Fig. 6a. The quenching of THP fluorescence intensity referred to the accumulation of THP within the cells. The THP accumulation was low because of the function of P-gp pump. The fluorescence intensity of THP continuously decreased when VER was added. This result presents the pattern of P-gp inhibition by P-gp inhibitor. The low THP quenching was observed after adding free quercetin (Fig. 6b), whereas QCT-loaded polymeric micelles revealed high THP quenching (Fig. 6c). These results indicated that QCT-loaded polymeric

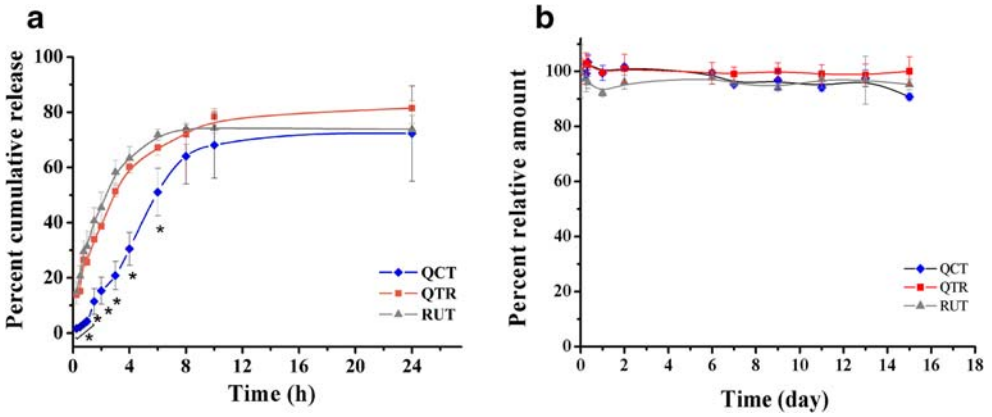

Fig. 4. The release profiles of QCT, QTR, and RUT from mPEG-*b*-OCL-Bz micelles (**a**) and the flavonoid content of the flavonoid-loaded micelles kept at room temperature for 2 weeks (**b**)

micelles had much stronger P-gp inhibition than free QCT. Interestingly, empty polymeric micelles also had an inhibition effect on P-gp function (Fig. 6d).

The ability of the P-gp inhibitor to inhibit the P-gp function was present in the ratio of $C_{n(i)}/C_N$ as shown in Fig. 7. The efficacy of VER to inhibit the P-gp function increased as a function of concentration (Fig. 7a). Interestingly, the ratio of $C_{n(i)}/C_N$ of QCT-loaded micelles and empty polymeric micelle continuously increased in a dose-dependent manner (Fig. 7b). However, it was found that the ratio of $C_{n(i)}/C_N$ of free QCT did not change in a dose-dependent manner. Taken together, QCT-loaded polymeric micelles had an excellent ability to inhibit the function of P-gp.

Assessment of Mitochondrial Membrane Potential

JC-1 was used to evaluate mitochondrial membrane potential. JC-1 yields red fluorescence at high mitochondrial membrane potential while JC-1 yields green fluorescence at low mitochondrial membrane potential. A decrease in the JC-1 R/G ratio is indicative of mitochondrial depolarization (non-functional mitochondria). The JC-1 R/G ratio in K562/ADR cells treated with empty polymeric micelles was not significantly different from cell control ($p < 0.05$), whereas the JC-1 R/G ratio in resistant cells treated with free QCT for 15 min decreased to 36% of cell control. This decrease did not change in a time-dependent manner as shown in Fig. 8. Moreover, the decreasing of JC-1 R/G ratio in resistant cells treated with QCT-loaded polymeric micelles (decreased to 30% of the cell control) was not significantly different from free QCT, suggesting that QCT (in its free form and micellar formation) had an effect on mitochondrial membrane potential.

DISCUSSION

In the present study, QCT glycosides incorporated mPEG-*b*-OCL-Bz micelles were successfully prepared using a film hydration method. The particle size of the obtained polymeric micelles was around 13–18 nm. The sugar moieties of QCT did not show any effect on the particle size of flavonoid-loaded mPEG-*b*-OCL-Bz micelles, but a difference in the loading efficiency was found. Many recent studies reported that compatibility optimization between the micellar hydrophobic segment and the incorporated drug improved the drug loading efficiency and its retention, resulting in long circulation time in the biological system (32,33). The hydrophobic interaction between the hydrophobic moieties of polymer and the entrapped hydrophobic drugs was successful in improving the efficiency of loading drug into polymeric micelles (34). However, the results from this study demonstrated that the loading content of QTR into the mPEG-*b*-OCL-Bz micelles was significantly higher than that of both QCT and RUT ($p < 0.05$). This may be due to the optimum affinity between the aglycone (non-polar) and the glycone (polar) groups of QTR and the amphiphilic molecules of the mPEG-*b*-OCL-Bz oligomers. QTR is more hydrophilic than QCT but more hydrophobic than RUT. These results present

Table II. IC_{50} Values of Various Compounds Against K562 and K562/ADR Cells. The Values Are Presented as Mean ± S.D. ($n = 3$)

Compounds	IC_{50} value (μM)		RF
	K562	K562/ADR	
DOX	0.019 ± 0.001	0.678 ± 0.137	35.5
DAU	0.018 ± 0.001	0.388 ± 0.075	22.1
Free QCT	15.0 ± 4.0	10.0 ± 0.7	0.7
QCT-loaded mPEG-*b*-OCL-Bz micelles	8.7 ± 1.6	7.0 ± 2.6	0.8
Empty mPEG-*b*-OCL-Bz micelles	ND	ND	–

DOX, doxorubicin; *DAU*, daunorubicin; *QCT*, quercetin; *mPEG-b-OCL-Bz*, (poly [ethylene glycol]-b-oligo [e-caprolactone]) with benzoyl end groups; *IC_{50}*, half maximal inhibitory concentration; *RF*, resistance factor; *ND*, not detectable

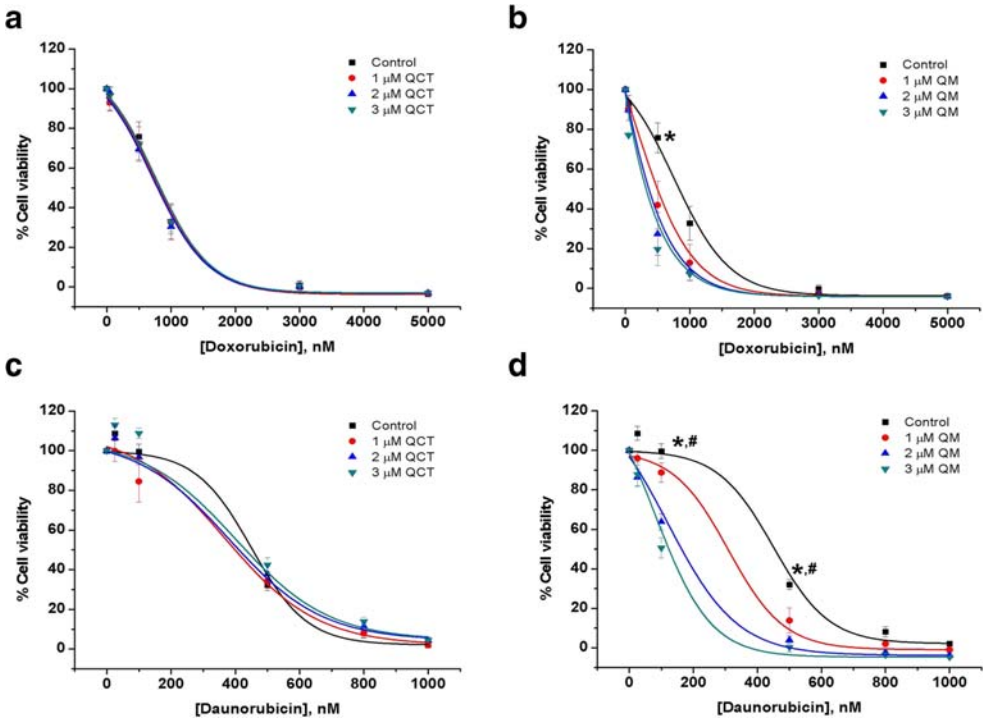

Fig. 5. The P-gp reversing effect of free QCT (QCT: **a**, **c**) and QCT-loaded mPEG-*b*-OCL-Bz micelles (QM: **b**, **d**) with various concentrations of DOX and DAU against K562/ADR. The cell viability assay was conducted by counting the cell numbers using a flow cytometer after 72 h of incubation

that the efficiency of incorporation of flavonoids into polymeric micelles was influenced by the balance between hydrophobicity and hydrophilicity.

In the release study, the interaction between the drug and the micellar core affected the drug release. The difference in the release rate between aglycone and the glycosides of the flavonoids contributed to the degree of interaction between the flavonoids and the mPEG-*b*-OCL-Bz polymer. The π-π interaction between QCT (aglycone) and the micellar core of mPEG-*b*-OCL-Bz micelles was stronger than that of QCT glycosides. The less π-π interaction, which was found from the QCT glycosides, was probably due to the steric factor of the sugar moieties of the QCT glycosides. Besides, the released QCT glycosides were more easily driven to the receiving medium than its aglycone (QCT) by Tween as the assistance in solubilization, based on the amphiphilic characteristic of the QCT glycosides and considering the "like dissolves like" theory, thus leading to the higher release rate.

Chemotherapy is the most frequently used approach in the treatment of cancer. Unfortunately, multidrug resistance (MDR) leads to the limitation in the success of cancer chemotherapy. The most common established mechanism of MDR is the overexpression of ATP-binding cassette (ABC) membrane (35,36). These membrane transporters pump anticancer drugs out of the cells by ATP consumption; therefore, only a small proportion of the administered drug reaches its intended target sites, leading to therapeutic failure. One of the main investigated efflux pumps is P-gp, a 170 kDa transport protein, which is known to limit the distribution of a broad spectrum of drugs. Strategies to overcome the P-gp

Table III. The MDR-Reversing Efficacy of QCT-Loaded mPEG-*b*-OCL-Bz Micelles in Increasing Cytotoxicity Effect of DOX and DAU on P-gp Expressing K562 (K562/ADR) Cells. The Values Are Presented as Mean ± S.D. ($n = 3$)

Test compound	MDR reversing efficacy (δ)	
	DOX	DAU
1-μM QCT-loaded mPEG-*b*-OCL-Bz micelles	0.39 ± 0.19	0.29 ± 0.21
2-μM QCT-loaded mPEG-*b*-OCL-Bz micelles	0.54 ± 0.05	0.63 ± 0.19
3-μM QCT-loaded mPEG-*b*-OCL-Bz micelles	0.71 ± 0.15	0.74 ± 0.20
10 μg/mL mPEG-*b*-OCL-Bz micelles	0.11 ± 0.04	ND
20 μg/mL mPEG-*b*-OCL-Bz micelles	0.13 ± 0.06	ND
30 μg/mL mPEG-*b*-OCL-Bz micelles	0.18 ± 0.05	ND
2-μM VER	0.93 ± 0.03	0.93 ± 0.07

*Not determine
MDR, multidrug resistance; *DOX*, doxorubicin; *DAU*, daunorubicin; *QCT*, quercetin; *VER*, verapamil hydrochloride; *ND*, not detectable

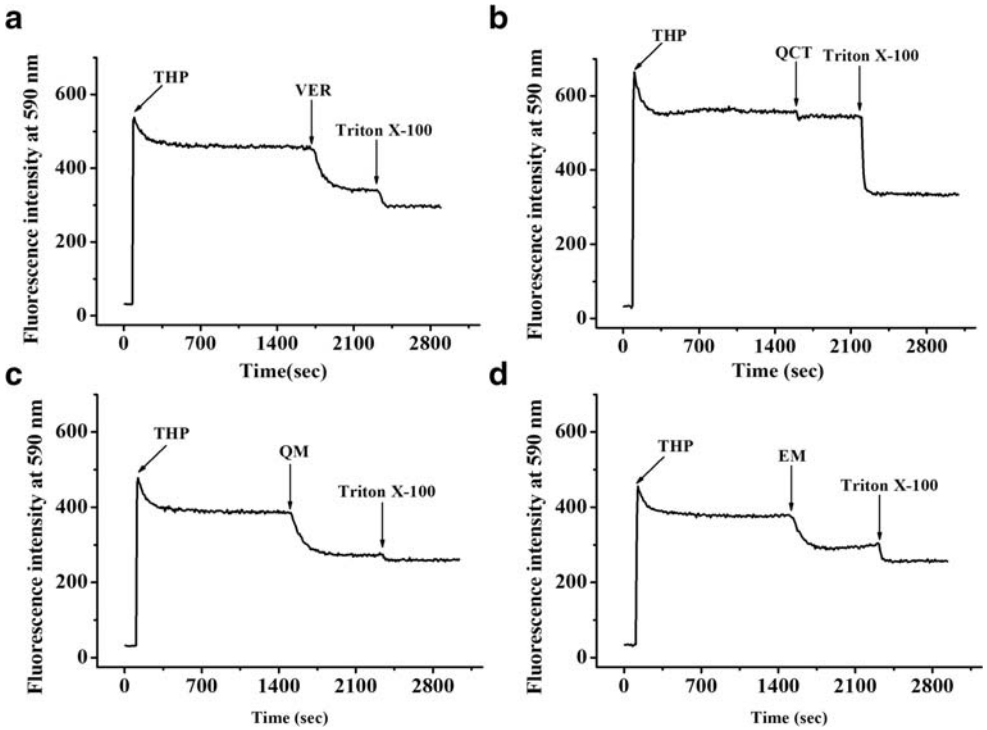

Fig. 6. Typical kinetic uptake of THP in K562/ADR in the presence of 2.5 μM verapamil (VER: **a**), 2.5 μM free quercetin (QCT: **b**), 2.5 μM quercetin-loaded micelles (QM: **c**) and 2.5 μM empty polymeric micelles (EM: **d**)

protein have been extensively studied, including silencing MDR-related miRNAs, combinative drug strategy, applying monoclonal antibodies against P-gp, and designing novel agents that are not recognized as P-gp substrate (2,3,37,38). Among these strategies, reversing drug resistance by the inhibition of the drug efflux of P-gp, including the use of MDR chemosensitizers, is a major challenge to overcome MDR in cancer treatment. Moreover, the nano drug delivery system is one of the novel strategies in the approach to fight MDR.

Natural substances could be a potent anticancer agent or MDR transporter inhibitors with less cytotoxicity (39,40). The cytotoxicity results of this study present that free QCT and QCT-loaded micelles had stronger anticancer activity toward both sensitive and resistant leukemia cells than QTR and RUT (in its free form and micellar formations). Furthermore, similar efficacies in drug-resistant phenotypes and their corresponding sensitive cells (the low degree of the resistant factor) of both free QCT and QCT-loaded micelles were observed. This result suggests that free QCT and QCT-loaded micelles were not transported by P-gp. Moreover, the result also showed that free QCT (at a concentration of 1–3 μM) had no MDR-reversing effect on DOX or DAU. This result is in agreement with Choiprasert *et al.* (7) who reported that the MDR-reversing effect of QCT and QCT glycosides to DAU of K562/ADR and GLC4/ADR cells was not observed. Interestingly, empty mPEG-*b*-OCL-Bz micelles had MDR-reversing effect. A stronger MDR-reversing effect to both

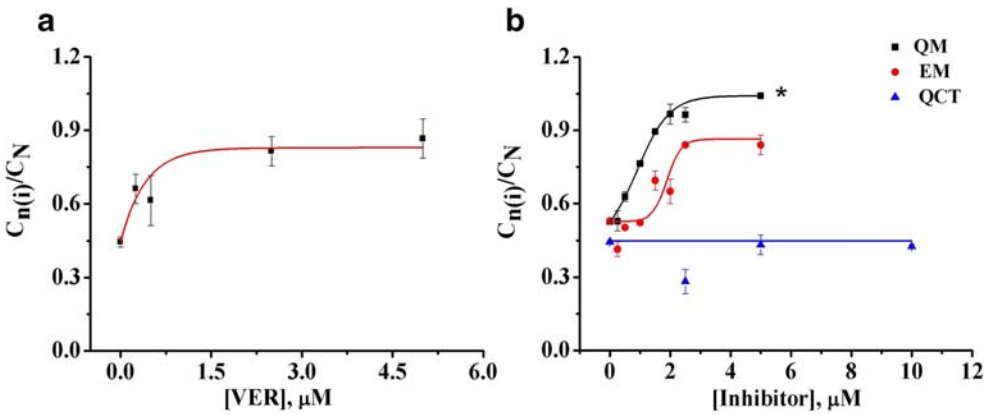

Fig. 7. The effect of verapamil (VER) (**a**), free quercetin (QCT), quercetin-loaded micelles (QM), and empty polymeric micelles (EM) (**b**) on the inhibition of P-gp function. The values of $C_{n(i)}/C_N$ are plotted as a function of the concentration of molecules

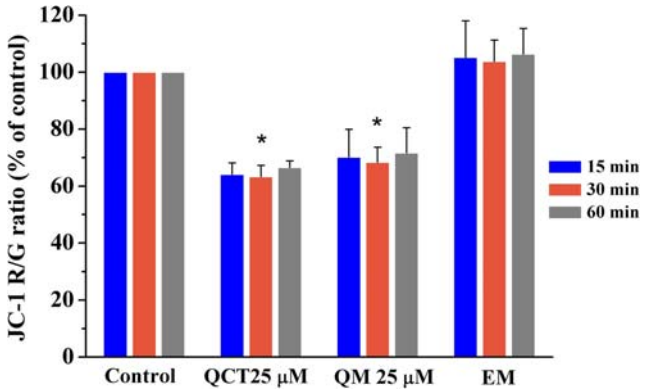

Fig. 8. The effect of quercetin (QCT), quercetin-loaded polymeric micelles (QM), and empty polymeric micelles (EM) on the mitochondrial membrane potential of K562/ADR cells

DOX and DAU of K562/ADR cells was observed from QCT-loaded micelles (at QCT concentration of 1–3 μM) with maximum MDR-reversing values around 70%.

In order to study the mode of action by which QCT-loaded micelles increased the efficacy of DOX or DAU in P-gp-overexpressing cells, the modulation of QCT-loaded micelles in the kinetics of P-gp-mediated pumping and mitochondrial membrane potential were investigated. For the assessment of the kinetics of P-gp-mediated pumping, the THP was studied as a model anticancer drug because its pKa is relatively low and it can move into the cells very rapidly (24–27). In the present study, the efflux of THP by P-gp was slightly inhibited by free QCT. Moreover, QCT-loaded micelles increased the inhibition of P-gp efflux of THP in a dose-dependent manner. Interestingly, empty polymeric micelles also had the ability to inhibit P-gp function. This finding reveals that empty mPEG750-*b*-OCL-Bz micelles could enhance the MDR reversal effects of the QCT-loaded mPEG750-b-OCL-Bz micelles by the inhibition of P-gp efflux. Polymeric micelles are amphiphilic molecules which may lead to membrane fluidization and enhanced permeability of cell membrane, resulting in P-gp interfering (41). It has been reported that drug resistance was altered by poly (ethylene oxide)–poly- (propylene oxide) copolymers (pluronic®) or poly (ethylene glycol)-poly (lactic acid) copolymers using several mechanisms such as affecting the membrane microviscosity, decreasing the P-gp ATPase activity, loss of the mitochondrial membrane potential, and a subsequent decrease in the ATP levels (42–44). Moreover, cellular drug accumulation was enhanced using nanocrystals and nanotubes through bypassing P-gp *via* endocytosis (45,46).

QCT has been recently recognized for its use as an anticancer agent alone or in combination therapy with conventional chemotherapeutic drugs. QCT was found to cause DNA fragmentation, cell cycle arrest, and apoptosis through the mitochondrial pathway (47–49). It has been reported that QCT was an effective inhibitor toward P-gp by directly interacting with transporter protein (50), whereas the less efficient inhibitor of P-gp by QCT glycosides was observed which might result from the steric effect of their sugar moieties (7,51). In this study, the mitochondrial membrane potential was altered by both QCT and QCT-loaded micelles. The main mechanism of MDR proteins pumping the chemical agents uses the energy of ATP. Mitochondria play key roles in energy production. Mitochondrial dysfunction has been shown to participate in the induction of apoptosis. Opening of the mitochondrial permeability transition pore induces depolarization of mitochondrial membrane potential, inhibition of ATP synthesis, release of apoptogenic factors, and subsequent cell death (52,53). The mitochondria targeting of MDR cancer cells and trigger cell apoptosis is one of the mechanisms to overcome MDR. Taken together, the potential mechanisms of reversing multidrug resistance of K562/ADR cells by QCT-loaded polymeric micelles might be the combination effects of polymeric micelles and QCT, interfering with P-gp function and mitochondrial membrane potential, respectively.

CONCLUSION

The results in this study exhibit that the potential anticancer flavonoids, QCT, QTR, and RUT, were successfully incorporated into mPEG-*b*-OCL-Bz micelles. The particle size of the flavonoid-loaded mPEG-*b*-OCL-Bz micelles was not affected by the chemical structure of flavonoids. However, the chemical structure of flavonoids plays important roles in the incorporation efficiency and release behavior of the micelles. The study demonstrates that free QCT and QCT-loaded micelles are not the substrates of P-gp. Moreover, the QCT-loaded micelles possess potential MDR-reversing action to the conventional chemotherapeutic drugs (DOX or DAU). It was found that empty polymeric micelles had the ability to inhibit P-gp function. A higher inhibition of P-gp efflux of THP was found from QCT-loaded micelles. On the other hand, the mitochondrial membrane potential was altered by both QCT and QCT loaded micelles. The combination effects of polymeric micelles, by interfering P-gp function, and QCT, by altering mitochondrial membrane potential, might be the potential mechanisms of reversing multidrug resistance of K562/ADR cells by QCT-loaded polymeric micelles. Finally, it can be concluded that mPEG750-*b*-OCL-Bz micelles are a promising carrier system of flavonoids for enhancing MDR reversal effects.

ACKNOWLEDGMENTS

We thank the Department of Pharmaceutics, Utrecht Institute for Pharmaceutical Sciences (UIPS), Utrecht University, the Netherlands, and Faculty of Associated Medical Sciences, Chiang Mai University, Thailand, for valuable technical support.

FUNDING INFORMATION

This work is fully financially supported by the Thailand Research Fund (TRF) grant for new researchers (grant number MRG6180038) and partially supported by Chiang Mai University.

REFERENCES

1. Assaraf YG, Brozovic A, Gonçalves AC, Jurkovicova D, Linē A, Machuqueiro M, et al. The multi-factorial nature of clinical multidrug resistance in cancer. Drug Resist Updat. 2019;46:100645.

2. Ranjbar S, Khonkarn R, Moreno A, Baubichon-Cortay H, Miri R, Khoshneviszadeh M, et al. 5-Oxo-hexahydroquinoline derivatives as modulators of P-gp, MRP1 and BCRP transporters to overcome multidrug resistance in cancer cells. Toxicol Appl Pharmacol. 2019;362:136–49.
3. Paterna A, Khonkarn R, Mulhovo S, Moreno A, Madeira Girio P, Baubichon-Cortay H, et al. Monoterpene indole alkaloid azine derivatives as MDR reversal agents. Bioorg Med Chem. 2018;26(2):421–34.
4. Tavsan Z, Kayali HA. Flavonoids showed anticancer effects on the ovarian cancer cells: involvement of reactive oxygen species, apoptosis, cell cycle and invasion. Biomed Pharmacother. 2019;116:109004.
5. Dury L, Nasr R, Lorendeau D, Comsa E, Wong I, Zhu X, et al. Flavonoid dimers are highly potent killers of multidrug resistant cancer cells overexpressing MRP1. Biochem Pharmacol. 2017;124:10–8.
6. van Zanden JJ, Wortelboer HM, Bijlsma S, Punt A, Usta M, Bladeren PJ, et al. Quantitative structure activity relationship studies on the flavonoid mediated inhibition of multidrug resistance proteins 1 and 2. Biochem Pharmacol. 2005;69(4):699–708.
7. Choiprasert W, Dechsupa N, Kothan S, Garrigos M, Mankhetkorn S. Quercetin, quercetrin except rutin potentially increased pirarubicin cytotoxicity by non-competitively inhibiting the P-glycoprotein-and MRP1 function in living K562/adr and GLC4/adr cells. Am J Pharmacol Toxicol. 2010;5:24–33.
8. Ofer M, Wolffram S, Koggel A, Spahn-Langguth H, Langguth P. Modulation of drug transport by selected flavonoids: involvement of P-gp and OCT? Eur J Pharm Sci. 2005;25:263–71.
9. Xiao Y, Wang S, Zong Q, Yin Z. Co-delivery of metformin and paclitaxel via folate-modified ph-sensitive micelles for enhanced anti-tumor efficacy. AAPS PharmSciTech. 2018;19(5):2395–406.
10. Woraphatphadung T, Sajomsang W, Rojanarata T, Ngawhirunpat T, Tonglairoum P, Opanasopit P. Development of chitosan-based pH-sensitive polymeric micelles containing curcumin for colon-targeted drug delivery. AAPS PharmSciTech. 2018;19(3):991–1000.
11. Danhier F, Danhier P, De Saedeleer CJ, Fruytier AC, Schleich N, des Rieux A, et al. Paclitaxel-loaded micelles enhance transvascular permeability and retention of nanomedicines in tumors. Int J Pharm. 2015;479(2):399–407.
12. Zhang J, Zhao X, Chen Q, Yin X, Xin X, Li K, et al. Systematic evaluation of multifunctional paclitaxel-loaded polymeric mixed micelles as a potential anticancer remedy to overcome multidrug resistance. Acta Biomater. 2017;50:381–95.
13. Wang Z, Li X, Wang D, Zou Y, Qu X, He C, et al. Concurrently suppressing multidrug resistance and metastasis of breast cancer by co-delivery of paclitaxel and honokiol with pH-sensitive polymeric micelles. Acta Biomater. 2017;62:144–56.
14. Xu P, Van Kirk EA, Li S, Murdoch WJ, Ren J, Hussain MD, et al. Highly stable core-surface-crosslinked nanoparticles as cisplatin carriers for cancer chemotherapy. Colloids Surf. B: Biointerfaces. 2006;48:50–7.
15. Peng CL, Shieh MJ, Tsai MH, Chang CC, Lai PS. Self-assembled starshaped chlorin-core poly(ε-caprolactone)–poly (ethylene glycol) diblock copolymer micelles for dual chemo-photodynamic therapies. Biomaterials. 2008;29:3599–608.
16. Cuong NV, Li YL, Hsieh MF. Targeted delivery of doxorubicin to human breast cancers by folate-decorated star-shaped PEG–PCL micelle. J Mater Chem. 2012;22:1006–20.
17. Liang Y, Deng X, Zhang L, Peng X, Gao W, Cao J, et al. Terminal modification of polymeric micelles with π-conjugated moieties for efficient anticancer drug delivery. Biomaterials. 2015;71:1–10.
18. Carstens MG, de Jong PHJLF, van Nostrum CF, Kemmink J, Verrijk R, de Leede LGJ, et al. The effect of core composition in biodegradable oligomeric micelles as taxane formulations. Eur J Pharm Biopharm. 2008;68:596–606.
19. Carstens MG, Bevernage JJL, van Nostrum CF, van Steenbergen MJ, Flesch FM, Verrijk R, et al. Small oligomeric micelles based on end group modified mPEG-oligocaprolactone with monodisperse hydrophobic blocks. Macromolecules. 2007;40:116–22.
20. Khonkarn R, Mankhetkorn S, Hennink WE, Okonogi S. PEG-OCL micelles for quercetin solubilization and inhibition of cancer cell growth. Eur J Pharm Biopharm. 2011;79:268–75.
21. Cabral H, Matsumoto Y, Mizuno K, Chen Q, Murakami M, Kimura M, et al. Accumulation of sub-100 nm polymeric micelles in poorly permeable tumours depends on size. Nat Nanotechnol. 2011;6:815–23.
22. Merz L, Höbel S, Kallendrusch S, Ewe A, Bechmann I, Franke H, et al. Tumor tissue slice cultures as a platform for analyzing tissue-penetration and biological activities of nanoparticles. Eur J Pharm Biopharm. 2017;112:45–50.
23. Tennant JR. Evaluation of the trypan blue technique for determination of cell viability. Transplantation. 1964;2:685–94.
24. Mankhetkorn S, Teodori E, Scapecchi S, Garnier-Suillerot A. Study of P-glycoprotein functionality in living resistant K562 cells after photolabeling with a verapamil analogue. Biochem Pharmacol. 1996;52:213–7.
25. Reungpatthanaphong P, Mankhetkorn S. Modulation of multidrug resistance by artemisinin, artesunate and dihydroartemisinin in K562/adr and GLC4/adr resistant cell lines. Biol Pharm Bull. 2002;25:1555–61.
26. Meesungnoen J, Jay-Gerin JP, Mankhetkorn S. Relation between MDR1 mRNA levels, resistance factor, and the efficiency of P-glycoprotein-mediated efflux of pirarubicin in multidrug-resistant K562 sublines. Can J Physiol Pharmacol. 2002;80:1054–63.
27. Daowtak K, Kothan S, Doloh S, Dankai W, Udomtanakunchai C. *In vitro* evaluation of P-glycoprotein functions in human neuroblastoma cell lines. J Assoc Med Sci. 2018;51(2):72–80.
28. Levchenko TS, Rammohan R, Lukyanov AN, Whiteman KR, Torchilin VP. Liposome clearance in mice: the effect of a separate and combined presence of surface charge and polymer coating. Int J Pharm. 2002;240:95–102.
29. Khonkarn R, Samlee M, Talelli M, Hennink WE, Okonogi S. Cytostatic effect ofxanthone-loaded mPEG-b-p (HPMAm-Lac_2) micelles towards doxoruribin sensitive and resistant cancer cells. Colloids Surf B: Biointerfaces. 2012;94:266–73.
30. Ishii K, Tanaka S, Kagami K, Henmi K, Toyoda H, Kaise T, et al. Effects of naturally occurring polymethyoxyflavonoids on cell growth, p-glycoprotein function, cell cycle, and apoptosis of daunorubicin-resistant T lymphoblas-toid leukemia cells. Cancer Investig. 2010;28:220–9.
31. Laochariyakul P, Ponglikitmongkol M, Mankhetkorn S. Functional study of intracellular P-gp- and MRP1-mediated pumping of free cytosolic pirarubicin into acidic organelles in intrinsic resistant SiHa cells. Can J Physiol Pharmacol. 2003;81:790–9.
32. Liu J, Xiao Y, Allen C. Polymer-drug compatibility: a guide to the development of delivery systems for the anticancer agent, ellipticine. J Pharm Sci. 2004;93:132–43.
33. Yamamoto T, Yokoyama M, Opanasopit P, Hayama A, Kawano K, Maitani Y. What are determining factors for stable drug incorporation into polymeric micelle carriers? Consideration on physical and chemical characters of the micelle inner core. J Control Release. 2007;123:11–8.
34. Yokoyama M, Opanasopit P, Okano T, Kawano K, Maitani Y. Polymer design and incorporation methods for polymeric micelle carrier system containing water-insoluble anti-cancer agent camptothecin. J Drug Target. 2004;12:373–84.
35. Gillet JP, Efferth T, Remacle J. Chemotherapy-induced resistance by ATP-binding cassette transporter genes. Biochim Biophys Acta. 1775;2007:237–62.
36. Johnson WW. P-glycoprotein-mediated efflux as a major factor in the variance of absorption and distribution of drugs: modulation of chemotherapy resistance. Methods Find Exp Clin Pharmacol. 2002;24:501–14.
37. Bao L, Hazari S, Mehra S, Kaushal D, Moroz K, Dash S. Increased expres-sion of P-glycoprotein and doxorubicin chemoresistance of metastatic breastcancer is regulated by miR-298. Am J Pathol. 2012;180:2490–503.
38. Pearson JW, Fogler WE, Volker K, Usui N, Goldenberg SK, Gruys E, et al. Reversal of drug resistancein a human colon cancer xenograft expressing MDR1 complementary DNA by *in vivo* administration of MRK-16 monoclonal antibody. J Natl Cancer Inst. 1991;83:1386–91.

39. Kuete V, Nkuete AH, Mbaveng AT, Wiench B, Wabo HK, Tane P, et al. Cytotoxicity and modes of action of 4′-hydroxy-2′, 6′-dimethoxychalcone and other flavonoids toward drug-sensitive and multidrug-resistant cancer cell lines. Phytomedicine. 2014;21:1651–7.
40. Michalak K, Wesolowska O. Polyphenols counteract tumor cell chemoresis-tance conferred by multidrug resistance proteins. Anti Cancer Agents Med Chem. 2012;12:880–90.
41. Agarwal A, Lariya N, Saraogi G, Dubey N, Agrawal H, Agrawal GP. Nanoparticles as novel carrier for brain delivery: a review. Curr Pharm Des. 2009;15(8):917–25.
42. Batrakova EV, Li S, Alakhov VY, Kabanov AV. Selective energy depletion and sensitization of multiple drug resistant cancer cells by Pluronic block copolymers. Polym Prepr. 2000;41:1639–40.
43. Xiao L, Xiong X, Sun X, Zhu Y, Yang H, Chen H, et al. Role of cellular uptake in the reversal of multidrug resistance by PEG-b-PLA polymeric micelles. Biomaterials. 2011;32(22):5148–57.
44. Batrakova EV, Li S, Vinogradov SV, Alakhov VY, Miller DW, Kabanov AV. Mechanism of pluronic effect on p-glycoprotein efflux system in blood brain barrier: contributions of energy depletion and membrane fluidization. J Pharmacol Exp Ther. 2001;299(2):483–93.
45. Li R, Zou H, Xiao H, Wu R. Carbon nanotubes as intracellular carriers for multidrug resistant cells studied by capillary electrophoresis-laser-induced fluorescence. Methods Mol Biol. 2010;625:153–68.
46. Liu Y, Huang L, Liu F. Paclitaxel nanocrystals for overcoming multidrug resistance in cancer. Mol Pharm. 2010;7(3):863–9.
47. Chou CC, Yang JS, Lu HF, Ip SW, Lo C, Wu CC, et al. Quercetin-mediated cell cycle arrest and apoptosis involving activation of a caspase cascade through the mitochondrial pathway in human breast cancer MCF-7 cells. Arch Pharm Res. 2010;33:1181–91.
48. Granado-Serrano AB, Martin MA, Bravo L, Goya L, Ramos S. Quercetin induces apoptosis via caspase activation, regulation of Bcl-2, and inhibition of PI-3-kinase/Akt and ERK pathways in a human hepatoma cell line (HepG2). J Nutr. 2006;136(11):2715–21.
49. Duraj J, Zazrivcova K, Bodo J, Sulikova M, Sedlak J. Flavonoid quercetin, but not apigenin or luteolin, induced apoptosis in human myeloid leukemia cells and their resistant variants. Neoplasma. 2005;52(4):273–9.
50. Limtrakul P, Khantamat O, Pintha K. Inhibition of P-glycoprotein function and expression by kaempferol and quercetin. J Chemother. 2005;17(1):86–95.
51. Kitagawa S, Nabekura T, Takahashi T, Nakamura Y, Sakamoto H, Tano H, et al. Structure–activity relationships of the inhibitory effects of flavonoids on P-glycoprotein mediated transport in KB-C2 cells. Biol Pharm Bull. 2005;28:2274–8.
52. Vayssi'ere J-L, Petit PX, RislerY MB. Commitment to apoptosis is associated with changes in mitochondrial biogenesis and activity in cell lines conditionally immortalized with simian virus 40. Proc Natl Acad Sci U S A. 1994;91:11752–6.
53. Bernardi P. The permeability transition pore. Control points of a cyclosporin A-sensitive mitochondrial channel involved in cell death. Biochim Biophys Acta. 1996;1275:5–9.

Journal of Pharmaceutical Sciences 108 (2019) 996-1006

Contents lists available at ScienceDirect

Journal of Pharmaceutical Sciences

journal homepage: www.jpharmsci.org

Pharmaceutical Nanotechnology

Delivery of Superparamagnetic Polymeric Micelles Loaded With Quercetin to Hepatocellular Carcinoma Cells

Korawith Srisa-nga [1], Samlee Mankhetkorn [2], Siriporn Okonogi [3, 4], Ruttiros Khonkarn [3, 4, *]

[1] Master's Degree Program in Pharmaceutical Science, Department of Pharmaceutical Sciences, Faculty of Pharmacy, Chiang Mai University, Chiang Mai, Thailand
[2] Laboratory of Physical Chemistry, Molecular and Cellular Biology, Department of Radiologic Technology, Faculty of Associated Medical Sciences, Chiang Mai University, Chiang Mai, Thailand
[3] Department of Pharmaceutical Sciences, Faculty of Pharmacy, Chiang Mai University, Chiang Mai, Thailand
[4] Research Center of Pharmaceutical Nanotechnology, Chiang Mai University, Chiang Mai, Thailand

ARTICLE INFO

Article history:
Received 3 October 2017
Revised 6 August 2018
Accepted 7 August 2018
Available online 16 August 2018

Keywords:
quercetin
superparamagnetic iron oxide nanoparticles
polymeric micelles
magnetic nanocarrier

ABSTRACT

The aim of this study is to develop co-encapsulation of quercetin (QCT) and superparamagnetic iron oxide nanoparticles (SPIONs) into methoxy-poly(ethylene glycol)-*b*-oligo(ε-caprolactone), mPEG750-*b*-OCL-Bz micelles (QCT-SPION-loaded micelles) for inhibition of hepatitis B virus-transfected hepatocellular carcinoma (HepG2.2.15) cell growth. QCT-SPION-loaded micelles were prepared using film hydration method. They were spherical in shape with an average size of 22-55 nm. The best QCT-SPION-loaded micelles showed entrapment efficiency and loading capacity of QCT at 70% and 3.5%, respectively, and of SPIONs at 15% and 0.8%, respectively. Transverse (T_2) relaxivity of SPIONs was 137 $mM^{-1}s^{-1}$. SPION clusters present inside the core of QCT-SPION-loaded micelles increased T_2 relaxivity value (246 $mM^{-1}s^{-1}$) indicating the good magnetic resonance imaging sensitivity of QCT-SPION-loaded micelles in comparison with SPIONs. QCT-SPION-loaded micelles could be taken up by HepG2.2.15 cells and showed higher cytotoxicity than QCT. Furthermore, these cells were arrested by QCT-SPION-loaded micelles at the G0/G1 phase of cell cycle. QCT-SPION-loaded micelles accumulated in the vicinity of Neodymium Iron Boron (NdFeB) magnetic disc, resulting in the potent inhibition of cancer cell growth at the strong magnetic field strength. In conclusion, mPEG750-*b*-OCL-Bz micelles are a promising multi-functional vehicle for co-delivery of QCT and SPIONs for disease monitoring and therapies of hepatocellular carcinoma.

Introduction

Liver cancer is the second-ranked cause of cancer-related mortality in the world, and is most prevalent in Southeast Asia, especially in Thailand.[1,2] Hepatocellular carcinoma (HCC), the major type of liver cancer, is difficult to diagnose. Most HCC patients in the advanced stage are not suitable for curative treatments such as surgical resection, local ablation, and liver transplantation. Therefore, chemotherapy is the only therapeutic option.[3] However, chemotherapy to liver cancer is associated with harmful side effects and low response rates (10%-15%).[4] Furthermore, multi-drug resistance (MDR) plays a major role in the chemoresistance of HCC.[5] Quercetin (QCT) presents interesting anti-proliferative effects on a variety of cancer cells such as colon, breast, and liver.[6] QCT also exhibits high antioxidant effects, induces cell apoptosis, and reverses cancer drug resistance.[7,8] It has been shown that in HCC, QCT induces cell apoptosis by activation of caspase-3 and caspase-9, regulation of B-cell lymphoma 2, and suppression of specificity protein-1.[9,10] Besides, adenosine triphosphate-binding cassette transporters including MDR-1, MDR-associated protein-1, and breast cancer resistance protein, which control drug efflux process, are inhibited by QCT.[8] Therefore, QCT is a potential drug candidate for HCC treatment. However, the very low aqueous solubility of QCT limits its therapeutic use.[11]

The aqueous solubility of QCT can be improved using microemulsions, liposomes, and polymeric micelles. Polymeric micelles

This article contains supplementary material available from the authors by request or via the Internet at https://doi.org/10.1016/j.xphs.2018.08.008.

* *Correspondence to:* Ruttiros Khonkarn (Telephone: +66-53-944-309).
E-mail address: pharrutty@gmail.com (R. Khonkarn).

https://doi.org/10.1016/j.xphs.2018.08.008
0022-3549/

are an interesting class of drug delivery systems for cancer therapy on account of their capability to solubilize hydrophobic compounds/drugs. Their small size leads to accumulation at the tumor site through the enhanced permeability and retention (EPR) effect.[12] In our previous study, methoxy-poly(ethylene glycol)-*b*-oligo(ε-caprolactone), mPEG750-*b*-OCL-Bz micelles increased the water solubility of QCT to about 110-fold and these micelles exhibited a higher cytotoxicity toward resistant human erythromyelogenous leukemia (K562) and small lung carcinoma (GLC4) cells than the parental sensitive cells.[13]

Drug targeting could decrease side effects and enhance therapeutic efficiency of anti-cancer drugs by reducing its systemic concentration and increasing the concentration at the target site. The EPR effect of nanoparticles can be improved by active targeting (use of a cell-specific ligand) as a result of enhancing the specificity to the target cells.[14]

Superparamagnetic iron oxide nanoparticles (SPIONs), magnetic resonance imaging (MRI) agents approved by the U.S. Food and Drug Administration, are interesting particles for imaging the *in vivo* fate of targeted nanomedicines.[15] Recent studies have developed nanomedicines loaded with SPIONs for targeted drug delivery to particularly liver tumors using an external magnetic field.[16,17] Nanocarrier platforms loaded with SPIONs and evodiamine have been developed to enable magnetic targeting ability and high accumulation at the target site.[17] SPION-loaded polymeric micelles show prolonged blood circulation times, increased MRI sensitivity, as well as improved biocompatibility.[18] This study aims to develop the magnetic nanocarrier of QCT using polymeric micelles in order to improve disease monitoring and therapy of HCC. The obtained polymeric micelles were characterized for their particle size, morphology, and magnetic properties. Finally, the micelles were evaluated for cytotoxicity, cellular uptake, cell cycle analysis, and magnetic targeting potential in hepatitis B virus-transfected HCC (HepG2.2.15) cells.

Methods

Materials

QCT and Dulbecco's modified Eagle's medium (DMEM) were from Sigma-Aldrich (St. Louis, MO). Penicillin-streptomycin and trypsin-ethylenediaminetetraacetic acid (EDTA) were from GIBCO™ Invitrogen (Grand Island, NY). Ethanol, dichloromethane, and dimethyl sulfoxide (DMSO) were from Merck (Darmstadt, Germany). Fetal bovine serum was from Biochrom AG (Berlin, Germany). The other chemicals were of the highest available grade. mPEG750-*b*-OCL-Bz was prepared as previously reported.[19] The average degree of polymerization of mPEG750 and caprolactone were 17 ($_{av17}$) and 4 ($_{av4}$), respectively.

Preparation of SPIONs

SPIONs were prepared using the co-precipitation method previously reported with some modification.[20] Ferrous sulfate heptahydrate ($FeSO_4 \cdot 7H_2O$, 9.25 mM) and ferric chloride hexahydrate ($FeCl_3 \cdot 6H_2O$, 18.50 mM) were dissolved in deionized (DI) water. The pH of the mixture was adjusted to 10 by 7% NH_4OH at room temperature and dark brown particles (Fe_3O_4) were formed. To avoid SPION agglomeration, oleic acid (35 mM) was added resulting in the coating of SPIONs. The mixture was heated to 90°C with vigorous stirring for 1 h under nitrogen atmosphere and reflux condition. SPIONs were separated using a Neodymium Iron Boron (NdFeB) magnetic disc (0.3 cm × 2 cm) and washed with DI water (2 times) and ethanol (2 times) by centrifugation at 4000 rpm for 10 min. Finally, SPIONs were dried in a hot air oven (45°C) overnight and kept at room temperature.

Preparation of QCT-SPION-Loaded mPEG750-b-OCL-Bz Micelles and QCT-Loaded mPEG750-b-OCL-Bz Micelles

QCT and SPIONs were loaded into mPEG750-*b*-OCL-Bz micelles by a film hydration method previously reported,[13] with some modifications. A solution of QCT (5 mg in 1 mL ethanol), dispersion of SPIONs (1-15 mg in 5 mL tetrahydrofuran), and solution of mPEG750-*b*-OCL-Bz (100 mg in 10 mL dichloromethane) were mixed in a round-bottom flask. The organic solvents were removed using a rotary evaporator to obtain a thin film. Subsequently, this film was hydrated by DI water at room temperature and sonicated for 30 min. Non-entrapped (precipitated) QCT or SPIONs were removed using a microfilter (0.2-μm nylon syringe filter).

Characterization of SPIONs, QCT-SPION-Loaded Micelles, and QCT-Loaded Micelles

Transmission electron microscopy (TEM) was performed on SPIONs, empty mPEG750-b-OCL-Bz micelles, and QCT-SPION-loaded mPEG750-*b*-OCL-Bz micelles to evaluate their morphology and particle size. Moreover, selected area electron diffraction patterns of SPIONs were also obtained with TEM. TEM samples were prepared on a copper grid, and the microscope (JEOL JEM-2200FS) was operated at 200 kV. Besides, magnetic property of the obtained SPIONs was characterized by vibrating sample magnetometry (Lakeshore Model 7404 with 4-inch electromagnet). All samples were freeze-dried in liquid nitrogen and lyophilized under vacuum. The magnetic field was applied at 12 kOe. Experimental type was hysteresis with time constant and total point values of 0.1 and 100, respectively. All measurements were carried out at room temperature.

The amount of loaded QCT in QCT-SPION-loaded micelles was determined by UV-Vis spectroscopy with absorbance wavelength of 375 nm. A sample of the QCT-SPION-loaded micelles dispersion (10 μL) was diluted with 2 mL DMSO before UV absorption measurement. Calibration of QCT was carried out by dissolving QCT in DMSO at 1-20 μg/mL. On the other hand, the loaded amount of the SPIONs was determined using a GBC/932 plus atomic absorption spectroscopy with a hollow cathode lamp. A sample of QCT-SPION-loaded micelles (100 μL) was added to 1 M HCl (5 mL). The instrumental parameters were set up in agreement with the manufacturer's recommendations. The flame composition was air-acetylene with fuel flow and air flow of 2 and 10 L/min, respectively. The lamp current was set at 7 mA and absorbance wavelength of SPIONs was 248 nm. Loading capacity (LC) and the entrapment efficiency (EE) were calculated by the following formulas: LC (%w/w) = (quantity of loaded QCT or SPIONs/quantity of initial polymer) × 100 and EE (%w/w) = (quantity of loaded QCT or SPIONs/quantity of initial QCT or SPIONs) × 100.

The hydrodynamic size of micelles was measured by dynamic light scattering (Zetasizer®; Malvern, Malvern, UK). FTIR spectroscopy of QCT, SPIONs, mPEG750-*b*-OCL-Bz polymer, QCT-loaded micelles, and QCT-SPION-loaded micelles were performed using a Nicolet Nexus 470 microscope in the transmission mode by the potassium bromide pellet method, with the wave number ranging from 400 to 4000 cm-1.

QCT-SPION-loaded micelle dispersions were stored at room temperature for 2 months. The particle size analyzer and HPLC (a Hewlett Packard with UV-visible detector) were used to check the stability of the QCT-SPION-loaded micelles. The HPLC column was C-18 column (250 × 4.6 mm, 5 μm particle size, SB-C18; Hypersil®) and the elution solvent was 85% methanol (15% water). Chromatograms were recorded at 254 nm.

Relaxivity Measurement

Transverse (T_2) relaxivity of SPIONs and QCT-SPION-loaded micelles were measured using a 1.5 T clinical magnetic resonance

scanner at room temperature. Samples were prepared using tissue equivalent phantom gel.[21] SPIONs and QCT-SPION-loaded micelles were mixed with acrylamide and bis-acrylamide to final concentration of 4% of both reagents. Subsequently, 0.05% ammonium persulfate and 0.05% tetramethylethylenediamine were added. The mixture was kept at room temperature for 90 min to allow polymerization. Subsequently, T_2-weighted images of the different samples were acquired using the following parameters: echo time (TE): 45-300 ms, field of view (FOV): 120 mm, slice thickness: 2.0 mm, and flip angle: 90°. The signal intensity of T_2-weighted images was plotted against TE. A fitting curve was obtained using OriginPro 2015 software to determine the T_2 values. Relaxation rate ($1/T_2$) versus SPION concentration was plotted to obtain a linear relationship. T_2 relaxivity value was calculated from the slope of the linear graph. High value of T_2 relaxivity represents high sensitivity of SPIONs and QCT-SPION-loaded micelles for negative contrast enhancement.[22]

Cell Culture

HepG2.2.15 cells which are more resistant to anti-cancer drugs than parental HCC (HepG2) cells[23] were cultured using a standard method for adherent cells. Briefly, the cells (2×10^6 cells) were cultured in 10 mL DMEM with 10% fetal bovine serum, penicillin (100 UI/mL), and streptomycin (100 μg/mL). The flask was kept in a humidified incubator (5% CO_2, 37°C). The culture medium (DMEM) was changed every 3 days to maintain the pH around 7.6-7.8.

Cellular Uptake of QCT-SPION-Loaded Micelles

This experiment was performed using HepG2.2.15 cells and Prussian blue staining technique.[24] HepG2.2.15 cells were seeded into 6-well plates at a density of 1×10^5 cells/well in 2 mL of DMEM and incubated for 24 h at 37°C. Subsequently, the cells were washed with phosphate buffered saline (PBS) twice and replaced by fresh medium containing QCT-SPION-loaded micelles (50 μM) and incubated at 37°C for 5 h. The cells were then washed with PBS twice and fixed with 10% paraformaldehyde for 20 min before washing twice with PBS. The fixed cells were incubated with fresh Pearl's Prussian blue reagent (5% potassium ferrocyanide: 5% HCl, 1:1 v/v) for 60 min and washed 3 times with distilled water. After that, eosin solution (1 mL, 0.5% w/v eosin in 1% HCl and 80% ethanol) was added and incubated for 1 min. The cells were subsequently washed with distilled water and dehydrated with ethanol in gradient concentrations from 30% to 100%. Finally, the cells were observed under a microscope to visualize the uptake of QCT-SPION-loaded micelles.

Inductively coupled plasma mass spectrometer (Agilent 7500 C, Tokyo, Japan) was performed to quantify the iron uptake. The QCT-SPION-loaded micelle-treated HepG2.2.15 cells were weighted and digested in 65% HNO_3 for 2 h at 95°C. The final iron concentration was calculated as weight percentage over the total weight of the cells.

Cellular Toxicity

The HepG2.2.15 cells (1×10^5 cells/well) were seeded into 6-well plates. Next, 0-40 μL solutions/dispersions with different concentrations were added (0-60 μM of QCT, 0-12 μM of SPIONs, and 0-260 μM of the polymer) to 2 mL culture medium. QCT was added using a stock solution in ethanol (the ethanol concentration in the cell culture medium did not exceed 0.5%). Next, the cells were incubated for 72 h in a humidified incubator (5% CO_2, 37°C) and the cells were analyzed using the 3-(4,5-dimethylthiazol-2-yl)-2,5-

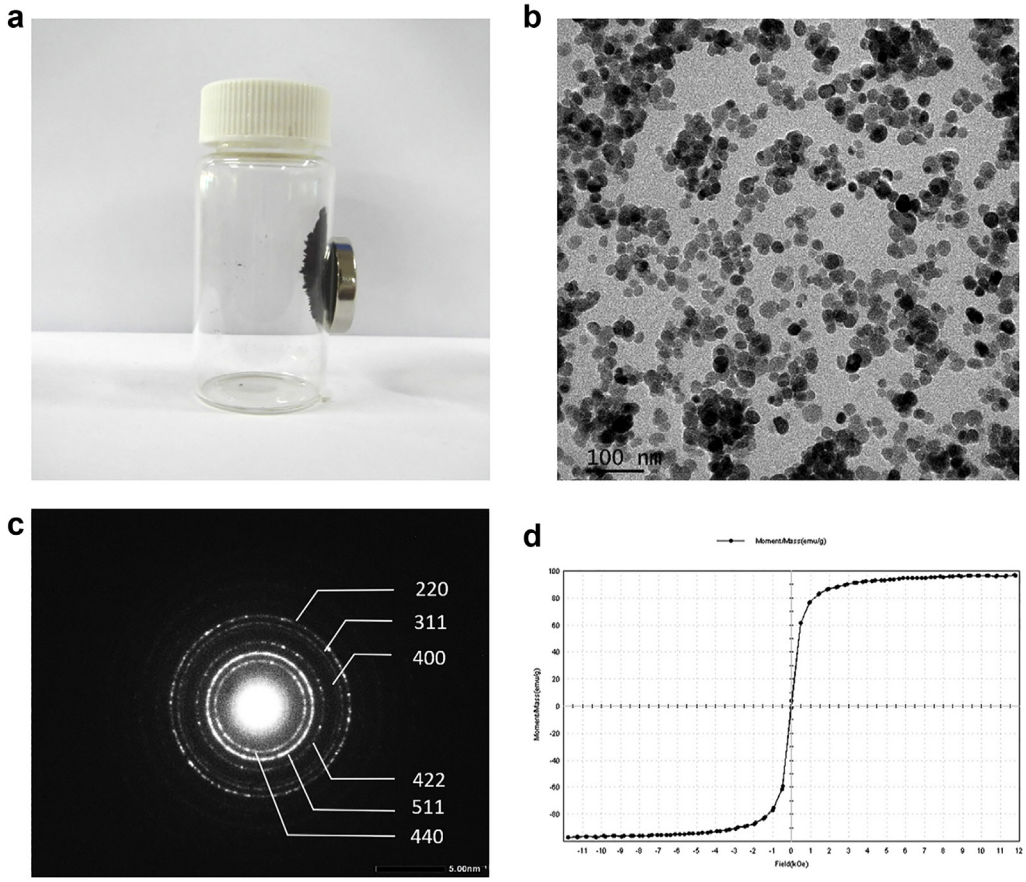

Figure 1. Characterizations of SPIONs: physical appearance (a), TEM image (b), SAED pattern (c), and hysteresis curve (d). SAED, selected area electron diffraction patterns.

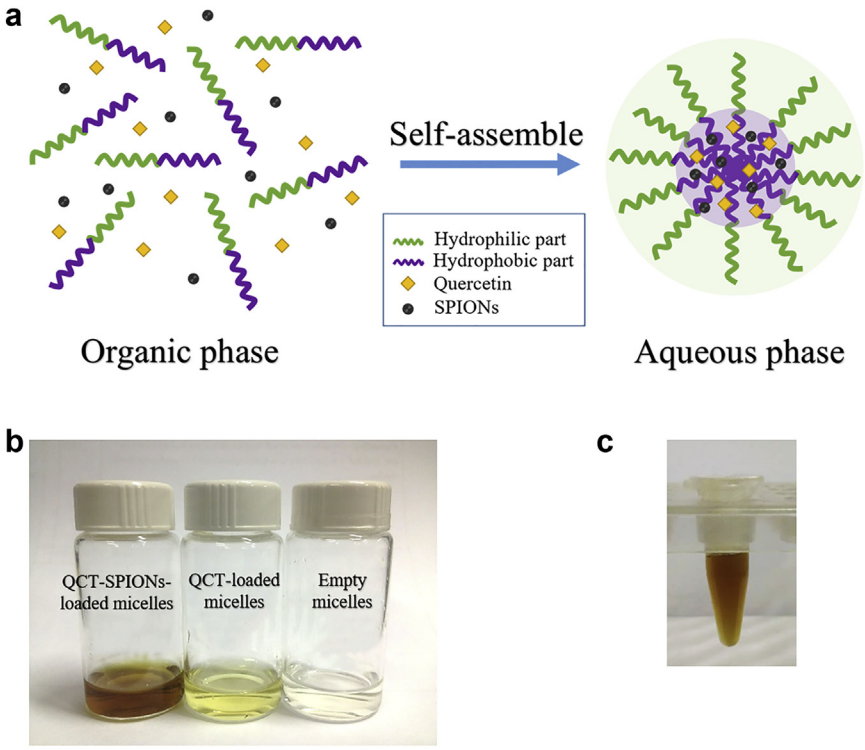

Figure 2. Self-assemble scheme of co-entrapment between QCT and SPIONs in polymeric micelle (a); physical appearance of QCT-SPION-loaded micelles, QCT-loaded micelles, and empty mPEG750-*b*-OCL-Bz micelles (b); and physical appearance of QCT-SPION-loaded micelles after storage at room temperature for 5 weeks (c).

diphenyltetrazolium bromide assay to determine cell viability. The IC_{50} value (50% inhibitory concentration) was determined from the graph plotted between % cell viability and sample concentrations.

Effect of QCT-SPION-Loaded Micelles on Cancer Cell Cycle Progression

Propidium iodide (PI) is the most frequently used for DNA binding in the experiment of cell cycle analysis determined by flow cytometry. Nevertheless, PI also binds with RNA, thus the staining process usually includes RNase to discard RNA and detergent (Triton X-100) to wipe out the cell membrane and cytoplasm. The measurements were performed in the same manner as described previously.[13] Briefly, HepG2.2.15 cells (5×10^5 cells) were seeded into 6-well plates and then exposed to the tested samples in a humidified incubator (5% CO_2, 37°C) for 24 h. After incubation, the treated cells were washed 2 times with PBS. Next, 0.05% trypsin containing 0.02% EDTA was directly added. The detached cells were washed with PBS and subsequently fixed with 70% ethanol overnight. After that, the cells were stained by PI containing RNase (0.2 mg/mL) and 0.1% Triton X-100 for 30 min at 37°C in the dark place. The cell cycle progression was analyzed using a flow cytometer (Beckman Coulter CyAn ADP). The experiment was carried out at a low flow rate for optimal resolution of PI fluorescence. PI fluorescence intensity was collected on FL2 of a flow cytometer. Flow cytometer was set at 488 nm laser illumination (excitation maximum = 493 nm; emission maximum = 636 nm). OriginPro software was used to analyze the DNA content of the cell cycle (phase G0/G1, S, G2/M).

Annexin V-fluorescein isothiocyanate (Annexin V-FITC) assay was performed for apoptosis detection. The detached cells were washed with PBS and subsequently added with binding buffer. Then Annexin V-FITC and PI were added. The prepared cells were incubated at room temperature with light protection for 10 min. The fluorescence of the cells was determined immediately with a flow cytometer. The flow cytometer was set at excitation 488 nm and emission 530 nm. PI and FITC fluorescence intensity were collected on FL2 and FL1, respectively. The apoptosis analysis was performed by Flowing Software.

Cellular Magnetic Targeting Properties

Cellular magnetic targeting properties of QCT-SPION-loaded micelles were investigated in HepG2.2.15 cells as described in a previous study.[17] HepG2.2.15 cells (1×10^6 cells) were seeded in a T25 culture

Table 1
Average Particle Size and Loading Efficiency of QCT-SPION-Loaded Micelles

Polymer/QCT/SPIONs (w/w/w)	Z_{ave} (nm)	PdI	QCT		SPIONs	
			EE (%)	LC (%)	EE (%)	LC (%)
20:1:0	14 ± 1	0.17 ± 0.03	97.19 ± 1.08	4.86 ± 0.05	–	–
20:1:0.2	22 ± 0	0.48 ± 0.02	69.76 ± 2.00	3.49 ± 0.10	7.32 ± 0.20	0.37 ± 0.01
20:1:0.5	20 ± 0	0.34 ± 0.02	66.11 ± 1.75	3.30 ± 0.09	8.13 ± 0.11	0.41 ± 0.01
20:1:1	40 ± 1	0.25 ± 0.04	64.15 ± 3.42	3.21 ± 0.17	15.08 ± 0.10	0.75 ± 0.01
20:1:2	49 ± 1	0.31 ± 0.04	61.82 ± 2.11	3.09 ± 0.10	7.79 ± 0.15	0.39 ± 0.01
20:1:3	55 ± 1	0.37 ± 0.06	53.54 ± 2.90	2.68 ± 0.15	8.51 ± 0.12	0.43 ± 0.01

PdI, polydispersity index.

flask containing DMEM and incubated in a humidified incubator (5% CO_2, 37°C) for 24 h. QCT-SPION-loaded micelles was added into the culture flask and the NdFeB magnetic disc (0.3 cm × 2 cm) was subsequently placed at the bottom of the culture flask. The cells were incubated for 48 h to evaluate the magnetic targeting properties. Cellular morphology and distribution at the magnetic targeted area and the weak magnetic field area were observed under a light microscope.

Statistical Analysis

The results are reported as mean ± standard deviation for triplicate independent experiments. Statistical analysis was carried out using an unpaired t-test. p value less than 0.05 was considered statistically significant.

Results and Discussion

Preparation and Characterization of SPIONs

SPIONs with good magnetic property were successfully synthesized by the co-precipitate method (Fig. 1a). Aggregation behavior is the crucial limitation of SPIONs synthesized by the co-precipitate method. Naked SPIONs present a large surface-to-volume ratio and lead to high surface energies of these SPIONs. Therefore, naked SPIONs tend to aggregate to minimize the surface energies.[25] Surface modification with dextran, polyethyleneglycol (PEG), poly(vinylpyrrolidone), citric acid, and oleic acid has been utilized to reduce aggregation.[25-27] The mechanism to reduce the naked SPION aggregation by oleic acid coating has been reported, whereby oleic acid adsorbs on SPIONs by strong chemical bond between the carboxylic acid and amorphous SPIONs. This action enhances the osmotic pressure or repulsion force to balance the increasing Van der Waals energies (attraction) resulted from smaller size of SPIONs.[25,28] Surface modification of SPIONs with oleic acid coating was therefore performed in this study. TEM was used to determine the morphology and crystallinity of SPIONs. The results reveal that SPIONs were spherical in shape with an average size of 16 ± 2 nm (Fig. 1b), which is similar to the previous reports.[25,29] Selected area electron diffraction pattern (Fig. 1c) confirmed the magnetite structure of SPIONs. Besides, magnetization hysteresis curves with zero remanence represent the superparamagnetic behavior of the obtained SPIONs as shown in Figure 1d. The values of saturation magnetization and coercivity were 97.054 emu/g and 14.744 Oe, respectively. It has been reported that saturation magnetization values of SPIONs were around 65-78 emu/g.[25,28,29] Compared to previous reports, the obtained SPIONs from this study had high saturation magnetization value resulting in the pure and good crystal structure of SPIONs.

Preparation and Characterization of QCT-SPION-Loaded Micelles and QCT-Loaded Micelles

Co-entrapment of QCT and SPIONs into mPEG750-*b*-OCL-Bz co-polymer was investigated for specific targeted delivery (Fig. 2a). The obtained QCT-SPION-loaded micelles appeared as clear brown which is the blended color of QCT and SPIONs. QCT-loaded micelles and empty polymeric micelles appeared as yellow and colorless dispersions, which are the color of QCT and mPEG750-*b*-OCL-Bz co-polymer, respectively (Fig. 2b). To optimize the suitable formulation, the amount of SPIONs varied while the ratio of polymer/QCT was fixed at 20:1, corresponding to the highest EE of QCT loading.[13] The average hydrodynamic size (Z_{ave}) of QCT-SPION-loaded micelles was in the range of 22-55 nm, which was higher than QCT-loaded micelles (14 nm) and depended on the amount of SPIONs used for loading. An increase in the initial amount of SPIONs caused the increase in the average size of QCT-SPION-loaded micelles (Table 1). This is in line with the finding of Hong et al.[30] who found that the particle size of SPION-loaded PEG-PCL (38 nm) is bigger than that of empty micelles (28 nm).

The morphology of empty mPEG750-*b*-OCL-Bz micelles observed by TEM was near-spherical with average size of 20 ± 4 nm (Fig. 3a). TEM images of QCT-SPION-loaded micelles indicate that the particles of QCT-SPION-loaded micelles were also spherical in shape (Fig. 3b). Particle sizes of QCT-SPION-loaded micelles measured by TEM were in the range of 20-50 nm, which was in agreement with the findings of the dynamic light scattering analysis. In the liver, the particle size that enables tumor accumulation after intravenous administration by EPR effect and can fenestrate the liver sinusoid should be less than 100 nm.[31,32] The QCT-SPION-loaded micelles obtained from this study were therefore the appropriate size for liver tumor targeted therapy.

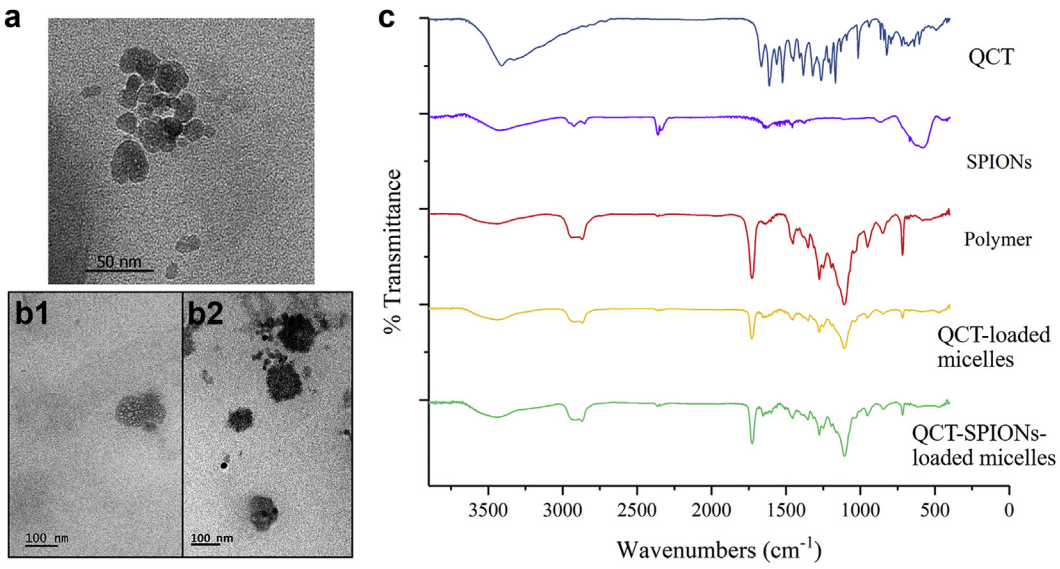

Figure 3. TEM image of empty mPEG750-*b*-OCL-Bz micelles (a); TEM image of QCT-SPION-loaded micelles (b); and FTIR spectrum of QCT, SPIONs, mPEG750-*b*-OCL-Bz polymer, QCT-loaded micelles, and QCT-SPION-loaded micelles (c).

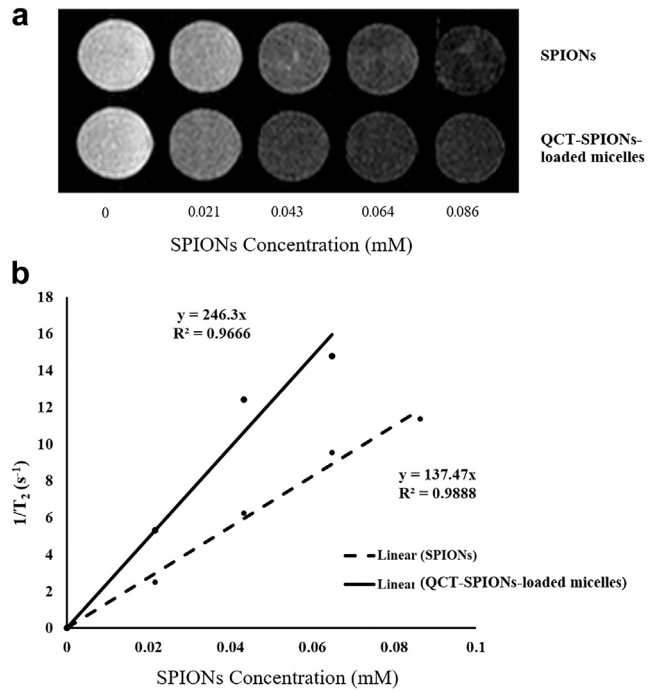

Figure 4. Relaxivity measurement: the T_2-weighted images of SPIONs and QCT-SPION-loaded micelles (a) and relationship between T_2 relaxivity rate ($1/T_2$, 1/s) and SPIONs concentration (mM) on MRI scanner (b).

The maximum EE and LC of QCT in QCT-SPION-loaded micelles were at 70% and 3.5%, respectively (Table 1). At the same time, the highest SPION content in QCT-SPION-loaded micelles was 15% (EE) and 0.8% (LC). Keeping QCT-SPION-loaded micelles at room temperature for 5 weeks, physical appearance of QCT-SPION-loaded micelles remain unchanged (as shown in Fig. 2c). Besides, the QCT content of the QCT-SPION-loaded micelles was not different and any degradation product could not be observed after HPLC analysis (Fig. 8). Table 2 shows that the average size of QCT-SPION-loaded micelles gradually increased (from 63 nm at fifth week to 83 nm at ninth week) indicating that some aggregation might have occurred. Besides, EE of QCT subsequently decreased with time (from 68% at fifth week to 27% at ninth week). Based on the size, polydispersity index, and loading efficiency, QCT-SPION-loaded micelles composed of polymer/QCT/SPIONs of 20:1:1 ratio was chosen for further study because this system gave appropriate properties of small size, low polydispersity index, and high EE.

FTIR Analysis

FTIR spectroscopy was used to find chemical bonding, molecular structure, and intermolecular interaction. The interaction among QCT, SPIONs, and mPEG750-*b*-OCL-Bz polymer was defined. Figure 3c shows FTIR spectra of QCT, SPIONs, mPEG750-*b*-OCL-Bz co-polymer, QCT-loaded micelles, and QCT-SPION-loaded micelles. The bands at 1700-1500 cm-1 and 3550-3200 cm-1 represent aromatic C=C bending and −OH stretching phenolics of QCT, respectively. The characteristic peak of SPIONs (Fe-O) was observed at 580 cm-1. The bands of the co-polymer located at 1109 cm-1 and 1728 cm-1 represent aliphatic ether (R-O-R′) and ester C=O stretches, respectively. The spectra of QCT-loaded micelles and QCT-SPION-loaded micelles also showed the co-polymer signature without shift in the single band. These results indicated that interaction among QCT, SPIONs, and polymeric micelles was not observed.

Table 2
Colloidal Stability of QCT-SPION-Loaded Micelles, Particle Size, and Loading Efficiency

Duration (wk)	Z_{ave} (nm)	PdI	Loaded QCT	
			%EE	%LC
1	59 ± 1	0.20 ± 0.01	64.23 ± 1.35	3.21 ± 0.07
3	64 ± 1	0.32 ± 0.05	61.66 ± 1.37	3.08 ± 0.07
5	63 ± 2	0.30 ± 0.04	67.67 ± 0.51	3.38 ± 0.03
7	76 ± 4	0.37 ± 0.07	46.59 ± 0.92	2.33 ± 0.05
9	83 ± 1	0.31 ± 0.02	27.45 ± 1.97	1.37 ± 0.10

PdI, polydispersity index.

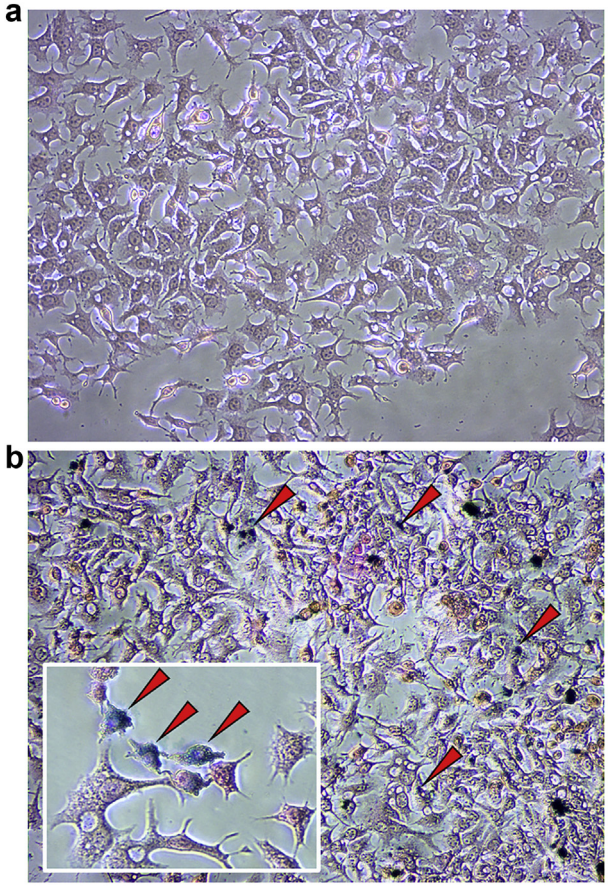

Figure 5. Cellular uptake was performed by the Prussian blue staining. The images of the control HepG2.2.15 cells (a) and HepG2.2.15 cells after treatment with QCT-SPION-loaded micelles; QCT concentration of 50 μM (b) at 37°C for 5 h, ×100 magnification.

Relaxivity Measurement

The magnetic property of SPIONs and QCT-SPION-loaded micelles was verified using a clinical 1.5 T MRI scanner. The intensity of T_2-weighted images gradually decreased when SPION concentration of both QCT-SPION-loaded micelles and SPIONs increased (Fig. 4a). Therefore, QCT-SPION-loaded micelles and SPIONs could be good MRI contrast agents. The signal loss of the T_2-weighted images of QCT-SPION-loaded micelles was higher than that of SPIONs confirming that QCT-SPION-loaded micelles were better MRI contrast agent than SPIONs. Figure 4b presents that both SPIONs and QCT-SPION-loaded micelles had good MRI sensitivity with T_2 relaxivity values of 137.47 $mM^{-1}s^{-1}$ and 246.30 $mM^{-1}s^{-1}$, respectively. Interestingly, T_2 relaxivity value of QCT-SPION-loaded

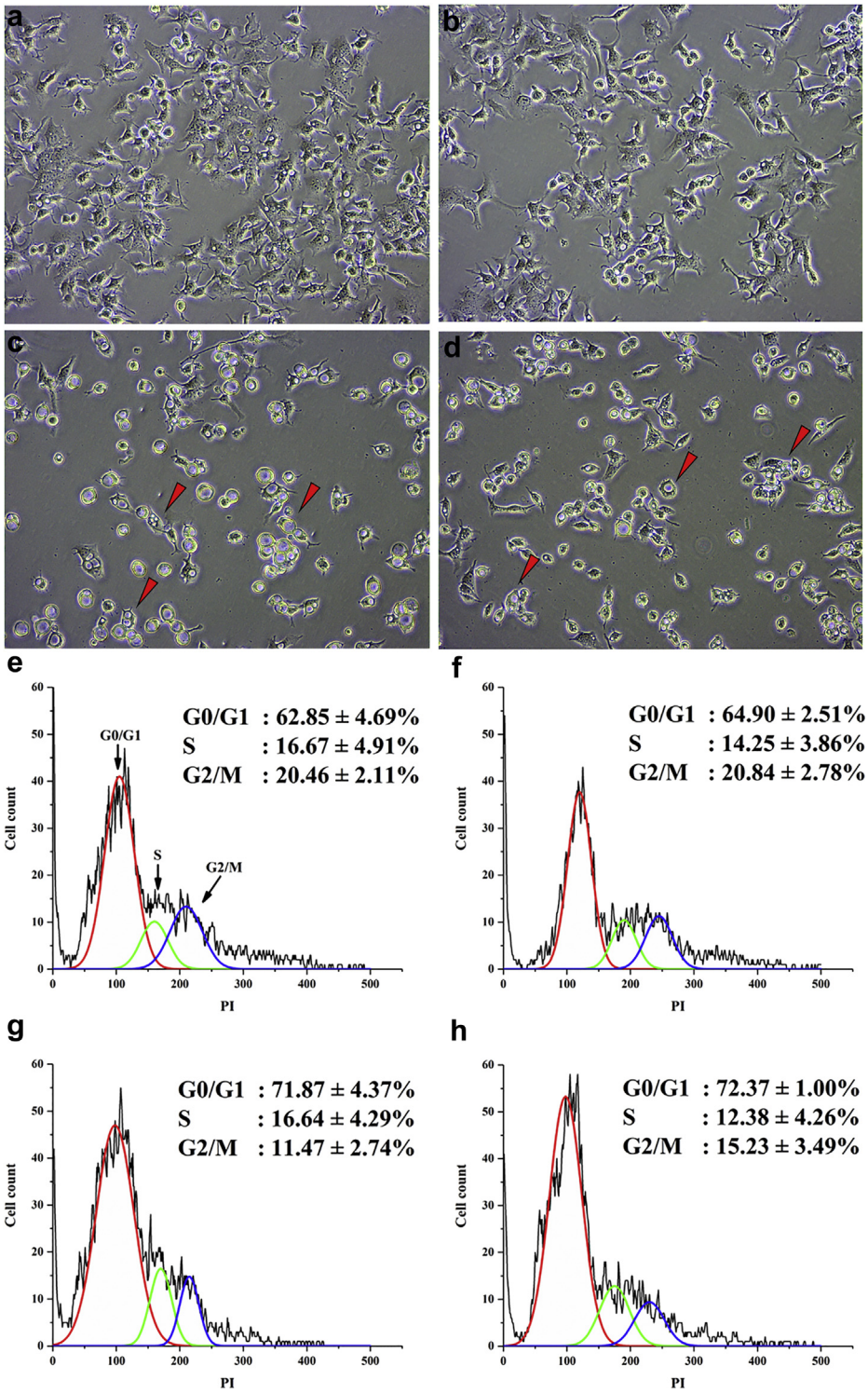

Figure 6. Morphology of the control HepG2.2.15 cells (a), HepG2.2.15 cells after incubation with SPION-loaded mPEG750-*b*-OCL-Bz micelles; SPIONs concentration of 14 μM (b); with QCT, QCT concentration of 50 μM (c) and with QCT-SPION-loaded micelles, QCT concentration of 50 μM (d) at 37°C for 24 h, ×100 magnification. Cell cycle analysis of DNA content of the control HepG2.2.15 cells (e) and HepG2.2.15 cells after incubation with SPION-loaded mPEG750-*b*-OCL-Bz micelles; SPIONs concentration of 14 μM (f); with QCT, QCT concentration of 50 μM (g) and with QCT-SPION-loaded micelles, QCT concentration of 50 μM (h) at 37°C for 24 h. The values are presented as mean ± SD ($n = 3$), which applies only to panels (e), (f), (g), and (h).

micelles was 2 times higher than that of SPIONs. This may be due to the clustering effect of SPIONs in polymeric micelles. Our finding is in line with other reports using other polymers. For examples, SPION-loaded mPEG-*b*-p(HPMAm-Lac2) (50-70 $mM^{-1}s^{-1}$) has higher T_2 relaxivity value than SPIONs coated with dextran (30-50 $mM^{-1}s^{-1}$), and SPION-loaded PEG-PCL (110 $mM^{-1}s^{-1}$) presents better MRI signal than hydrophilic Fe_3O_4 nanoparticles (40 $mM^{-1}s^{-1}$).[27,33] The high T_2 relaxivity value of the QCT-SPIONs-loaded micelles obtained in this study was resulting in their better accuracy of MRI.

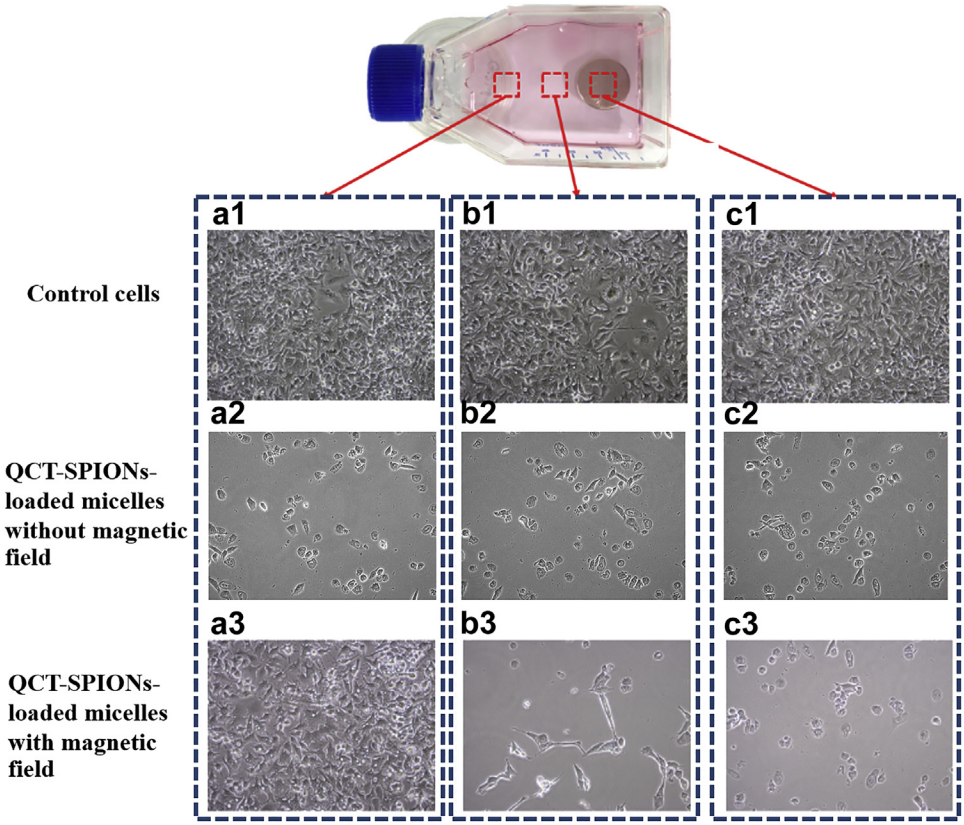

Figure 7. Magnetic targeting: the microscopic images of the control HepG2.2.15 cells (1); HepG2.2.15 cells incubated with QCT-SPION-loaded micelles; QCT concentration of 50 μM, without magnetic field (2) and HepG2.2.15 cells incubated with QCT-SPION-loaded micelles; QCT concentration of 50 μM, after external magnetic field was applied (3) at 37°C for 72 h. Area (a) indicates the weakest magnetic field strength, while area (b) and area (c) indicate higher magnetic field strength, in ascending order, ×100 magnification.

Determination of QCT-SPION-Loaded Micelles Uptake

Intracellular drug concentration is an important factor for effectiveness of treatment. To clarify this issue, QCT-SPION-loaded micelles were tracked using Prussian blue staining technique which is used to detect SPIONs in cells. The presence of SPIONs results in blue color staining. The result presented in Figure 5 shows that blue color was not observed in the control HepG2.2.15 cells but

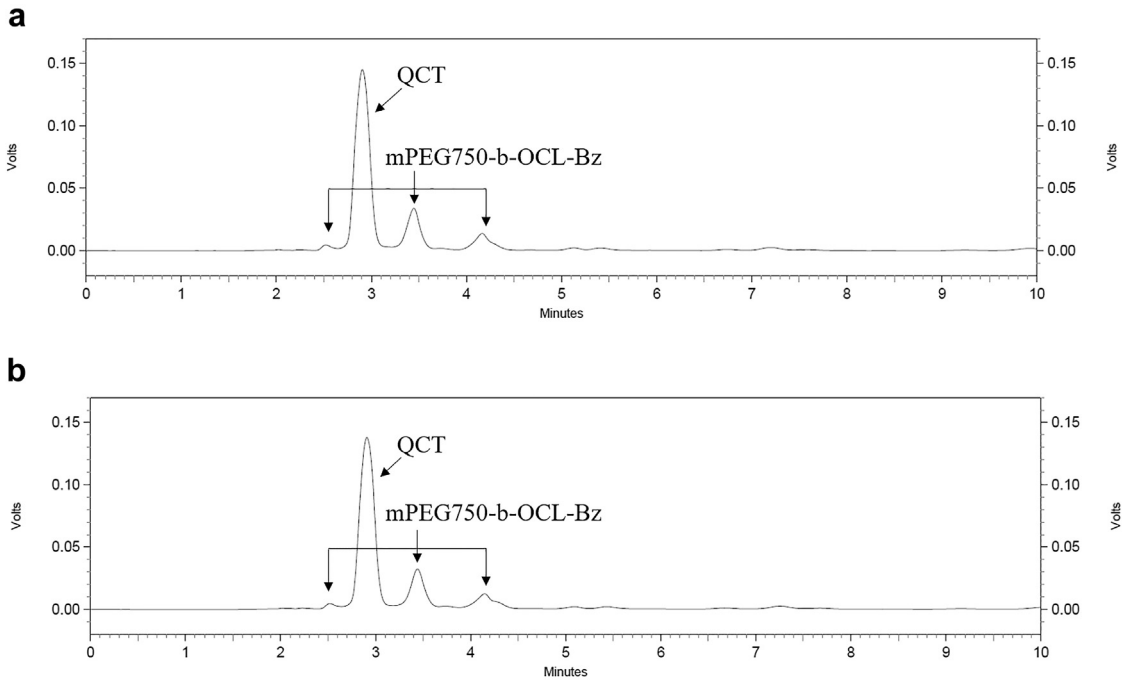

Figure 8. HPLC chromatogram at 254 nm of QCT-SPION-loaded micelles at room temperature on the 1st day (a) and 5th week (b).

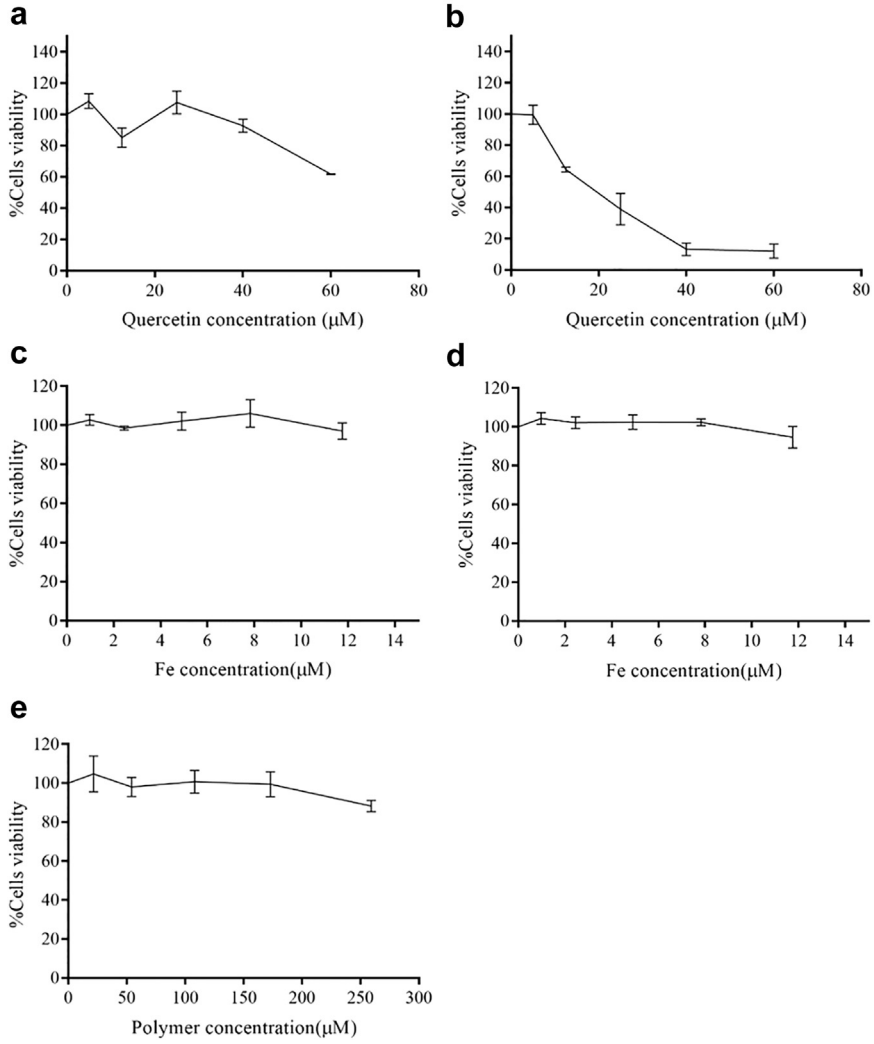

Figure 9. Cytotoxicity of HepG2.2.15 cells treated with free QCT (a), QCT-SPION-loaded micelles (b), SPIONs (c), SPION-loaded micelles (d), and empty mPEG750-*b*-OCL-Bz micelles (e).

was clearly observed in the QCT-SPION-loaded micelle-treated cells indicating that QCT-SPION-loaded micelles were taken up into the HepG2.2.15 cells. In addition, inductively coupled plasma mass spectrometer result shows that the total amount of ion per cells of QCT-SPION-loaded micelles (48.80 ± 10.18 pgFe/cell) was higher than control HepG2.2.15 cells (0.31 ± 0.07 pgFe/cell). In other studies, PEG-*b*-PLA polymeric micelles and PEG-PCL were previously reported to be taken up by human ovarian (A2780) and HepG2 cells, respectively.[34,35] The cellular uptake mechanism of colloidal particles is influenced by important parameters such as surface property, rigidity, shape, and size. The uptake of large particles (>500 nm) is usually through phagocytosis pathway, whereas the small particle (<200 nm) is usually through pinocytosis pathway.[36,37] According to the small size of QCT-SPION-loaded micelles (22-55 nm), the cellular uptake mechanism of QCT-SPION-loaded micelles is considered by pinocytosis which might be via clathrin-mediated endocytosis, caveolin-mediated endocytosis, and clathrin/caveolin independent endocytosis pathways which may depend on both the chemical structure of colloidal particles and cell types.[36]

Cellular Toxicity

HepG2.2.15 cells were transfected by hepatitis B virus to induce multiple drug resistance.[23] QCT-SPION-loaded micelles and QCT showed cytotoxicity effect against HepG2.2.15 cells with IC_{50} values of 17.02 ± 2.82 and 207.90 ± 63.08 μM, respectively. In a previous study, the cytotoxicity of QCT in sensitive breast cancer cells (MCF-7) and resistant breast cancer cells (MCF-7/ADR) was reported with IC_{50} values of 16.32 and 16.87 μg/mL, respectively.[38] It was also reported that QCT (0.1-100 μM) has no toxicity against HepG2.2.15 cells.[39] In this study, the IC_{50} value of QCT against HepG2.2.15 cells was higher than 100 μM. Moreover, SPIONs (0-12 μM), empty mPEG750-*b*-OCL-Bz micelles (0-260 μM), and SPION-loaded micelles did not exhibit any cytotoxicity against HepG2.2.15 cells (Fig. 9). Remarkably, this result indicates that QCT-SPION-loaded micelles had significantly ($p < 0.05$) higher cytotoxicity against HepG2.2.15 cells than QCT. Furthermore, SPIONs and QCT did not display synergistic effect (data not shown), presenting no synergism on cancer cell treatment from QCT-SPION-loaded micelles. Cellular uptake of doxorubicin-conjugated poly(lactic-co-glycolic acid)-PEG block co-polymers has been found to become enhanced due to their facilitated endocytotic transport (likely, fluid-phase endocytotic), and higher cytotoxicity against HepG2 cells than doxorubicin has also been observed.[40] Recent study reported that polymeric micelles can inhibit P-glycoprotein function. The micelles cause cell membrane depolarization and enhance membrane microviscosity, leading to inhibition of P-glycoprotein function.[41] This mechanism decreases the loss of intracellular drug concentration. Therefore, the

enhancement cytotoxic effect found in this study was due to the improved intracellular concentration of QCT by mPEG750-*b*-OCL-Bz micelles.

Effect of QCT-SPION-Loaded Micelles on Cancer Cell Cycle Progression

In this experiment, HepG2.2.15 cells without treatment were used as a negative control group. HepG2.2.15 cells treated with SPION-loaded micelles (without QCT) were used as vehicle control. QCT treated groups consisted of HepG2.2.15 cells treated with QCT and QCT-SPION-loaded micelles. Figures 6a-6d show that morphological alteration occurred in QCT and QCT-SPION-loaded micelle-treated cells. These cells showed bigger vacuoles, rounder cell shape, and higher number of detached cells than the negative and vehicle control groups.

Most cells can regenerate new cells to replace damaged and dead cells by doubling its DNA content with 2 sets of chromosomes and subsequently cells division. The cell division can split into 5 main phases: G0, G1, S, G2, and M. Cell cycles start with the DNA synthesis phase (S phase) before entering the cell mitotic phase (M phase). The gap between the end of the mitotic phase and the synthesis phase is G0 or G1 phases, as well as between the end of the synthesis phase and the mitotic phase is the G2 phase. In this study, the HepG2.2.15 DNA content of the QCT treated groups was different from the control group. The percentage cells of the QCT treated groups at the G0/G1 phase significantly ($p < 0.05$) increased, while the number of cells at the G2/M phase decreased in comparison with the control groups (Figs. 6e-6h). Yang et al.[42] reported that the cell cycle of human lung cancer cells is arrested at G2/M by QCT, and that QCT induces apoptosis through caspase-3. The G0/G1 cell cycle arrest phenomenon can be observed after treating HepG2 cells with QCT which is caused by decreased expression of cyclin D1 (controlled transition of G1/S cell cycle phase).[43] Moreover, the apoptotic cell death induced by QCT-SPION-loaded micelles was found by Annexin V-FITC-PI assay. In this study, the mechanism of HCC cell death induced by QCT-SPION-loaded micelles was mediated through the inhibition of cell cycle progression at G0/G1 phase followed by apoptosis cell death.

Magnetic Targeting Properties

Figure 7 presents that the morphology of cells, which were incubated with QCT-SPIONs-loaded micelles and applied with external magnetic field, in the very low magnetic field area (area A3) had epithelial-like shape. This cellular morphology was similar to that of the control cells. As far as the moderate magnetic field area (area B3) is concerned, not only low cellular density but also morphological alteration was observed in this area. In the high magnetic targeted area (area C3), the cell morphology changed from polygonal shape to spherical shape, indicating the cytotoxicity of the targeting QCT-SPION-loaded micelles. These results clearly demonstrate that the extrinsic magnetic field can increase the accumulation of QCT-SPION-loaded micelles in the targeted area. The cytotoxicity efficacy of QCT can increase in the targeted area (high magnetic field) and decrease in the non-targeted area (low magnetic field). The SPION-loaded polymeric micelles were previously reported to increase the concentration of evodiamine in the targeted area using the external magnetic field.[17] Furthermore, SPION-poly(caprolactone)-carbazole nanoparticles can transfer drugs to the target via the external magnetic field.[44] The result of this study clearly reveals that magnetic nanocarrier for inhibition of HCC cell growth was successful developed by co-encapsulation of QCT and SPIONs into mPEG750-*b*-OCL-Bz micelles.

Conclusion

A promising nanomagnetic drug delivery of QCT can be fabricated by co-delivery of QCT and SPIONs into mPEG750-*b*-OCL-Bz micelles. This drug delivery platform can improve the drug targeting properties of HepG2.2.15 cells. This is not only to enhance the efficiency but also to decrease the adverse side effects of both anti-cancer compound and imaging agent leading to the improvement of both disease monitoring and therapeutic efficacy. The best system is composed of mPEG750-*b*-OCL-Bz polymer/QCT/SPIONs at a weight ratio of 20:1:1 ratio. This system is suitable for further study in *in vivo* MRI imaging and targeting of drug delivery.

Acknowledgment

The authors would like to acknowledge the financial support by the Thailand Research Fund (TRF) grant for new researchers (grant number MRG6180038) and the research grant from Faculty of Pharmacy, Chiang Mai University. We also thank the Research Center of Pharmaceutical Nanotechnology, Chiang Mai University, Thailand, and the Department of Pharmaceutics, Utrecht Institute for Pharmaceutical Sciences (UIPS), Utrecht University, the Netherlands, for the facility and equipment support.

References

1. El-Serag HB, Rudolph KL. Hepatocellular carcinoma: epidemiology and molecular carcinogenesis. *Gastroenterology*. 2007;132(7):2557-2576.
2. Torre LA, Bray F, Siegel RL, Ferlay J, Lortet-Tieulent J, Jemal A. Global cancer statistics, 2012, CA. *Cancer J Clin*. 2015;65:87-108.
3. Topp ZZ, Sigal DS. Beyond chemotherapy: systemic treatment options for hepatocellular carcinoma. *Translational Cancer Res*. 2013;2(6):482-491.
4. Abou-Alfa GK, Huitzil-Melendez FD, O'Reilly EM, Saltz LB. Current management of advanced hepatocellular carcinoma. *Gastrointest Cancer Res*. 2008;2(2):64-70.
5. Sukowati CH, Rosso N, Crocè LS, Tiribelli C. Hepatic cancer stem cells and drug resistance: relevance in targeted therapies for hepatocellular carcinoma. *World J Hepatol*. 2010;2(3):114-126.
6. Sak K. Cytotoxicity of dietary flavonoids on different human cancer types. *Pharmacogn Rev*. 2014;8(16):122-146.
7. Lamson DW, Brignall MS. Antioxidants and cancer, part 3: quercetin. *Altern Med Rev*. 2000;5(3):196-208.
8. Chen C, Zhou J, Ji C. Quercetin: a potential drug to reverse multidrug resistance. *Life Sci*. 2010;87(11):333-338.
9. Granado-Serrano AB, Martín MA, Bravo L, Goya L, Ramos S. Quercetin induces apoptosis via caspase activation, regulation of Bcl-2, and inhibition of PI-3-kinase/Akt and ERK pathways in a human hepatoma cell line (HepG2). *J Nutr*. 2006;136(11):2715-2721.
10. Lee RH, Cho JH, Jeon YJ, et al. Quercetin induces antiproliferative activity against human hepatocellular carcinoma (HepG2) cells by suppressing specificity protein 1 (Sp1). *Drug Dev Res*. 2015;76(1):9-16.
11. Chavan KM. Novel formulation strategy to enhance solubility of quercetin. *Pharmacophore An Int Res J*. 2014;5(3):358-370.
12. Fang J, Nakamura H, Maeda H. The EPR effect: unique features of tumor blood vessels for drug delivery, factors involved, and limitations and augmentation of the effect. *Adv Drug Deliv Rev*. 2011;63(3):136-151.
13. Khonkarn R, Mankhetkorn S, Hennink WE, Okonogi S. PEG-OCL micelles for quercetin solubilization and inhibition of cancer cell growth. *Eur J Pharm Biopharm*. 2011;79(2):268-275.
14. Van der Meel R, Vehmeijer LJC, Kok RJ, Storm G, van Gaal EVB. Ligand-targeted particulate nanomedicines undergoing clinical evaluation: current status. *Adv Drug Deliv Rev*. 2013;65(10):1284-1298.
15. Mody V, Cox A, Shah S, Singh A, Bevins W, Parihar H. Magnetic nanoparticle drug delivery systems for targeting tumor. *Appl Nanosci*. 2014;4(4):385-392.
16. Lee CM, Jeong HJ, Kim SL, et al. SPION-loaded chitosan-linoleic acid nanoparticles to target hepatocytes. *Int J Pharm*. 2009;371(1):163-169.
17. Lv Y, Ding G, Zhai J, Guo Y, Nie G, Xu L. A superparamagnetic Fe_3O_4-loaded polymeric nanocarrier for targeted delivery of evodiamine with enhanced antitumor efficacy. *Colloids Surf B Biointerfaces*. 2013;110:411-418.
18. Torchilin VP. PEG-based micelles as carriers of contrast agents for different imaging modalities. *Adv Drug Deliv Rev*. 2002;54(2):235-252.
19. Carstens MG, Bevernage JJL, Van Nostrum CF, et al. Small oligomeric micelles based on end group modified mPEG-oligocaprolactone with monodisperse hydrophobic blocks. *Macromolecules*. 2007;40(1):116-122.
20. Massart R. Preparation of aqueous magnetic liquids in alkaline and acidic media. *IEEE Trans Magn*. 1981;17(2):1247-1248.

21. McDonald M, Lochhead S, Chopra R, Bronskill MJ. Multi-modality tissue-mimicking phantom for thermal therapy. *Phys Med Biol*. 2004;49(13):2767-2778.
22. Simon GH, Bauer J, Saborovski O, et al. T1 and T2 relaxivity of intracellular and extracellular USPIO at 1.5T and 3T clinical MR scanning. *Eur Radiol*. 2006;16(3):738-745.
23. Gripon P, Rumin S, Urban S, et al. Infection of a human hepatoma cell line by hepatitis B virus. *Proc Natl Acad Sci U S A*. 2002;99(24):15655-15660.
24. Jouihan H. Iron - Prussian blue reaction - Mallory's method. *Bioprotocol*. 2012;2(13):3-6.
25. Mahdavi M, Ahmad M, Haron M, et al. Synthesis, surface modification and characterisation of biocompatible magnetic iron oxide nanoparticles for biomedical applications. *Molecules*. 2013;18(7):7533-7548.
26. Gupta AK, Gupta M. Synthesis and surface engineering of iron oxide nanoparticles for biomedical applications. *Biomaterials*. 2005;26(18):3995-4021.
27. Kim HC, Kim E, Jeong SW, et al. Magnetic nanoparticle-conjugated polymeric micelles for combined hyperthermia and chemotherapy. *Nanoscale*. 2015;7(39):16470-16480.
28. Zhang L, He R, Gu H-C. Oleic acid coating on the monodisperse magnetite nanoparticles. *Appl Surf Sci*. 2006;253(5):2611-2617.
29. Yin C, Wei XY, Li JH, Wang F. Synthesis and properties of superparamagnetic Fe_3O_4 nanoparticles by co-precipitation process. *Appl Mech Mater*. 2013;377:173-179.
30. Hong G, Zhou J, Yuan R. Folate-targeted polymeric micelles loaded with ultrasmall superparamagnetic iron oxide: combined small size and high MRI sensitivity. *Int J Nanomedicine*. 2012;7:2863-2872.
31. Cabral H, Matsumoto Y, Mizuno K, et al. Accumulation of sub-100 nm polymeric micelles in poorly permeable tumours depends on size. *Nat Nanotechnol*. 2011;6(12):815-823.
32. Hattori Y, Kawakami S, Yamashita F, Hashida M. Controlled biodistribution of galactosylated liposomes and incorporated probucol in hepatocyte-selective drug targeting. *J Control Release*. 2000;69(3):369-377.
33. Talelli M, Rijcken CJF, Lammers T, et al. Superparamagnetic iron oxide nanoparticles encapsulated in biodegradable thermosensitive polymeric micelles: toward a targeted nanomedicine suitable for image-guided drug delivery. *Langmuir*. 2009;25(4):2060-2067.
34. Zhang Z, Xiong X, Wan J, et al. Cellular uptake and intracellular trafficking of PEG-b-PLA polymeric micelles. *Biomaterials*. 2012;33(29):7233-7240.
35. Hu Y, Xie J, Tong YW, Wang CH. Effect of PEG conformation and particle size on the cellular uptake efficiency of nanoparticles with the HepG2 cells. *J Control Release*. 2007;118(1):7-17.
36. Mao Z, Zhou X, Gao C. Influence of structure and properties of colloidal biomaterials on cellular uptake and cell functions. *Biomater Sci*. 2013;1(9):896-911.
37. Conner SD, Schmid SL. Regulated portals of entry into the cell. *Nature*. 2003;422(6927):37-44.
38. Zhao L, Shi Y, Zou S, Sun M, Lil L, Zhail G. Formulation and in vitro evaluation of quercetin loaded polymeric micelles composed of pluronic P123 and D-a-tocopheryl polyethylene glycol succinate. *J Biomed Nanotechnol*. 2011;7(3):358-365.
39. Cheng Z, Sun G, Guo W, et al. Inhibition of hepatitis B virus replication by quercetin in human hepatoma cell lines. *Virol Sin*. 2015;30(4):261-268.
40. Yoo HS, Park TG. Biodegradable polymeric micelles composed of doxorubicin conjugated PLGA-PEG block copolymer. *J Control Release*. 2001;70(1):63-70.
41. Xiao L, Xiong X, Sun X, et al. Role of cellular uptake in the reversal of multidrug resistance by PEG-b-PLA polymeric micelles. *Biomaterials*. 2011;32(22):5148-5157.
42. Yang JH, Hsia TC, Kuo HM, et al. Inhibition of lung cancer cell growth by quercetin glucuronides via G2/M arrest and induction of apoptosis. *Drug Metab Dispos*. 2006;34(2):296-304.
43. Zhou J, Li L, Fang L, et al. Quercetin reduces cyclin D1 activity and induces G1 phase arrest in HepG2 cells. *Oncol Lett*. 2016;12(1):516-522.
44. Chomoucka J, Drbohlavova J, Huska D, Adam V, Kizek R, Hubalek J. Magnetic nanoparticles and targeted drug delivering. *Pharmacol Res*. 2010;62(2):144-149.

รายงานสรุปการนำผลงานวิจัยไปใช้ประโยชน์

สัญญาเลขที่ MRG6180038 **โครงการ** การเพิ่มประสิทธิภาพยารักษามะเร็งในเซลล์ที่มีการแสดงพีจีพีด้วยสารฟลาโวนอยด์ที่ถูกกักเก็บในพอลิเมอริกไมเซลล์.

หัวหน้าโครงการ ผศ.ดร.ภญ.รัตติรส คนการณ์ **หน่วยงาน** คณะเภสัชศาตร์ มหาวิทยาลัยเชียงใหม่
โทรศัพท์ 053-944309, 0846102544 **โทรสาร** 053-944390 **อีเมล์** ruttiros.khonkarn@cmu.ac.th, pharrutty@gmail.com

สถานะผลงาน ☐ **ปกปิด** ☑ **ไม่ปกปิด**

ความสำคัญ / ความเป็นมา

กระบวนการขนส่งสารผ่านเยื่อหุ้มเซลล์ที่มีจำนวนมากในเซลล์มะเร็งที่ดื้อยาเป็นสาเหตุหลักของการดื้อยา ซึ่งส่งผลให้การรักษามะเร็งล้มเหลว ดังนั้นการยับยั้งกระบวนการขนส่งสารผ่านเยื่อหุ้มเซลล์จึงเป็นวิธีที่น่าสนใจในการนำมารักษามะเร็ง

วัตถุประสงค์ของโครงการ

1. เพื่อกักเก็บฟลาโวนอยด์ในพอลิเมอริกไมเซลล์ชนิดเบนโซอิล เมทอกซี โพลิ เอทิลีน ไกลคอล โอลิโกคาโพลแลคโทน
2. เพื่อเพิ่มประสิทธิภาพยารักษามะเร็งในเซลล์ที่มีการแสดงพีจีพีด้วยสารฟลาโวนอยด์ที่ถูกกักเก็บในพอลิเมอริกไมเซลล์

ผลการวิจัย *(สั้น ๆ ที่บ่งชี้ประเด็นข้อค้นพบ กระบวนการ ผลผลิต และการเรียนรู้)*

สารฟลาโวนอยด์ที่ถูกกักเก็บในพอลิเมอริกไมเซลล์มีประสิทธิภาพฆ่าเซลล์มะเร็งเม็ดเลือดขาวที่ดื้อยา และสามารถเพิ่มประสิทธิภาพของยาดอกโซรูบิซินและยาดาวโนรูบิซินเนื่องจากผลที่เกิดจากการรวมกันของพอลิเมอริกไมเซลล์ที่ไปยังยั้งการขนส่งยารักษามะเร็งโดยพี-ไกลโคโปรตีน และผลของฟลาโวนอยด์ที่ไปลดศักย์เยื่อเซลล์ของไมโทคอนเดรีย

คำสืบค้น (Keywords)

ฟลาโวนอยด์; พอลิเมอริกไมเซลล์; ดื้อยา; มะเร็ง; พี-จีพี

การนำผลงานวิจัยไปใช้ประโยชน์ *(ดูคำจำกัดความ และตัวอย่างด้านหลังแบบฟอร์ม)*

☐ **ด้านนโยบาย** **โดยใคร** *(กรุณาให้ข้อมูลเจาะจง)*.....
มีการนำไปใช้อย่างไร
.....

☐ **ด้านสาธารณะ** **โดยใคร** *(กรุณาให้ข้อมูลเจาะจง)* .....
มีการนำไปใช้อย่างไร
.....

☐ **ด้านชุมชนและพื้นที่** **โดยใคร** *(กรุณาให้ข้อมูลเจาะจง)* .....
มีการนำไปใช้อย่างไร
.....

☐ **ด้านพาณิชย์** **โดยใคร** *(กรุณาให้ข้อมูลเจาะจง)* .....
มีการนำไปใช้อย่างไร
.....

☐ **ด้านวิชาการ** **โดยใคร** *(กรุณาให้ข้อมูลเจาะจง)* ผศ.ดร.ภญ.รัตติรส คนการณ์
มีการนำไปใช้อย่างไร *(กรุณาให้ข้อมูลเจาะจง)*
ตีพิมพ์ผลงานในวารสารระดับนานาชาติจำนวน 2 เรื่อง

☐ **ยังไม่มีการนำไปใช้** (โปรดกรอกในกรอบถัดไป)

(กรณีที่ยังไม่มีการใช้ประโยชน์) **ผลงานวิจัยมีศักยภาพในการนำไปใช้ประโยชน์**

☐ **ด้านนโยบาย** ☐ **ด้านสาธารณะ** ☐ **ด้านชุมชนและพื้นที่** ☐ **ด้านพาณิชย์** ☐ **ด้านวิชาการ**

ข้อเสนอแนะเพื่อให้ผลงานถูกนำไปใช้ประโยชน์

.....

.....

การเผยแพร่/ประชาสัมพันธ์ *(กรุณาให้รายละเอียด พร้อมแนบหลักฐาน)*

1. สิ่งพิมพ์ หรือสื่อทั่วไป

   ☐ **หนังสือพิมพ์** ☐ **วารสาร** ☐ **โทรทัศน์** ☐ **วิทยุ** ☐ **เว็บไซต์** ☐ **คู่มือ/แผ่นพับ** ☐ **จัดประชุม/อบรม** ☐ **อื่น ๆ**

   .....

2. สิ่งพิมพ์ทางวิชาการ *(วารสาร, การประชุม ให้ระบุรายละเอียดแบบการเขียนเอกสารอ้างอิง เพื่อการค้นหาซึ่งควรประกอบด้วย ชื่อผู้แต่ง ชื่อเรื่อง แหล่งพิมพ์ ปี พ.ศ. (ค.ศ.) ฉบับที่ หน้า)*

   1. **Khonkarn R**, Daowtak K, Okonogi S. Chemotherapeutic Efficacy Enhancement in P-gp-Overexpressing Cancer Cells by Flavonoid-Loaded Polymeric Micelles. *AAPS PharmSciTech* 2020;21:121.
   2. Srisa-nga K, Mankhetkorn S, Okonogi S, **Khonkarn R**. Delivery of Superparamagnetic Polymeric Micelles Loaded with Quercetin to Hepatocellular Carcinoma Cells. *Journal of pharmaceutical sciences*. 2019;108(2):996-1006.

<u>คำอธิบายและตัวอย่างการนำไปใช้ประโยชน์ในแต่ละด้าน</u>

1. การใช้ประโยชน์ด้านนโยบาย

คำจำกัดความ : การนำความรู้จากงานวิจัยไปใช้ในกระบวนการกำหนดนโยบาย ซึ่งนโยบายหมายถึง หลักการ แนวทาง กลยุทธ์ ในการดำเนินงานเพื่อให้บรรลุวัตถุประสงค์ อาจเป็นนโยบายระดับประเทศ ระดับภูมิภาค ระดับจังหวัด ระดับท้องถิ่น หรือระดับหน่วยงาน นโยบายที่ดีจะต้องประกอบด้วยวัตถุประสงค์ แนวทาง และกลไกในการดำเนินงานที่ชัดเจน สอดคล้องกับปัญหาและความต้องการการใช้ประโยชน์ด้านนโยบายจะรวมทั้งการนำองค์ความรู้ไปสังเคราะห์เป็นนโยบายหรือทางเลือกเชิงนโยบาย (policy options) แล้วนำนโยบายนั้นไปสู่ผู้ใช้ประโยชน์

2. การใช้ประโยชน์ด้านสาธารณะ

คำจำกัดความ : การดำเนินงานเพื่อนำผลงานวิจัยและนวัตกรรม ไปใช้ในวงกว้างเพื่อประโยชน์ของสังคม และประชาชนทั่วไป ให้มีความรู้ความเข้าใจ เกิดความตระหนัก รู้เท่าทันการเปลี่ยนแปลง ซึ่งนำไปสู่การเปลี่ยนวิธีคิด พฤติกรรม เพื่อเพิ่มคุณภาพชีวิตของประชาชน สร้างสังคมคุณภาพ และส่งเสริมคุณภาพสิ่งแวดล้อม

3. การใช้ประโยชน์ด้านพาณิชย์

คำจำกัดความ : การนำนวัตกรรม เทคโนโลยี ผลิตภัณฑ์ใหม่ พันธุ์พืช พันธุ์สัตว์ ไปสู่การผลิตในเชิงพาณิชย์ การสร้างมูลค่าเพิ่มของผลิตภัณฑ์ การแปรรูป การสร้างตราสินค้า การเพิ่มประสิทธิภาพในกระบวนการผลิต และการลดต้นทุนการผลิต การสร้างอาชีพ และทางเลือกให้กับผู้ประกอบการ เกษตรกรหรือผู้ประกอบอาชีพอื่น ๆ

4. การใช้ประโยชน์ด้านชุมชนและพื้นที่

คำจำกัดความ : การนำกระบวนการ วิธีการ องค์ความรู้ การเปลี่ยนแปลง การเสริมพลัง อันเป็นผลกระทบที่เกิดจากการวิจัยและพัฒนาชุมชน ท้องถิ่น พื้นที่ ไปใช้ให้เกิดประโยชน์การขยายผลต่อชุมชน ท้องถิ่นและสังคมอื่น

5. การใช้ประโยชน์ด้านวิชาการ

คำจำกัดความ : การนำองค์ความรู้จากผลงานวิจัยที่ตีพิมพ์ในรูปแบบต่าง ๆ เช่น ผลงานตีพิมพ์ในวารสารระดับนานาชาติ ระดับชาติ หนังสือ ตำรา บทเรียน ไปเป็นประโยชน์ด้านวิชาการ การเรียนรู้ การเรียนการ

สอน ในวงนักวิชาการและผู้สนใจด้านวิชาการ รวมถึงการนำผลงานวิจัยไปวิจัยต่อยอด หรือการนำไปสู่ product และ process ไปใช้ในการเสริมสร้างนวัตกรรม และเทคโนโลยี